

University of Windsor

Scholarship at UWindor

Electronic Theses and Dissertations

Theses, Dissertations, and Major Papers

2022

Elucidating Mechanisms for S-Nitrosoglutathione Reductase Activity and Control in Plants Using O-Aminobenzoyl-S-Nitrosoglutathione and a Novel Photo-Sensitive Probe

Leslie Ventimiglia
University of Windsor

Follow this and additional works at: <https://scholar.uwindsor.ca/etd>



Part of the [Biochemistry Commons](#), and the [Organic Chemistry Commons](#)

Recommended Citation

Ventimiglia, Leslie, "Elucidating Mechanisms for S-Nitrosoglutathione Reductase Activity and Control in Plants Using O-Aminobenzoyl-S-Nitrosoglutathione and a Novel Photo-Sensitive Probe" (2022). *Electronic Theses and Dissertations*. 8976.

<https://scholar.uwindsor.ca/etd/8976>

This online database contains the full-text of PhD dissertations and Masters' theses of University of Windsor students from 1954 forward. These documents are made available for personal study and research purposes only, in accordance with the Canadian Copyright Act and the Creative Commons license—CC BY-NC-ND (Attribution, Non-Commercial, No Derivative Works). Under this license, works must always be attributed to the copyright holder (original author), cannot be used for any commercial purposes, and may not be altered. Any other use would require the permission of the copyright holder. Students may inquire about withdrawing their dissertation and/or thesis from this database. For additional inquiries, please contact the repository administrator via email (scholarship@uwindsor.ca) or by telephone at 519-253-3000ext. 3208.

**Elucidating mechanisms for *S*-nitrosoglutathione Reductase activity and control in plants using
O-aminobenzoyl-*S*-nitrosoglutathione and a novel photo-sensitive probe**

By

Leslie Ventimiglia

A Thesis

Submitted to the Faculty of Graduate Studies
through the Department of Chemistry and Biochemistry
in Partial Fulfillment of the Requirements for
the Degree of Master of Science
at the University of Windsor

Windsor, Ontario, Canada

© 2022 Leslie Ventimiglia

**Elucidating mechanisms for *S*-nitrosoglutathione Reductase activity and control in plants using
O-aminobenzoyl-*S*-nitrosoglutathione and a novel photo-sensitive probe**

By

Leslie Ventimiglia

APPROVED BY:

J. Hudson

Department of Biomedical Sciences

P. Vacratsis

Department of Chemistry and Biochemistry

B. Mutus, Advisor

Department of Chemistry and Biochemistry

December 14th, 2022

DECLARATION OF ORIGINALITY

I hereby certify that I am the sole author of this thesis and that no part of this thesis has been published or submitted for publication.

I certify that, to the best of my knowledge, my thesis does not infringe upon anyone's copyright nor violate any proprietary rights and that any ideas, techniques, quotations, or any other material from the work of other people included in my thesis, published or otherwise, are fully acknowledged in accordance with the standard referencing practices. Furthermore, to the extent that I have included copyrighted material that surpasses the bounds of fair dealing within the meaning of the Canada Copyright Act, I certify that I have obtained a written permission from the copyright owner(s) to include such material(s) in my thesis and have included copies of such copyright clearances to my appendix.

I declare that this is a true copy of my thesis, including any final revisions, as approved by my thesis committee and the Graduate Studies office, and that this thesis has not been submitted for a higher degree to any other University or Institution.

ABSTRACT

S-nitrosoglutathione reductase, (GSNOR) is widely accepted as the master regulator of stress through NO signaling and protein *S*-nitrosylation. GSNOR mediates stress response through the catalysis of its principal substrate *S*-nitrosoglutathione (GSNO). The instigation of various stressors in plants cause observable changes in plant phenotype, which are associated with changes in GSNOR activity. There are no current methods for measuring GSNOR activity directly in living plants. In this paper, a previously developed fluorogenic pseudo-substrate for human GSNOR, OAbz-GSNO, was applied to the *Solanum lycopersicum* plant model. OAbz-GSNO was identified as a promising novel pseudo-substrate to study changes in GSNOR activity in the presence of stressors, using fluorescence microscopy and living plant tissue. Ammonium is one of the most prevalent nitrogen sources available, however, ammonium becomes toxic to plants at over 0.5mM. GSNOR activity was assessed in roots grown in high ammonium stress conditions where activity was shown to decrease despite an up-regulation in GSNOR synthesis. These results suggest that GSNOR can also be controlled through post-translational modifications.

Previous studies have identified a possible modification at an allosteric site at residues Lys323, Gly321, Asn185, and Lys188, which may cause an increase in activity at high GSNO concentration. A photo-labile affinity probe, *p*-azidophenacyl glutathione (papaGS) was designed to interact with GSNO binding sites. In dark conditions, enzyme kinetic experimentation identified a reduction in cooperativity binding when HmGSNOR is exposed to papaGS, indicating specificity to the allosteric site. When irradiated the HmGSNOR function was also inhibited to 50% activity by azide non-specific crosslinking at the allosteric site causing a conformational change, indicating the importance of the site in proper enzyme function and the usefulness of papaGS as an allosteric site probe for GSNOR.

DEDICATION

For a younger version of myself

ACKNOWLEDGEMENTS

This project was made possible by the support and guidance of my supervisor, Dr. Bulent Mutus. I cannot thank him enough for accepting me into his research group and allowing me the opportunity to develop as a researcher under his leadership.

I also extend my gratitude to many of the past and present Mutus Lab members, as well as members of the Chemistry and Biochemistry department who have taken their time to assist me over the years. Their willingness to extend their knowledge to me has made me a more confident researcher. Particularly, I would like to thank current lab members Mark Potter, and Sara Hassanzadehroknabadi for their willingness to provide support wherever necessary, as well as past lab members Sara Aljoudi, Nneamaka Onukuwe, and Kathleen Fontana, for laying the groundwork for my project. Additionally, I express my gratitude to Dr. Ashley Dadalt, Adrian Luiso and Sanam Mohammadzadeh for taking time to offer me their expertise as well as our neighboring lab groups, Marquardt lab and Trant lab for their availability and assisting where-ever needed. I must also thank Angela Awada for her continued support and encouragement over the years.

I would also like to thank Dr. Otis Vacratsis for agreeing to be on my committee, and for having spent many hours assisting me with mass spectral analysis, for which I am very grateful. Additionally, thank-you to Dr. John Hudson for being on my graduate committee. I would also like to extend my appreciation to Dr. Zelinski and Zeenat Aurangzeb for their assistance with immunocytochemistry.

Additionally, I extend my gratitude to the graduate secretaries, Marlene Bezaire for keeping me on track during my graduate studies, and now Linda Hudson-Chapman for her continued guidance as I complete my studies.

Lastly, I must thank my friends and my family for their persistent support, without whom, many of my aspirations would not be possible.

TABLE OF CONTENTS

DECLARATION OF ORIGINALITY	iii
ABSTRACT	iv
DEDICATION.....	v
ACKNOWLEDGEMENTS	vi
LIST OF TABLES.....	xii
LIST OF FIGURES	xiii
LIST OF APPENDICES.....	xv
LIST OF ABBREVIATIONS/SYMBOLS	xvi
CHAPTER 1	1
GENERAL INTRODUCTION.....	1
1.1 INTRODUCTION	2
1.2 THE STUDY OF STRESS IN PLANTS.....	3
1.2.1 STRESS DETECTION.....	3
1.2.2 THE ANTIOXIDANT DEFENCE SYSTEM	5
1.2.3 THE ROLE OF GLUTATHIONE IN OXIDATIVE ENVIRONMENTS	5
1.3 NITRIC OXIDE AS A SIGNALLING MOLECULE.....	6
1.3.1 NITRIC OXIDE POST-TRANSLATIONAL MODIFICATIONS	7
1.3.2 <i>S</i> -NITROSATION OF PROTEIN THIOLS	7
1.3.3 OTHER MODIFICATIONS ON CYSTEINE THIOLS	8
1.3.4 NITRIC OXIDE GENERATION IN PLANTS.....	9
1.3.5 THE ROLE OF NITRATE REDUCTASE IN NO PRODUCTION	10
1.3.6 OTHER POSSIBLE SOURCES OF NITRIC OXIDE MEDIATION IN PLANTS	10
1.4 <i>S</i> -NITROSOGLUTATHIONE.....	11

1.5 <i>S</i> -NITROSOGLUTATHIONE REDUCTASE	12
1.5.1 GSNOR AS A FORMALDEHYDE DEHYDROGENASE	13
1.5.2 THE STRUCTURE OF GSNOR.....	13
1.6 GSNOR INHIBITION	14
1.6.1 GSNOR HAS POSSIBLE INHIBITION THROUGH <i>S</i> -NITROSYLATION.....	15
1.7 GSNOR'S ROLE IN PLANT GROWTH AND STRESS RESPONSE.....	15
1.8 DOWN-STREAM RESPONSES OF GSNOR ACTIVITY	16
1.8.1 THE ROLE OF PHYTOHORMONES IN TANDEM WITH GSNOR IN PLANT DEVELOPMENT	17
CHAPTER 2	19
A NOVEL FLUOROGENIC PSUEDO-SUBSTRATE APPLIED TO THE CHARACTERIZATION OF <i>S</i> -NITROSOGLUTATHIONE REDUCTASE IN LIVING PLANTS	19
2.1 INTRODUCTION	20
2.1.1 MICRO-TOM AS A RELEVANT PLANT RESEARCH MODEL.....	20
2.1.2 CURRENT METHOD FOR DETERMINING GSNOR ACTIVITY IN LIVING PLANTS	20
2.1.3 CHALLENGES WITH THE NADH ASSAY	21
2.1.4 APPLICATIONS OF FLUORESCENT MICROSCOPY IN LIVING PLANT STUDIES	21
2.1.5 TARGETS FOR FLUORESCENT MICROSCOPY ON LIVING TISSUES.....	22
2.1.6 OABZ-GSNO AS A FLUOROGENIC SUBSTRATE FOR GSNOR	23
2.1.7 EFFECT OF EXOGENOUSLY APPLIED AMMONIUM ON PLANT GROWTH AND GSNOR ACTIVITY.....	25
2.2 MATERIALS AND METHODS.....	27
2.2.1 Materials.....	27
2.2.2 Methods.....	27

2.2.3 Seedling preparation and culture	27
2.2.4 GSNO synthesis	28
2.2.5 OAbz-GSNO synthesis and purification	28
2.2.6 Microscopy kinetic experimentation	29
2.2.7 Immunolocalization of GSNOR in roots	29
2.2.8 Crude protein extraction.....	30
2.2.9 Western blots.....	30
2.2.10 Protoplast isolation.....	31
2.3 RESULTS AND DISCUSSION	33
2.3.1 GSNOR LOCALIZATION IN SOLANUM LYCOPERSICUM ROOTS.....	33
2.3.2 FLOW CHAMBER METHOD FOR VISUALIZING OABZ-GSNO ACTIVITY ...	36
2.3.3 OABZ-GSNO KINETIC ASSAYS	38
2.3.4 CHANGES IN ACTIVITY DUE TO AMMONIUM STRESS.....	46
2.4 CONCLUSION.....	51
CHAPTER 3	52
DEVELOPING A PHOTOREACTIVE AFFINITY LABEL FOR THE CHARACTERIZATION OF S-NITROSOGLUTATHIONE REDUCTASE.....	52
3.1 INTRODUCTION	53
3.1.1 GSNOR ACTIVITY IS MODIFIED POST-TRANSLATIONALLY BY GSNO	53
3.1.2 AN ALLOSTERIC SITE FOR GSNO MODIFICATION ON GSNOR WAS IDENTIFIED	54
3.1.3 P-AZDIOPHENACYL BROMIDE	57
3.2 MATERIALS AND METHODS.....	58
3.2.1 Materials.....	58
3.2.2 Methods.....	58
3.2.3 papaGS synthesis and purification	58

3.2.4 HmGSNOR expression and purification.....	59
3.2.5 Kinetic assays.....	60
3.2.6 Mass Spectrometry.....	60
3.3 RESULTS AND DISCUSSION.....	62
3.3.1 THE DEVELOPMENT OF PAPAGS.....	62
3.3.2 EVIDENCE OF SUCCESSFUL PAPAGS SYNTHESIS AND ACTIVITY.....	63
3.3.4 MASS SPECTROMETRY TO DETERMINE PAPAGS BINDING SITE.....	72
3.4 CONCLUSION.....	74
CHAPTER 4: GENERAL CONCLUSION.....	75
REFERENCES.....	76
APPENDICES.....	87
VITA AUCTORIS.....	95

LIST OF TABLES

Table 2.3.4-2 Western blot band intensities	46
Table 3.3.3-1 Michaelis-Menten parameters from Figure 3.3.3-1	66
Table 3.3.3-2 Hill-Langmuir parameters from Figure 3.3.3-2	68

LIST OF FIGURES

Figure 1.2.1-1 Examples of ROS and RNS that may be present in plants and the ways they may affect cellular processes	4
Figure 2.1.5-1 Structure of lignin polymer and most abundant monolignols	21
Figure 2.1.6-1 Fluorescence generation of OAbz-GSNO	22
Figure 2.3.1-1 Immunolocalization of GSNOR in <i>S. lycopersicum</i> vs controls	31
Figure 2.3.1-2 GSNOR immunolocalization in <i>S. lycopersicum</i> roots	32
Figure 2.3.2-1 Diagram of flow chamber	34
Figure 2.3.3-1 <i>S. lycopersicum</i> roots displaying fluorescent increase over time when exposed to OAbz-GSNO	38
Figure 2.3.3-2 Competitive Inhibition of OAbz-GSNO as a function of [GSNO]	39
Figure 2.3.3-3 GSNOR activity reduction by N6022 Inhibitor	40
Figure 2.3.3-4 GSNOR activity localization assay	41
Figure 2.3.3-5 Initial rates of OAbz-GSNO reduction as a function of [OAbz-GSNO]	42
Figure 2.3.4-1 The phenotypic changes in seedlings when grown in ammonium vs control conditions	45
Figure 2.3.4-2 Western Blot to determine GSNOR content in ammonium vs control Roots	46
Figure 2.3.4-3 GSNOR activity in ammonium treated roots as determined by Oabz-GSNO reduction <i>in vivo</i>	47
Figure 3.1.2-1 GSNO Binding Site on GSNOR at residues Lys323, Gly321, Asn185, Lys188	51
Figure 3.1.2-2 wtGSNOR activity vs mutants	52
Figure 3.1.3-1 Possible structural changes in azide group in response to irradiation	53

Figure 3.3.1-1 The proposed structure of photo-labile papaGS	59
Figure 3.3.2-1 papaGS light-sensitivity indicated by a colour change	61
Figure 3.3.2-2 GSNOR kinetic activity when exposed to papaGS in light and dark conditions vs control	62
Figure 3.3.2-4 Mass spectral analysis of papaGS	63
Figure 3.3.2-5 Proposed structural changes based on Mass Spectral analysis of irradiated papaGS	64
Figure 3.3.3-1 Michaelis-Menten GSNOR kinetics in samples containing papaGS	66
Figure 3.3.3-2 Cooperativity binding indicating possible allosteric binding site	67
Figure 3.3.4-1 Mass analysis of trypsin digested GSNOR with papaGS	69

LIST OF APPENDICES

Appendix A—Michaelis Menten Kinetics

Figure A.1 Image series for Michaelis-Menten experiments

Appendix B—Human GSNOR sequence used containing tags and start methionine

Figure B.1 Sequence of hmGSNOR used containing tags and start methionine with allosteric site residues Asn205, Lys208, Gly341, and Lys343

Table B.1 peptide masses from HmGSNOR trypsin digestion

Appendix C—papaGS adducts

Figure C.1 Possible Molecular Weights of irradiated papaGS adducts.

Appendix D—Protoplast Isolation

Figure B.1 Extracted protoplasts

LIST OF ABBREVIATIONS/SYMBOLS

AB	Ammonium Bicarbonate
ACN	Acetonitrile
ADH	Alcohol dehydrogenase
AOX	Alternative Oxidase
AsA	Ascorbic acid
AUX	Auxin
Aux/IAA	Auxin/indole 3-acetic acid
APX3	Ascorbate peroxidase 3
ATP	Adenosine Triphosphate
B+J	Burdick & Jackson Water for LC-MS and HPLC
BSA	Bovine Serum Albumin
CK	Cytokinin
DAPI	4',6-diamidino-2-phenylindole nuclear stain
ddH₂O	distilled water
DTT	Dithiothreitol
EDTA	Ethylenediaminetetraacetic acid
ETOH	Ethanol
ESI	Electrospray Ionization

FA	Formic Acid
FAD	Flavin adenine dinucleotide
FALDH	Formaldehyde dehydrogenase
FCS	Fluorescence correlation spectroscopy
FITC	Fluorescein Isothiocyanate
FLIM	Fluorescence lifetime imaging microscopy
FP	Fluorescent protein
FRET	Forster/Fluorescence Resonance Energy transfer
GR	Glutathione reductase
GSH	Glutathione, reduced
GSNO	<i>S</i> -nitrosoglutathione
GSNOR	<i>S</i> -nitrosoglutathione reductase
HCl	Hydrochloric acid
HmGSNOR	Human <i>S</i> -nitrosoglutathione reductase
HMGSH	Hemithioacetal <i>S</i> -hydromethylglutathione
HPLC	High performance liquid chromatography
HRP	Horseradish peroxidase
IAM	iodoacetamide
IPTG	Isopropyl β -D-1-thiogalactopyranoside

LC-MS/MS	Liquid chromatography tandem mass spectrometry
LMM	Low molecular weight
MeOH	Methanol
MES	2-(N-morpholino)ethanesulfonic acid
MilliQ	Highly purified water using Millipore Milli-Q lab water system
MS	Mass spectrometry
MS media	Murashige and Skoog Basal media
NAD⁺	β -nicotinamide adenine dinucleotide, oxidized
NADH	β -nicotinamide adenine dinucleotide, reduced
NADPH	Nicotinamide adenine dinucleotide phosphate (reduced)
NADP⁺	Nicotinamide adenine dinucleotide phosphate
Ni-NR	Nitrite reduction activity of Nitrate reductase
NO	Nitric Oxide
NOFNiR	Nitric Oxide-forming Nitrite reductase
NOS	Nitric Oxide Synthase
NR	Nitrate Reductase
NRT	Nitrate Transporter
OAbz-GSNO	<i>O</i> -aminobenzoyl- <i>S</i> -nitrosoglutathione
papaBr	<i>p</i> -azidophenacyl bromide

papaGS	<i>p</i> -azidophenacyle glutathione
PMSF	Phenylmethanesulfonyl fluoride
PrxII E	Peroxiredoxin II E
PTM	Post translational modification
PVDF	Polyvinylidene Fluoride
RFU	Relative fluorescence units
ROS	reactive oxygen species
RNS	reactive nitrogen species
SDS-PAGE	Sodium dodecyl-sulfate polyacrylamide gel electrophoresis
SNO	<i>S</i> -nitrosothiol
TIR1	Transport Inhibitor Response 1
THB1	Truncated hemoglobin 1
TGB	trypsin digestion buffer
UPLC	Ultra pure liquid chromatography
VTC1	Vitamin C 1
2XYT	2 times yeast extract-tryptone broth

CHAPTER 1
GENERAL INTRODUCTION

1.1 INTRODUCTION

Stress is an innate part of all life. It is defined as an event that occurs within an organism that exceeds its natural homeostatic range ¹. From life's inception, organisms have evolved in ways to mitigate stress, and the result is a series of remarkable physical characteristics and molecular processes across species, allowing life to thrive in the multitude of environmental conditions that exist across the planet. For this reason, the study of how an organism responds to its changing environment is very interesting, particularly in the plant kingdom. Plants cannot find shelter from harsh conditions when they arise, they must rely on their adapted traits like a cactus which depends on its thorns to keep predators from eating it or a maple tree which has adapted to store sap to keep itself alive during a cold winter. Stressors are such an important part of plant physiology that they determine how a plant will grow. Across the animal kingdom, genetics plays a major role in which features the animal will express, where in plant biology the environment plays a much more equitable role in the organisms resulting phenotype. Root structure, fruit production, and the number and size of leaves are all determined by a plant's degree of exposure to stressors as well as the type of stressor. Low water content in the soil may cause the plant to express longer and more branched roots, low nutrients may result in low fruiting in favour of nutrient conservation, and intense heat or cold may cause a plant to go 'dormant' to allow it to survive on low energy production until a more favourable temperature occurs.

Though stress is often thought of as a negative aspect of plant growth, it is also documented that plants often thrive on an optimal level of stress. Wind is often introduced into greenhouses because it strengthens stems allowing plants to grow upright without falling over as they get heavier and begin to bear heavier structures and fruits. Plants have a

somewhat ‘symbiotic’ relationship with the stressors they are exposed to within their environments.

As climate change continues to impact ecosystems and native environments to which organisms have adapted, the study of plant stress will continue to become a more significant area of research. Stressors can limit agriculture, native plant productivity and CO₂ uptake, leading to disastrous potential consequences, in global warming and food availability². Understanding stress response will allow for the development of new ways of mitigating stress and creating a more sustainable future.

1.2 THE STUDY OF STRESS IN PLANTS

Stressors inflicted on plants are defined as either biotic or abiotic³. A biotic stressor refers to its biological origin, like pathogens infecting plants, animals and insects eating plants or other vegetation out competing another for access to nutrients and light. An abiotic stressor is one that is not of biological origin, like extreme temperature, drought, nutrient deficiency, or high levels of salts and metals present in the soil^{3,4}. The elevating degree of abiotic stress on plants is linked to climate change³ and improper waste management². As global warming and pollution continue to change the environment of the planet, its impact on agriculture will become a more prevalent area of study.

1.2.1 STRESS DETECTION

On the onset of a stressor, stress signals, detected by receptors on the membrane of plant cells, will induce a downstream event leading to up/down-regulation of genes at the

transcription level ³. All stress responses lead to some level of oxidative stress and generation of reactive oxygen species (ROS) ^{1,5} or reactive nitrogen species (RNS) ^{4,6}, a nitrogen containing ROS. Either the stressor itself is responsible for an increase in ROS/RNS or it may occur as a downstream event, resulting from signaling cascades where ROS/RNS are produced to activate a stress response ^{5,6}. In response to ROS/RNS stimuli, redox-sensitive proteins can be activated or inhibited leading to signal transduction, gene activation or inhibition and the antioxidant defense system may be induced ⁵.

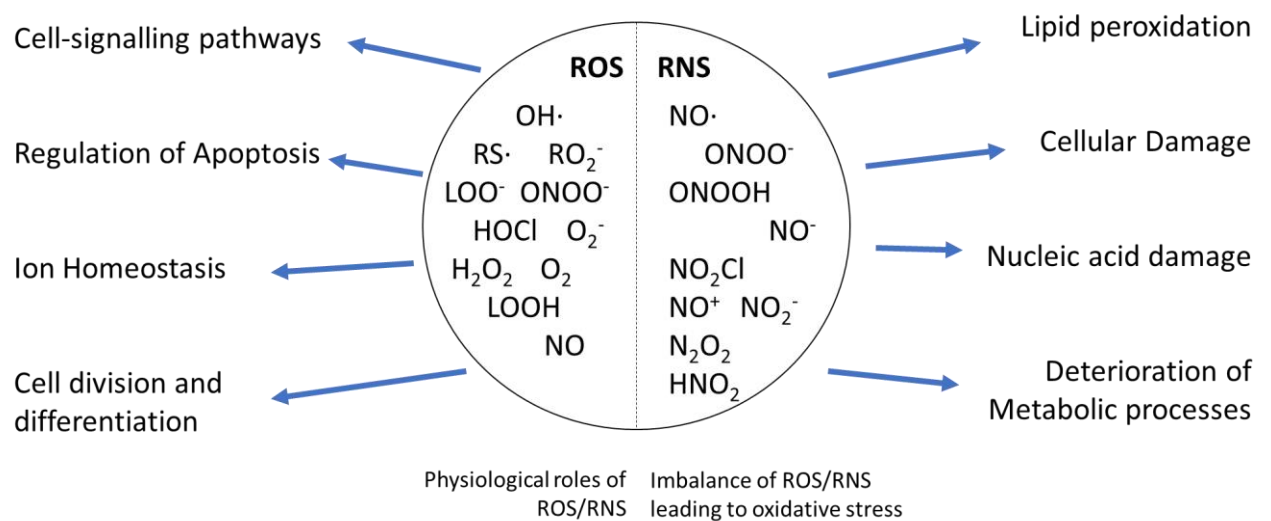


Figure 1.2.1-1 Examples of ROS and RNS that may be present in organisms and the ways they may affect cellular processes ⁶

1.2.2 THE ANTIOXIDANT DEFENCE SYSTEM

Antioxidants are capable of neutralizing free radicals. Within plant systems ascorbic acid (AsA) and glutathione (GSH) are some of the most prevalent low molecular weight non-enzymatic antioxidants ⁷. However the antioxidant defense system is made up of both non-enzymatic and enzymatic antioxidants, like superoxide dismutase, ascorbate peroxidase, catalase, monodehydroascrobate reductase, glutathione reductase, and glutathione *S*-transferase as well and carotenoids and tocopherols ^{2,8}. GSH is present at high concentrations, in the millimolar range, across most plant and animal systems and found in the cytosol, and other cellular machinery like endoplasmic reticulum, mitochondria, chloroplasts and peroxisomes as well as apoplast ⁹. However, some plants, like peanut and soybean, do not contain GSH but rather a similar antioxidant, homoglutathione which has a similar antioxidant role to GSH ¹⁰.

1.2.3 THE ROLE OF GLUTATHIONE IN OXIDATIVE ENVIRONMENTS

Generally, GSH is synthesized in the chloroplast, cytosol, or mitochondria ¹¹ through the amide bond formation between the amino acids, cysteine, glutamate, and glycine ¹². Cysteine and glutamate are reacted through the ATP dependent enzyme, γ -glutamylcysteine synthetase, to form γ -glutamylcysteine. Then GSH is formed by the ATP dependent reaction between γ -glutamylcysteine and glycine, catalyzed by GSH synthase ^{12,13}. In highly oxidative conditions, where there are ROS like the hydroxy radical ($\cdot\text{OH}$), hydrogen peroxide (H_2O_2) and superoxide (O_2^-) present, GSH will donate a proton to the free radical and oxidize to its disulfide GSSG, making the ratio of GSH:GSSG reflective of the level of oxidative stress on a plant system ^{5,12,13}. Similarly, when there are high levels of RNS like NO or peroxynitrite

(ONOO⁻) GSH can spontaneously react with RNS to neutralize oxidative environments ¹⁴. Additionally, GSH has been identified in other systems of detoxification like heavy metal and electrophilic xenobiotic elimination ¹⁵. In order for GSH to maintain its antioxidant properties it must regenerate after it is oxidized to GSSG, this occurs through the Ascorbate-Glutathione (AsA-GSH) cycle which coordinates with the antioxidant enzymes to regenerate both GSH and AsA so they may continue to maintain the redox state of the plant ¹¹. GSH and redox state also have profound implications in signaling pathways, where alterations in GSH:GSSG concentrations may lead to the release of phytohormones which have more specific downstream effects like, reduced growth, productivity, or apoptosis ¹⁶. GSH is also capable of reacting with nitric oxide (NO), a highly reactive nitrogen species (RNS), to form S-nitrosoglutathione (GSNO) and generally thought of as a more stable form of NO ¹⁴. NO has been identified as an important signaling molecule across species and must be considered when elucidating downstream effects of oxidative stress and GSH detoxification due to their close relationship ¹⁷.

1.3 NITRIC OXIDE AS A SIGNALLING MOLECULE

NO is a highly reactive, uncharged, gaseous free radical which is capable of degrading important cellular components, like lipids, proteins and nucleic acids leading to cellular death, when present in high concentrations ^{4,6}. However, at low endogenous concentrations NO has been identified and accepted as an important signaling molecule in many organisms and in applications of stress response ¹⁷⁻¹⁹. Due to its small size NO can pass through cellular membranes readily without a carrier, and due to its high reactivity, it is short lived when generated and reacts spontaneously in cellular environments ^{4,14,19}. When acting

as a signaling molecule NO is often shown to modify enzyme activity through post translational modifications (PTMs) on thiol groups and by tyrosine nitration ²⁰.

1.3.1 NITRIC OXIDE POST-TRANSLATIONAL MODIFICATIONS

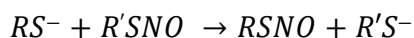
Nitric Oxide has been shown to modulate stress response both directly, through enzyme modification and indirectly by interacting with other cellular components ²¹. It is well known as an inhibitor of lipid peroxidation as well as an inhibitor of protein oxidation by forming a metal-nitrosyl complex (M-NO) with relevant metal ions, like copper, iron, and zinc, which are common oxidizers in metal ion containing proteins. By forming these M-NO interactions, strong positively charged metal ions are blocked from forming ROS which commonly degrade lipids and proteins through oxidation ^{22,23}. Additionally, NO will commonly form protein tyrosine nitration, where peroxynitrite (ONOO⁻), a species present under high stress where NO and superoxide (O₂⁻) have reacted together, adds a nitro group (NO₂) to tyrosine when the phenolic ring is oxidized to its tyrosyl radical, to form, 3-nitrotyrosine ²⁴. Certain proteins are more susceptible to this form of modification at times of high stress, by this mechanism tyrosine nitration on proteins can be a mediator of plant stress ²⁴. However, the most common NO PTM is *S*-nitrosylation, where NO covalently binds with the thiol group (-SH) of cysteine, forming an *S*-nitrosothiol (SNO) ²¹.

1.3.2 *S*-NITROSYLATION OF PROTEIN THIOLS

NO is not an oxidant on its own and in low oxidizing conditions will not react directly with protein thiol groups. It is proposed that to transfer its NO moiety onto thiols it

must first react with oxygen to form nitrogen oxides like NO₂ or N₂O₃ which react with a thiol to form a thiol radical that may react with NO to form an SNO. Or that a metal group may oxidize NO to form a nitrosonium ion (NO⁺) that may react directly with a thiol group to form an SNO ^{25,26}. SNOs can also be formed by transnitrosation (**Equation 1.3.2-1**), where the NO moiety is transferred between low molecular weight (LMM) thiols and protein thiols, one of the main LMM thiols being GSNO ²⁷. Additionally, there are limitations to which protein thiol groups may react to form SNOs, where some studies suggest these modifications may occur on thiols which are in hydrophobic environments and where acidic and basic residues are present ²⁸. A common feature amongst these PTMs is their reversibility, which allows these sites to be mediated quite sensitively by the levels of RNS, ROS and GSH present in the system ²⁵. There is an effort to identify more of these S-nitrosylation sites across common crop species to determine how they function in plant stress tolerance ²⁹.

Equation 1.3.2-1



1.3.3 OTHER MODIFICATIONS ON CYSTEINE THIOLS

Cysteine thiol groups are a common target of oxidative stress, and under oxidating conditions thiols can take on a variety of different modifications ³⁰. Because of cysteines sensitivity to the oxidation state of its environment, cysteine is capable of changing the structure and function of enzymes ³¹. Additionally, pathways which respond to oxidative environments often aim to reduce thiols and restore through the upregulation of thioredoxin or glutaredoxin ³⁰⁻³². Under oxidating cellular conditions, hydrogen peroxide, H₂O₂, can react

with thiols to form sulfenic acid (-SOH), sulfinic acid (-SO₂H) or sulfonic acid (-SO₃H) thiol modifications. Sulfenic acid formation can lead to further modification like disulfide formation with nearby thiols on the same protein, or thiols on associated proteins. Additionally, thiol groups may react with glutathione to form *S*-glutathionylated proteins ³⁰. Because these modifications on thiols are often reversible, and may modify protein activity, they are thought to act in signal transduction pathways ³⁰⁻³².

1.3.4 NITRIC OXIDE GENERATION IN PLANTS

In most prokaryote and eukaryote applications, NO is synthesized endogenously by nitric oxide synthase (NOS), which catalyzes the reaction between L-arginine, O₂ and NADPH, to L-citrulline, NADP⁺, H⁺ and produces NO ³³. Though there are emerging studies which have identified a possible NOS homolog in plants which may contribute to NO production, NOS is not currently accepted as the main source of endogenous NO production in plants ^{34,35}. Rather, NO is proposed to be generated through nitrate reduction by Nitrate Reductase (NR) present in the cytoplasm, an enzyme associated with the nitrogen assimilation pathway and metabolism ³⁶. Nitrates are taken up by plant roots and are a necessary element of growth. Once nitrate (NO₃⁻) enters a plant system through its nitrate transporters in roots, NRT1.1 and NRT2.1, NR will initiate reduction to nitrite (NO₂⁻) and it is further transported to chloroplasts where it is reduced to ammonium (NH₄⁺) and amino acids to contribute to growth or further reduced to NO ³⁷⁻³⁹. Nitrate uptake is thought of as a sensitive process mediated by NR and the NRT2.1 transport protein, a transporter which is activated only in times of low soil nitrate concentration (<1mM) ^{40,41}. Both NR and NRT2.1 have been found to be heavily regulated by the level of GSNO present and contribute to the regulation of NO ^{39,40}.

1.3.5 THE ROLE OF NITRATE REDUCTASE IN NO PRODUCTION

NR reduces nitrate to nitrite by using NAD(P)H as an electron donor, and molybdenum, heme group and FAD as cofactors. Additionally, NR is thought to be capable of nitrite reduction to NO in a similar manner (Ni-NR activity), however this activity accounts for about 1% of NRs nitrate reducing capability^{37,42}. Despite this low activity, some studies suggest that Ni-NR activity may increase in times of low oxygen or high acidity, supporting the suggestion that Ni-NR activity occurs in the roots where oxygen levels are low⁴³. Though it is supported that NR has a significant role in the ultimate NO levels within the plant and contains two highly protease sensitive regions by which it can be heavily regulated through protein degradation, it remains unclear how NR functions in endogenous NO production⁴⁴.

1.3.6 OTHER POSSIBLE SOURCES OF NITRIC OXIDE MEDIATION IN PLANTS

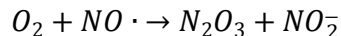
A possible partner protein to NR has also been identified, NOFNiR (nitric-oxide—forming nitrite reductase), which may reduce nitrite to NO by electrons donated by NAD(P)H oxidation in NR⁴⁵. In a similar manner, NR might form an alliance with a truncated hemoglobin 1 (THB1), where in this case the opposite effect is observed where the electron donated to THB1 converts NO to nitrate in the presence of oxygen⁴⁶. Another suggested source of nitrite reduction *in vivo* is through molybdoenzymes. Of the enzymes previously stated both NR and NOFNiR are molybdenum containing. There are five known molybdenum containing enzymes in plants and all five have been shown to be capable of nitrite reduction to NO *in vitro* and under anaerobic conditions³⁸.

1.4 S-NITROSOGLUTATHIONE

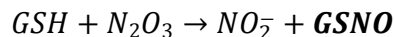
Once generated *in vivo* NO is likely to react spontaneously with GSH in aerobic conditions to form S-nitrosoglutathione (GSNO), the most abundant LMM S-nitrosothiol. Its formation is influenced by NO production and oxygen levels as limiting factors ⁴⁷. Though there is speculation over the mechanism of GSNO formation from NO, a popular theory is that GSNO is formed when NO is first oxidized by O₂, to form N₂O₃ which further S-nitrosates GSH, or that NO is added to a glutathionyl radical formed during NO oxidation ⁴⁸

Equation 1.4-1 to 1.4-4. Some newer studies also suggest that GSNO formation may be mediated by ferric cytochrome c ⁴⁹. GSNO is thought of as a NO reservoir due to its stability, and accepted as an NO donor, capable of S-nitrosylation, and S-transnitrosation of proteins to mediate their function. At high endogenous concentrations of GSNO, levels of S-nitrosylation on proteins is higher. GSNO can be mediated by GSNOR to alter the equilibrium of S-nitrosylated proteins to GSNO, and indirectly, the activity of proteins commonly modified by S-nitrosylation ⁵⁰. Within the plant model, GSNO has been localized in all organs and within the vasculature contributing to its possible role as an NO transporter by which it can be carried to other cellular locations where it can act as a mediator of stress response ^{51,52}. Additionally, the highest concentration of GSNO within a pepper plant model has been found in roots, despite roots containing the most aerobic environment ⁵³.

Equation 1.4-1

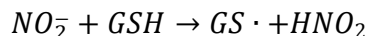


Equation 1.4-2

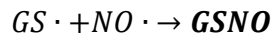


or

Equation 1.4-3



Equation 1.4-4



Equations 1.4-1 to 1.4-4: The proposed mechanism of GSNO formation in vivo

1.5 S-NITROSOGLUTATHIONE REDUCTASE

GSNO is mediated primarily by the cytosolic enzyme *S*-nitrosoglutathione reductase (GSNOR), to which GSNO is its principal substrate. This activity was first identified in *E. coli*⁵⁴, and later in *Arabidopsis thaliana*⁵⁵ but has since been identified in nearly all prokaryotic and eukaryotic organisms. GSNOR is an Alcohol Dehydrogenase (ADH) class III (ADH3) enzyme which belongs to the ADH superfamily of enzymes due to their role in the interchange between alcohols and aldehydes⁵⁶. They have been recognized for their significance in anerobic metabolism in plants, and of high relevance in root development⁵⁷. ADH3 is the only class with limited or absent ethanol activity, however ADH3 enzymes are the most highly conserved of all ADH superfamily enzymes across organisms⁵⁸. GSNOR/ADH3 catalyzes the NADH dependent reduction of GSNO, ultimately to the products GSSG and NH₄⁺. This occurs by first reducing GSNO to the intermediate, N-hydroxysulfonamide (GSNHOH), and in the presence of GSH, GSNHOH may further decompose to GSSG. However, when there is little GSH present the intermediate GSNHOH

will convert to glutathione sulfinamide which may be further hydrolyzed to glutathione sulfinic acid and ammonia ⁵⁹.

1.5.1 GSNOR AS A FORMALDEHYDE DEHYDROGENASE

Despite its current relevance as an enzyme capable of GSNO reduction, GSNOR was initially recognized by its relevance in formaldehyde detoxification as a GSH dependent formaldehyde dehydrogenase (FALDH) in the liver ^{60,61}. Formaldehyde can react spontaneously with GSH to form hemithioacetal *S*-hydromethylglutathione (HMGS), and in the presence of NAD⁺ GSNOR can catalyze its conversion to *S*-formylglutathione ⁶¹.

1.5.2 THE STRUCTURE OF GSNOR

GSNOR is a homodimer composed of two 40kDa subunits which each contain two domains complexed with Zinc metal ions (Zn²⁺). In each monomer, one Zinc ion is coordinated with two cysteines, a histidine and a water molecule or glutamate, and functions in catalysis as a Lewis acid ⁶² and the other takes on a role in maintaining the enzymatic structure and is coordinated with four cysteine residues ⁶³. The crystal structure of GSNOR has been isolated from *Solanum lycopersicum* (SIGSNOR) as an apoenzyme and in complex with NAD⁺. The NAD⁺ cofactor binding site, active site, along with the structural zinc and catalytic zinc coordination site residues are all conserved across elucidated GSNOR sequences ⁶³. SIGSNOR has 67% sequence identity with HmGSNOR (*Homo sapien* GSNOR) as well as 90% identity with AtGSNOR (*Arabidopsis thaliana* GSNOR) ⁶³. However, there are slight differences within the composition of the anion-binding pocket between HmGSNOR and SIGSNOR. In the HmGSNOR active site, the GSNOR substrate

HMGSNOR has been found to form hydrogen bonds with the residues Thr47, Asp56, Glu58, Arg115, and Tyr140, within the site, where the residues, Gln112, Arg115, and Lys248 form the anion-binding pocket ⁶². SIGSNOR has conserved residues which correspond to the HmGSNOR catalytic site at its residues Thr49, Asp58, Glu60, Arg117 and Lys287, however it is lacking corresponding residues Gln112 and Tyr140 ⁶³.

1.6 GSNOR INHIBITION

Some inhibitors of GSNOR have been designed for applications in treating human diseases. Cavenostat (N91115), C3, C2, and N6022 have all been developed and are undergoing clinical trials for their applications in treating cystic fibrosis, asthma, neurological damage, and myocardial damage ^{64–66}. Some plant studies have used N6022, a reversible mixed non-competitive inhibitor against GSNO, to show how reducing the activity of GSNOR can modulate plant stress response ^{63,65,67–69}. N6022 is also a mixed competitive inhibitor for HMGSNOR, and binds to GSNOR within the HMGSNOR anion binding pocket ⁶⁵. Despite N6022's ability to inhibit SIGSNOR within the nM concentrations, it has a lower affinity for SIGSNOR vs HmGSNOR due to not having a glutamine residue within the anion binding pocket ⁶³. In plants the inhibition of GSNOR has been associated with the upregulation of GSH, possibly through the upregulation of Glutathione reductase (GR) and thereby an initiation of the antioxidant defense system through positive feedback, to protect plants against ROS ⁶⁷. A downregulation of GSNOR leading to an upregulation of its primary substrate GSNO, a mark of concentrated NO, creates a highly *S*-nitrosylating environment, and an inhibitor to disease progression ⁶⁸. In a study where *S. lycopersicum* roots are exposed to ROS through cadmium and high salinity stress, primary root growth is slowed along with the *S*-nitrosylation of APX (ascorbate peroxidase), leading to its upregulation, and the *S*-

nitrosylation of NADPHox (NADPH oxidase) leading to its down regulation, which are both PTMs associated with a reduction in ROS ⁶⁸.

1.6.1 GSNOR HAS POSSIBLE INHIBITION THROUGH S-NITROSYLATION

GSNOR may be down regulated through GSNO mediation. Some studies suggested that there is a possible allosteric *S*-nitrosylation site on GSNOR that may downregulate the enzyme when NO levels are high. A study on the nitrogen assimilation pathway identified that high concentrations of GSNO within roots, and thus high NO levels, inhibited nitrate uptake through a nitrate transporter (NRT2.1), Nitrate reductase (NR) activity, as well as GSNOR ⁴⁰. In another study Cys271 from SIGSNOR, was identified as a potential *S*-nitrosylation site through biotinylation and LC-MS/MS analysis ⁷⁰. Additionally, the modification was found to be reversible when exposed to the reducing agent DTT (dithiothreitol) as further evidence of the modification ⁷¹. However other studies suggest that the inhibitory effect of GSNO on GSNOR could indicate another allosteric binding site on GSNOR rather than a cysteine *S*-nitrosylation site ⁷².

1.7 GSNOR'S ROLE IN PLANT GROWTH AND STRESS RESPONSE

Because GSNOR mediates GSNO bioavailability, it also indirectly regulates levels of protein *S*-nitrosylation leading to changes in protein function, and thus protein control. Over 1000 *S*-nitrosylated peptides have been identified in the *Arabidopsis thaliana* proteome which may be subject to control by GSNOR ⁷³. Different cellular conditions may lead to the upregulation and downregulation of GSNOR. In a study which exposed wild type (wt)

GSNOR, and GSNOR knock out (ko), young *Arabidopsis thaliana* seedlings to paraquat, a herbicide capable of creating a highly oxidizing environment, ko GSNOR seedlings were less susceptible to oxidative damage⁷⁴. This might occur because a reduction in GSNOR can lead to the accumulation of NO. NO is capable of reducing paraquat toxicity by scavenging superoxide radicals to form peroxynitrite which is less damaging, and which may further lead to tyrosine nitration leading to further stress response^{75,76}. These observations contrast similar studies done in heavy metal stress mechanisms, where ko GSNOR enhances the oxidative damage done by iron toxicity, possibly through the reaction between NO and H₂O₂ to form the hydroxyl radical ·OH⁷⁷. Among other common stress conditions, studies where plants were exposed to temperature extremes, consistent light or dark conditions, or wounding lead to increases in GSNOR activity⁷⁶. Moreover, loss of GSNOR function is associated with a series of phenotypic characteristics, like faster germination rates, reduction in root development and overall plant growth including reduction in photosynthesis, as well as loss in productivity^{29,74}.

1.8 DOWN-STREAM RESPONSES OF GSNOR ACTIVITY

Down-stream effects of GSNOR activity are likely a result of the *S*-nitrosylation states of reactive thiol groups responsible for stress response. Among proteins mediated in this manner are peroxiredoxin II E (PrxII E), which is responsible for the detoxification of peroxynitrite. *S*-nitrosylation down-regulates PrxII E, leading to the promotion of tyrosine nitration⁷⁸. *S*-NO formation also leads to increased activity in NADPH oxidase, which promotes apoptosis in some tissues, leading to loss of some structures⁷⁹. In addition to mediating oxidating environments, GSNOR activity will often result in the mediation of

certain phytohormones necessary to mitigate the harmful effects of stressors on plants and adapt development to these conditions ³.

1.8.1 THE ROLE OF PHYTOHORMONES IN TANDEM WITH GSNOR IN PLANT DEVELOPMENT

Starting at germination, all developmental processes that occur within a plant are mitigated by phytohormones. They are termed phytohormones due to their light sensitivity and susceptible to light and dark conditions, similar to the circadian rhythm in mammals ⁸⁰. There are nine kinds of phytohormones, which include salicylic acid (SA), jasmonic acid (JA), auxin (AUX), cytokinin (CK), gibberellins (GA), abscisic acid (ABA), ethylene (ET), brassinosteroids, and strigolactones. Each phytohormone is associated with a set of molecular processes that occur within plants, maintaining growth of structures like, root development and fruit ripening, or disease resistance and stress response. Due to the vital relationship between a plant's development and its unpredictable environment, it is understandable that both development and stress response are mitigated by the same network of phytohormones.

Phytohormone activity occurs in connection with NO signaling and GSNOR activity ⁸¹. Many proteins which act in connection to phytohormones are regulated through *S*-nitrosylation. Auxin and cytokinin are responsible for root and shoot development respectively. Both are mediated by GSNOR indirectly through *S*-nitrosylation. In root development auxin upregulation promotes apical growth. Auxin production is repressed by AUX/IAA repressors, and upon increases in GSNO or NO donors AUX/IAA repressors are inhibited by an interaction with *S*-nitrosylated TIR1 (Transport Inhibitor Response 1) stimulating root development ⁸². Cytokinin is also associated with growth in plant shoots as well as in regulating root growth in conjunction with auxin and mediated by NO. Opposite to

AUX, CK activity is attenuated by *S*-nitrosylation in the associated protein, AHP1, which represses its phosphorylation leading to a loss in downstream growth response⁸³.

CHAPTER 2

A NOVEL FLUOROGENIC PSUEDO-SUBSTRATE APPLIED TO THE CHARACTERIZATION OF S-NITROSOGLUTATHIONE REDUCTASE IN LIVING PLANTS

2.1 INTRODUCTION

2.1.1 MICRO-TOM AS A RELEVANT PLANT RESEARCH MODEL

Micro-tomato, ‘Micro-Tom’ or *Solanum Lycopersicum cultivar* was originally developed by Scott and Harbaugh in 1989 as an ornamental plant intended for home gardening⁸⁴. Though *S. lycopersicum* was not originally intended for fruit cultivation, its small size, relatively short growth cycle of about 90 days between sowing and fruiting as well as high cold tolerance and post-harvest ripening, has made it a suitable greenhouse tomato⁸⁵. For similar reasons Micro-Tom is an attractive research model in agricultural applications where fruit production and quality are of high importance. Additionally, on the onset of cold stress conditions, *S. lycopersicum* has a high antioxidant response, giving insight into the molecular processes that are initiated on the onset of stressors⁸⁶. There is already an abundance of research studies surrounding the response of *S. lycopersicum* to oxidative stressors^{29,63,68,87}.

2.1.2 CURRENT METHOD FOR DETERMINING GSNOR ACTIVITY IN LIVING PLANTS

There is currently no way to measure GSNOR activity directly *in vivo*, in plant cells. GSNOR activity can be estimated through the NADH assay *in vitro* from crude cellular lysates. This method of detection exploits the depletion of GSNORs co-enzyme NADH which absorbs light at 340nm⁸⁸. Most plant studies use the NADH assay as their main method of GSNOR activity, along with other experiments which give insight into the level of SNOs, S-nitrosylated proteins, NO, and ROS, content in the lysates, to give a better picture of how GSNOR activity is changing in different conditions.

2.1.3 CHALLENGES WITH THE NADH ASSAY

Though current studies have elucidated some relevant information about how GSNOR activity changes during times of stress, there are some inherent challenges when studying GSNOR activity in vitro using the NADH assay. The NADH assay is not specific to GSNOR, NADH is a co-enzyme of many enzymes, so it is unclear whether GSNOR activity is being measured. Additionally, plant lysates contain high levels of protease, and even in cold conditions in the presence of protease inhibitors, GSNOR can be degraded quickly over the course of an experiment. Some studies also suggest that GSNOR may be modulated reversibly by its primary substrate, GSNO, either by *S*-nitrosylation or by some other PTM. If this is the case, GSNOR activity can only be preserved in its native environment and not when diluted into a lysate. Another downfall to the NADH assay is that the contents of various cell types and from different plant organs become homogenized, providing little insight into the overall plant response to a particular stressor.

2.1.4 APPLICATIONS OF FLUORESCENT MICROSCOPY IN LIVING PLANT STUDIES

Live cell imaging of whole plant organs is crucial when considering how a plant responds to its changing environment. Microscopy usually requires a lengthy process involving fixing, sectioning and staining tissue samples, a technique which can only apply to deconstructed tissue samples rather than for observing functioning cellular environments⁸⁹. New methods of plant microscopy are taking advantage of the small size of young seedlings to visualize whole living and intact plant organs. Specimens can be placed or grown in sealed

compartments that can act as microfluidic devices and visualized using microscopy^{90,91}. An example of one of these microfluidic devices is the root chip, which was developed to visualize the growth of young *Arabidopsis* roots. Seedling can be grown directly into the microfluidic device and observed under a microscope for fluorescent analysis of growth, additionally metabolites can be applied to the roots endogenously to create a controlled environment and visualize biochemical changes in roots upon the application of different metabolites⁹².

2.1.5 TARGETS FOR FLUORESCENT MICROSCOPY ON LIVING TISSUES

Fluorescing cellular components and fluorophores have characteristic excitation and emission wavelengths, therefore fluorescence microscopes can be outfitted with filters that are specific for certain metabolites and processes. Organisms can contain fluorescing molecules inherent to their development that can be visualized and measured using fluorescence microscopy termed autofluorescence^{93,94}. The two most relevant fluorescing molecules native to plants are chlorophyll and lignin, however there are a wide variety of fluorescing components to plants which emit across all wavelengths in the fluorescence range (~400nm- 700nm)⁹³. Many of these molecules are common markers for plant growth and health and can be measured as a label free method of assessing molecular processes. Chlorophyll is measured in the red-orange range and corresponds to CO₂ assimilation when measuring the rate of photosynthesis in leaves⁹⁴. Lignin (**Figure 2.1.5-1**) is a component of the cell wall and fluoresces in the blue-green range, it is a marker of plant growth as well as exploited in cell wall interaction studies using FRET microscopy (Förster/Fluorescent Resonant Energy Transfer)⁹³. Autofluorescence can be exploited in conjunction with fluorescent proteins (FPs) and exogenously applied dyes, along with microscopy techniques,

including FRET, FLIM (Fluorescence Lifetime Imaging), FRAP (Fluorescence Recovery after Photobleaching), and FCS (Fluorescence Correlation Spectroscopy), to elucidate mechanisms of response to changing environments and specified cellular interactions^{93–95}. Due to the highly specific and low-invasive requirement of fluorescence experimentation on plants, developing new fluorescent markers for use *in vivo* is a significant area of research.

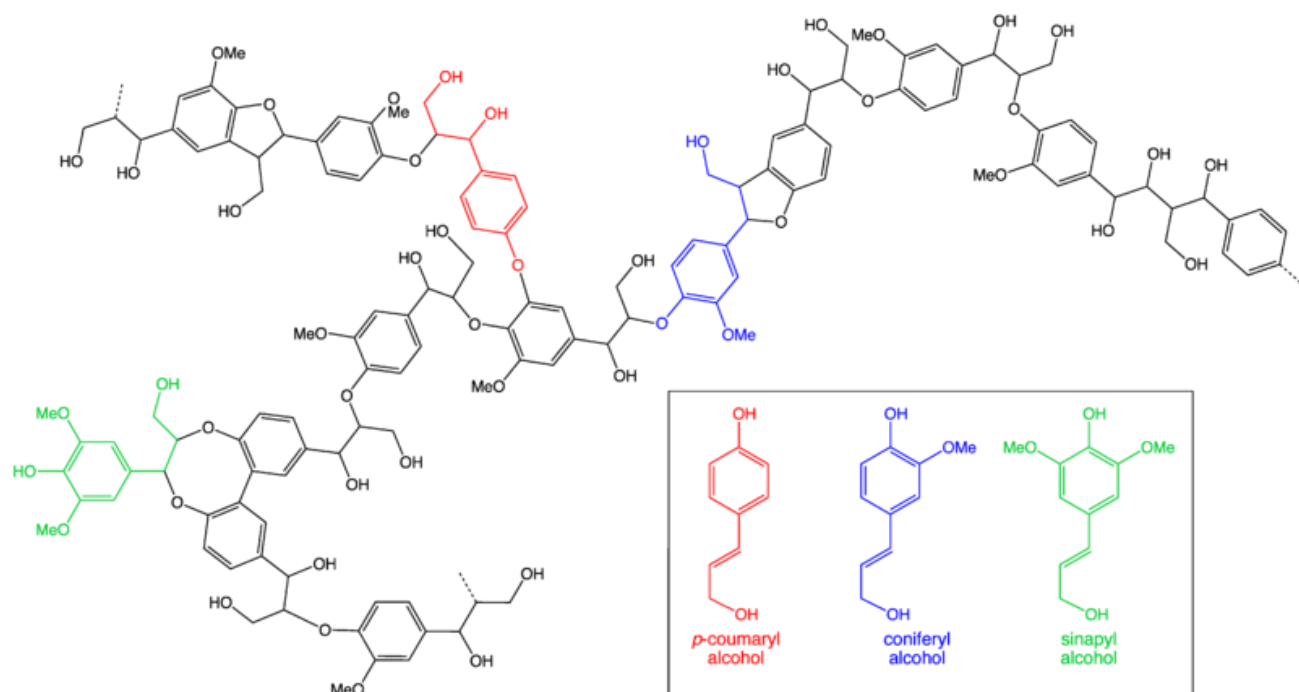


Figure 2.1.5-1 Structure of lignin polymer and most abundant monolignols^{96,97}

2.1.6 OABZ-GSNO AS A FLUOROGENIC SUBSTRATE FOR GSNOR

O-Aminobenzoyl-*S*-nitrosoglutathione (OAbz-GSNO) has been developed by Sun et al. as a fluorogenic pseudo-substrate for the kinetic characterization of GSNOR⁹⁸. OAbz-GSNO is formed by the reaction between the terminal amino group of GSNO and isatoic anhydride to produce GSNO labelled with the *o*-aminobenzoyl fluorescent group and CO₂. *o*-aminobenzoylated peptides are normally fluorescent and detectable when excited at 312nm,

however, the nearby NO group on OAbz-GSNO can quench the emittance of the *o*-aminobenzoyl group. Upon the reduction of OAbz-GSNO to OAbz-GSNHOH when interacting with the GSNOR active site the fluorescence of the *o*-aminobenzoyl group becomes detectable. Due to the fluorescence generation of this pseudo substrate when interacting with GSNOR it is cable of determining rate of GSNOR activity in varying conditions ⁹⁸. OAbz-GSNO was originally developed as a substrate for human GSNOR which has a Michaelis constant (K_M) of 320 μ M, however a lower affinity for the HmGSNOR active site than its principle substrate GSNO which has a K_M of 11 μ M ^{61,98}. Despite a lower affinity for the active site, similar V_{max} values and parallel inhibition upon the exposure to the well-known GSNOR inhibitors N6022 and C3, indicated that OAbz-GSNO interacts with GSNOR in a comparable manner to GSNO. The OAbz-GSNO pseudo substrate has also demonstrated cellular membrane permeability in animal cells, where the same locations containing high GSNOR content exhibited increased fluorescence over time showing the potential of this probe as a marker of GSNOR activity intravital studies.

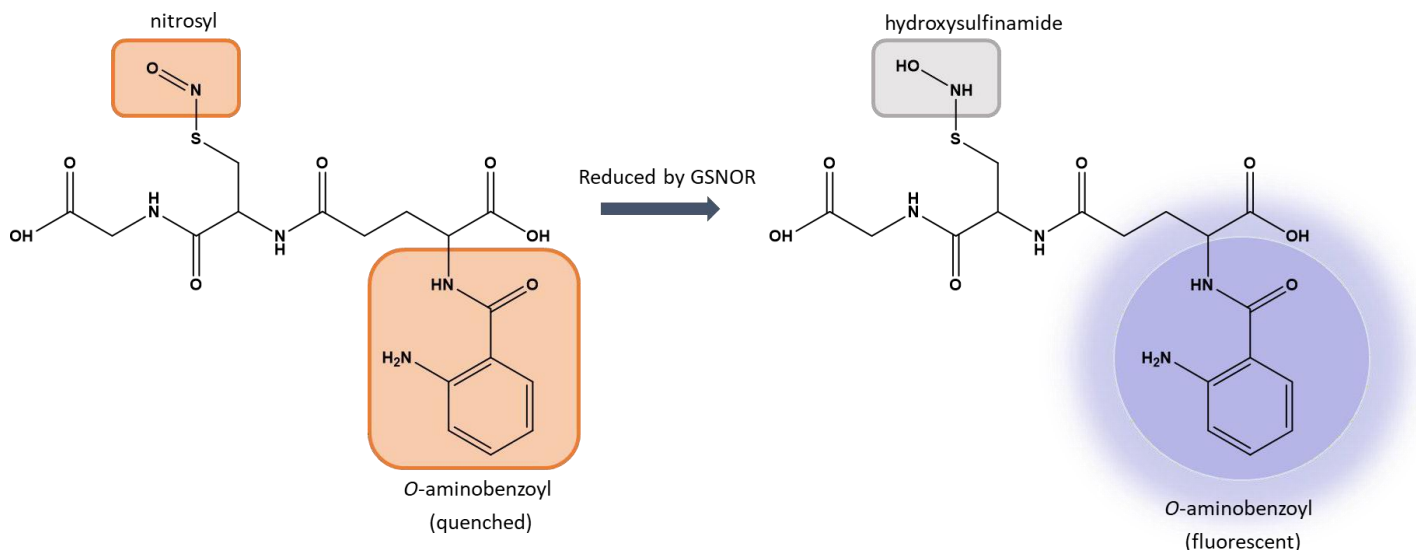


Figure 2.1.6-1 Fluorescence generation of OAbz-GSNO. OAbz-GSNO is quenched by proximity of *O*-aminobenzoyl group to *S*-nitrosyl group. When excited at 312nm and emission detected at 415nm the quenched OAbz-GSNO shows very low fluorescence. Once the *S*-nitrosyl group is reduced by GSNOR or by DTT (dithiothreitol) the fluorescence of the probe is observed at a higher than 10-fold increase in comparison to the unreduced probe.

2.1.7 EFFECT OF EXOGENOUSLY APPLIED AMMONIUM ON PLANT GROWTH AND GSNOR ACTIVITY

Nitrogen is an important macronutrient in soil and its assimilation is often a limiting factor in plant growth, when present in low concentrations. Among the most common forms of nitrogen in soils are nitrate and ammonium (NH₄⁺). In contrast to nitrates which must be reduced by NR to be used in amino acid synthesis, NH₄⁺ can be taken up and used directly by the plant^{99,100}. Despite the involvement of NH₄⁺ into amino acid production, and its lower energy cost, NH₄⁺ may not be the preferred nitrogen source. When NH₄⁺ is present in soil in relatively low concentrations (less than 0.5mM), it is observed to have deleterious effects on

plant growth and productivity, like disrupted root development in the apical root and accompanied by high branching in the lateral roots, in contrast to a reduction in lateral roots and longer apical roots observed in plants when soil nitrate concentration is higher ^{101,102}. as well as stunted overall growth and productivity. It is thought that the accumulation of cationic NH^+ may cause charge imbalances with negatively charged nitrate or may cause disparities in the uptake of other cations present in the soil, like potassium and calcium ¹⁰³. Because of this delicate relationship, there is an ideal ratio of nitrate to ammonium to optimize plant growth and productivity ¹⁰⁰.

Ammonium is linked to NO within respiratory pathways, where high ammonium in comparison to NO, elevates respiration rates by increasing oxygen uptake, as well as up-regulates the production of the enzyme, alternative oxidase (AOX), an enzyme associated with ROS accumulation under stress conditions ^{104,105}. When NH_4^+ is present in high concentrations, NO production is stimulated in tissues, and the observed response to this increase in NO is an upregulation of GSNOR enzyme production, to manage NO formation ⁹⁹. GSNOR overexpression was also linked to the enzyme co-factor, ascorbic acid, through the enzyme, Vitamin C1 (VTC1), another molecule which may regulate root growth. Mutant plants containing a knock out VTC1 enzyme resulted in no over production of GSNOR when exposed to high exogenous levels of NH_4^+ ^{99,106}.

2.2 MATERIALS AND METHODS

2.2.1 Materials

All reagents were purchased from Sigma Aldrich unless otherwise stated.

Solanum lycopersicum seeds were purchased from Ontario Seed Company (OSC), MS media, Ammonium Chloride, Glutathione (reduced), sodium nitrite, isatoic anhydride (recrystallized from isopropanol), potassium phosphate dibasic, potassium phosphate monobasic, sodium chloride, dithiothreitol, MES, sucrose, BSA, Triton-x 100, Tris-HCl, sodium azide, goat serum, rabbit polyclonal primary antibody against tomato GSNOR (PhytoAB Inc), goat anti-rabbit IgG (H+L) conjugated with FITC, VECTASHIELD Antifade Mounting Medium with DAPI, PMSF, EDTA, MeOH, glycine, Tris-Base, Tween-20, rabbit polyclonal primary antibody against tomato APX3 (PhytoAB Inc.), goat anti-rabbit IgG (H+L) secondary antibody conjugated with HRP, chemiluminescence SuperSignal West Femto Maximum Sensitivity Substrate (Thermo Fisher), mannitol, KCl, Cellulase R10, Macerozyme R10 (plant media), CaCl₂, N6022 (AbMole BioScience)

2.2.2 Methods

2.2.3 Seedling preparation and culture

Approximately 100 seeds were counted then washed with 70% ETOH for 30 seconds. Seeds were rinsed with ddH₂O three times then left in a 10% bleach solution for 20 minutes and subsequently rinsed three times with autoclaved milliQ. Seeds were submerged in 3mm of milliQ in a sealed sterile container for 4-7 days on a bench top until the majority of seeds had sprouted. The milliQ was removed using a sterile pipette and replaced with 10ml of pH 5.7 MS media or MS media containing 10mM or 100mM Ammonium salt. Seedlings were

left to grow in the media under a blue grow light for 9hr/15hr day-night cycles for 4-7 days, until leaves began to present.

2.2.4 GSNO synthesis

5mmol of reduced Glutathione was dissolved in 8mls of cold water. 2.5ml of 2M HCl and 5mmol of sodium nitrite were then added and the mixture was stirred in the dark at 4°C for 40 minutes. 10ml of cold acetone was added to the mixture and allowed to stir for 10 minutes until the bright pink GSNO had precipitated. The mixture was scooped onto a filter paper and the precipitate was separated from the unreacted component using vacuum filtration. The precipitate was washed five times with 1ml cold water, then three times with 10ml of cold acetone and three times with 10ml of ether. The product was then lyophilized and stored in the dark at -20°C.

2.2.5 OAbz-GSNO synthesis and purification

0.15mmol of GSNO was dissolved into 3ml of 1M pH 8.5 potassium phosphate buffer. 0.9mmol of isatoic anhydride was added to the mixture and allowed to stir at 4°C overnight in the dark. The mixture was then transferred to a centrifuge tube and centrifuged at approximately 100 rpm for 5 minutes. The clear pink supernatant was applied to a BioRad econo-column containing 2ml of QAE-Sephadex which was rehydrated, packed, and equilibrated with ddH₂O. Once added, the unreacted isatoic anhydride was washed off the column using 10mls of a 0.1M phosphate buffer, pH 7.4. The Oabz-GSNO was eluted with a 0.1M phosphate buffer, pH 7.4 containing 1M NaCl. Once the elution buffer was added, fractions were collected. To determine which fractions had the most Oabz-GSNO present, 5µl of each fraction was added to a fluorescent cuvette containing 500µl of 20mM Tris buffer pH 8.5 and kinetics measured using a Cary Eclipse fluorescence spectrophotometer for a few

seconds at excitation and emission 415nm/312nm. 5 μ l of 1M dithiothreitol was added to the cuvette and mixed well then measured for a few seconds. Fractions which showed the highest fold increase were pooled and their concentration measured using UV/vis spectroscopy where extinction coefficient $\epsilon \approx 2800 \text{ M}^{-1} \text{ cm}^{-1}$ at an absorbance of 320nm. The pooled fractions were then aliquoted and stored in the dark at -80°C for no longer than six months without repeat freeze/ thaw cycles.

2.2.6 Microscopy kinetic experimentation

Microscopy was performed using a Zeiss Axiovert 200 inverted epifluorescence microscope with optical filters from Chroma Technology corporation (10 Imtec Lane, Bellows Falls, VT 05101 USA) optimized for excitation and emission in the 346 and 510 nm range, respectively. 10-day old roots were incubated for 10 minutes in a small dish containing 10mM MES buffer pH 5.7. MES buffer containing OAbz-GSNO concentrations of 0.25mM, 0.375mM, 0.75mM, 1mM, 2mM, 4mM were prepared. Using a sharp scalpel blade a 1mm piece of root was cut and placed on a microscope slide. 10 μ l of OAbz-GSNO solution was applied to the root section then covered with a coverslip, pressing down gently so to not rupture most of the cells. Clear nail polish was quickly applied around the edges of the coverslip and then observed at 200x magnification focusing on the vascular tissue. Fluorescence images were taken every second for 15 seconds at an exposure of 500ms. These trails were done in triplicate for each concentration and analyzed on ImageJ (NIH and LOCI, University of Wisconsin), using their average greyscale value.

2.2.7 Immunolocalization of GSNOR in roots

Sectioning of roots was done by Zeenat Aurangzeb from Dr. Zelinski lab. 14-day old *Solanum lycopersicum* roots were cut into 1cm long sections and submerged in 20% sucrose

until the sections sink and then 30% sucrose overnight. Roots were then sliced into 18µm sections using a cryostat. The sections were incubated for 1hr on a shaker in a blocking buffer containing TBSA-BSAT (5mM Tris-HCl pH 7.6, 0.1% BSA, 0.9% NaCl, 0.05% Triton X-100, 0.05% Sodium azide), and 3% goat serum. The slides were then transferred into 1:500 rabbit polyclonal primary antibody against tomato GSNOR into TBSA-BSAT buffer containing no Triton X-100 and 3% goat serum, at 4°C on a shaker overnight. The slides were washed three times in TBSA-BSAT buffer containing no Triton X-100 for 20-minute intervals at room temperature. Slides were then incubated in 1:250 goat anti-rabbit IgG (H+L) secondary antibody conjugated with FITC for 1hr on a shaker at room temperature, then were washed three times in TBSA-BSAT buffer containing no Triton X-100 for 20-minute intervals. The slides were mounted using VECTASHIELD Antifade Mounting Medium with DAPI and imaged on a Leica inverted fluorescent microscope at 200X and 400X magnification.

2.2.8 Crude protein extraction

One month old roots were frozen with liquid nitrogen and ground into a fine powder using a mortar and pestle. The powder was mixed with a 1:2 (w/v) ratio of a freshly prepared cold extraction buffer containing 50mM Tris-HCl pH 7.5, 0.2% Triton X-100, 2mM DTT, 1mM PMSF, and 1mM EDTA. The extracts were centrifugated at 100 rpm for 10 minutes and the pellet discarded.

2.2.9 Western blots

The protein concentration of the crude extracts were measured using a Bradford assay and diluted to 50µg/ml and 100µg/ml using 50mM Tris-HCl pH 7.5. Following standard western blotting procedure, proteins were separated using SDS-PAGE (sodium dodecyl

sulphate polyacrylamide gel electrophoresis) and resolved on 12% gels. Proteins were transferred for 1hr at 100V onto a PVDF (polyvinylidene difluoride) membrane using a transfer buffer containing 20% MeOH, 0.192M glycine, 0.025M Tris-Base pH 8.3. Blots were blocked by incubating in 5% BSA in TBST buffer containing 0.068M NaCl, 0.1% Tween-20, and 8.3mM Tris-Base pH 7.6, on a shaker at room temperature for 1hr. Separate blots were exposed to 1:1000 rabbit polyclonal primary antibody against tomato GSNOR in 5% BSA or 1:1000 rabbit polyclonal primary antibody against tomato APX3 in 5% BSA on shaker at 4°C overnight then washed with TBST three times with 5-minute intervals. Blots were then exposed to 1:5000 goat anti-rabbit IgG (H+L) secondary antibody conjugated with HRP in 5% BSA for 45 minutes and washed with TBST three times in 5-minute intervals and ready for imaging on imager using chemiluminescence SuperSignal West Femto Maximum Sensitivity Substrate according to Manufacturer's instructions to visualize bands.

2.2.10 Protoplast isolation

Cotyledons and root caps were severed from 14-day old *Solanum lycopersicum* seedlings using a sharp scalpel. Hypocotyls and apical roots of approximately 100 seedlings were carefully sliced into 1mm sections, ensuring not to mechanically crush cells. Once sliced, root sections were immediately transferred to a small petri dish containing an enzyme solution which can digest the cellulose, hemicellulose and pectin which make up the cell wall. The fresh enzyme solution was prepared by heating a 20mM MES solution, pH 5.7 containing 0.4M mannitol and 20mM KCl to 70°C for 5 minutes. The solution was then cooled to 55°C, where 1.5% (wt/vol) Cellulase R10 and 0.4% (wt/vol) Macerozyme R10 and the solution incubated for 10 minutes to inactivate DNase and proteases. The solution was further cooled to 25°C and 10mM CaCl₂ was added along with 0.1% BSA. The final solution was passed through 0.2-µm syringe filter and into a sterile petri dish. Root sections were

incubated in the enzyme solution in the dark for 15hrs then gently agitated by swirling to release the protoplasts and visualized under a light microscope at 400x magnification to ensure protoplast extraction. To separate protoplasts from cellular debris the enzyme/protoplast mixture was diluted to 50% with a W5 buffer (2mM MES pH 5.7, 154mM NaCl, 125mM CaCl₂, 5mM KCl) and separated using a 100 µm nylon mesh filter. The solution was left at room temperature in a 15ml conical vial for 15 minutes until protoplasts settled to the bottom and as much buffer as possible was removed from the top of the protoplasts to concentrate them.

2.3 RESULTS AND DISCUSSION

2.3.1 GSNOR LOCALIZATION IN SOLANUM LYCOPERSICUM ROOTS

Previous studies have indicated that GSNOR has a significant role in root development and is most abundant in the cytoplasm of cells contributing to the vasculature of plants, including the phloem and xylem parenchyma cells^{107,108}. GSNOR immunolocalization experiments were performed to verify the cellular location of GSNOR in young *Solanum lycopersicum* seedlings. **Figure 2.3.1-1** shows the increased brightness of roots treated with both primary anti-GSNOR and secondary fluorescent antibodies, in comparison to autofluorescence in roots and controls containing only one antibody. In **Figure 2.3.1-2** increased magnification on young roots show GSNOR localization. The yellow filter corresponds to GSNOR location, it is primarily visualized in the phloem however some yellow fluorescence is also visible in the parenchyma cells. These results indicate that GSNOR activity may be visualized in these various locations during *in vivo* kinetic studies.

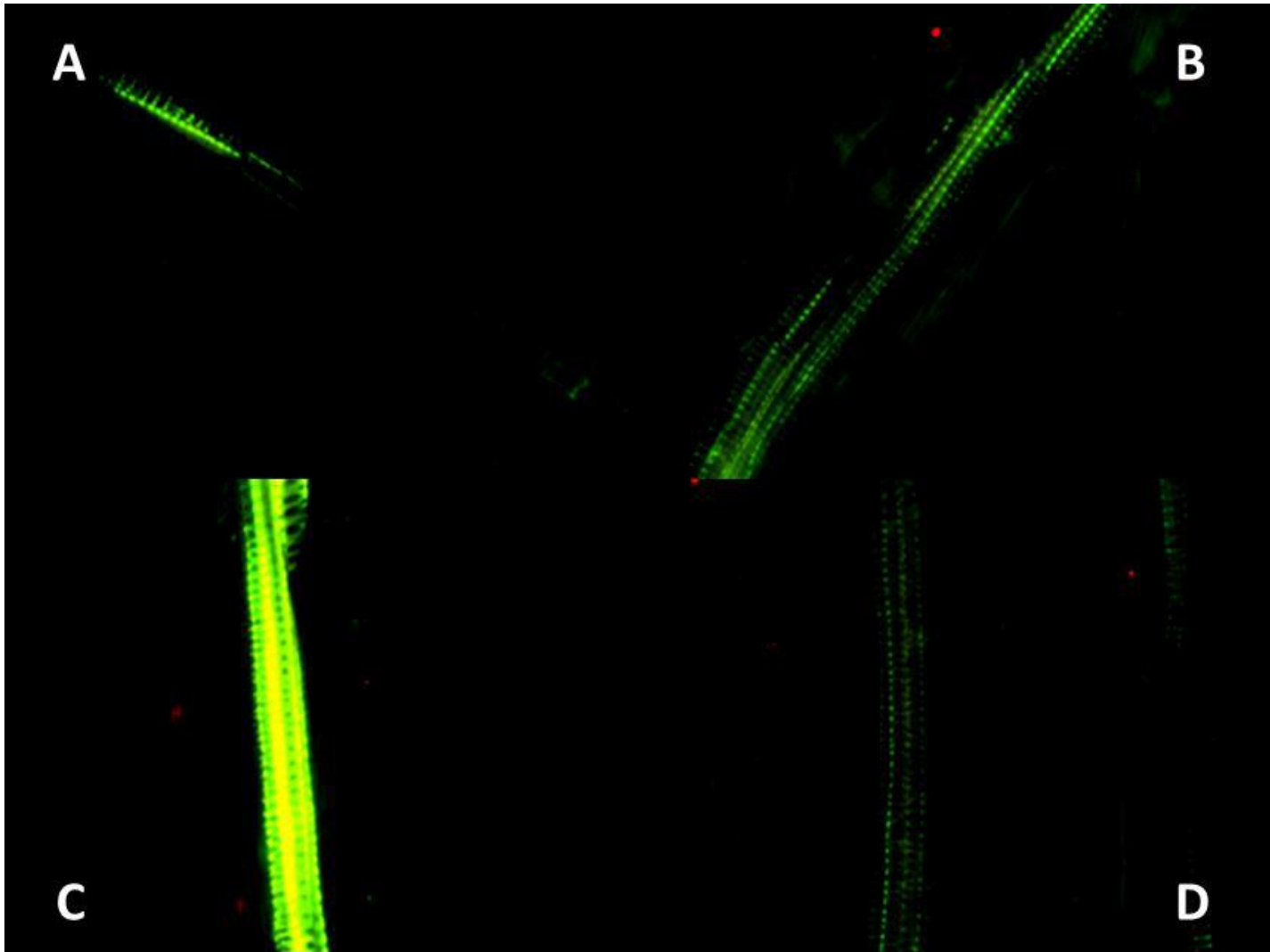


Figure 2.3.1-1 Immunolocalization of GSNOR in *S. lycopersicum* vs controls. layered images taken at 200x magnification and 300ms with Leica inverted fluorescent microscope with excitation/emission filters 430-510nm/475-575nm (pictured green) and 320-400nm/430-510nm (pictured yellow) **A.** roots exposed to TBST-BSAT blocking buffer only, shows native fluorescence. **B.** roots exposed to primary antibody only, shows native fluorescence only. **C.** roots exposed to both primary and secondary antibodies, indicating that GSNOR is present in roots. **D.** roots exposed to secondary antibody only, indicating that the fluorescent

secondary antibody is specific for *Solanum lycopersicum* GSNOR and the washing procedures successfully removed excess antibody.

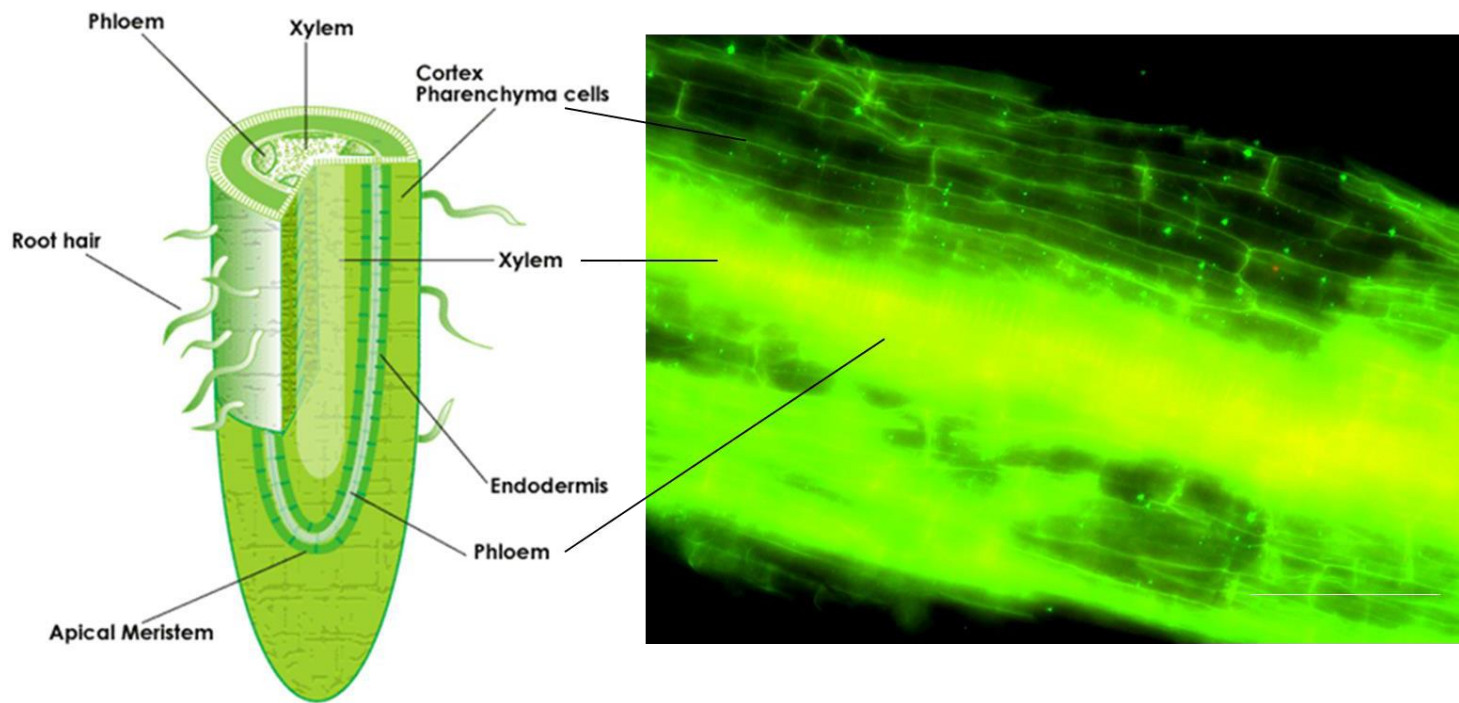


Figure 2.3.1-2 GSNOR immunolocalization in *S. lycopersicum* roots. left, diagram indicating the type of cells present in roots. Right, lateral root section imaged with a Leica inverted microscope as stated in **Figure 2.3.1-1** above at 400x magnification. Highest concentration of GSNOR is visualized at places of brightest yellow intensity, both in the vascular tissues (xylem and phloem) at the center of the root, and the outer most parenchyma cells of the cortex.

2.3.2 FLOW CHAMBER METHOD FOR VISUALIZING OABZ-GSNO ACTIVITY

A flow chamber, **Figure 2.3.2-1**, was developed to fulfill requirements of *in vivo* young root microscopy on a Ziess Axiovert 200 inverted epifluorescence microscope. When considering *in vivo* experimentation, it is crucial to maintain the native environment of plant tissues and to prevent the loss of cellular contents. The flow chamber contained a Teflon insert which was the same dimensions as the coverslip that was used to seal the chamber, allowing for intact roots to be visualized whole instead of sliced or crushed. The insert was mounted on an appropriate microscope slide using a clear epoxy. At the start of an experiment a large section of root was placed on the coverslip and secured with quick dry clear nail polish. After 30 seconds the coverslip could be secured to the Teflon insert using the same clear nail polish. The chamber was filled with an appropriate buffer through one of two holes drilled to the size of a 27.5-gauge diabetic needle and equilibrated for a few minutes before performing a kinetic experiment. Because roots were secured within the chamber the buffer could be removed and refilled with buffer containing a different metabolite environment, so controls and experiments could be performed on the same roots and visualized in the same location.

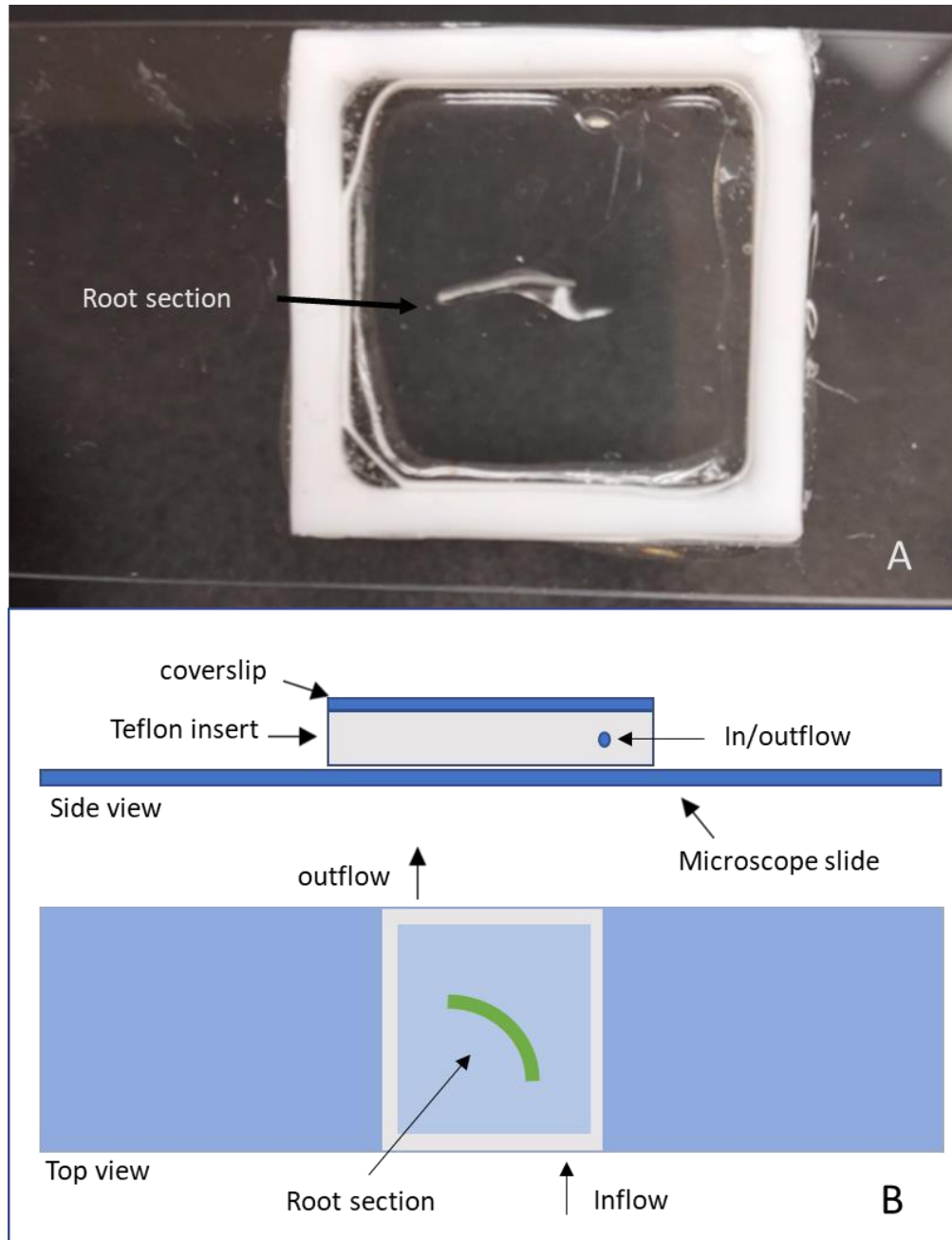


Figure 2.3.2-1 Diagram of flow chamber. **A.** The chamber consists of a square Teflon insert which sits between a microscope slide and coverslip, a root section is mounted to the coverslip on the inside of the chamber using nail polish. **B.** The buffer of the chamber can be replaced by aspirating old buffer through the In/outflow opening and reinjected with fresh buffer containing other metabolites. The total volume of the chamber is 500 μ l.

2.3.3 OABZ-GSNO KINETIC ASSAYS

Previous studies have identified OAbz-GSNO as a substrate for human GSNOR *in vitro* and mouse GSNOR *in vivo*, suggesting its potential as an indicator for GSNOR activity in living cells. *Solanum lycopersicum* GSNOR is homologous to mammalian GSNOR and retains conserved residues in its active site, indicating that OAbz-GSNO may act as an indicator for GSNOR activity in plants as well.

To determine whether OAbz-GSNO can also act as a fluorogenic pseudo-substrate for SIGSNOR, young *S. lycopersicum* roots were exposed to 1mM OAbz-GSNO and their fluorescence generation was compared to controls containing only MES buffer. In **Figure 2.3.3-1** control roots were demonstrated to exhibit a fluorescence decrease, corresponding to the autofluorescence of lignin, whereas the OAbz-GSNO containing roots exhibited a strong fluorescence increase, suggesting that the OAbz-GSNO probe has affinity to SIGSNOR. To further corroborate these results, subsequent inhibition experiments were performed to determine whether this fluorescence increase was a result of the interaction OAbz-GSNO with GSNOR.

Because previous studies have determined that the pseudo-substrate for GSNOR, OAbz-GSNO, has a lower affinity for GSNOR than its principal substrate GSNO, where GSNO has a K_M of 11 μ l in comparison to the K_M of 320 μ l for OAbz-GSNO *in vitro*, it was hypothesized that GSNO would outcompete OAbz-GSNO for catalysis. To ensure that this increase in fluorescence, in living tomato root tissue, was due to the interaction between OAbz-GSNO and GSNOR, it was assumed that in the presence of increasing concentrations of GSNO, GSNO would competitively inhibit the interaction between GSNOR and OAbz-GSNO. **Figure 2.3.3-2** depicts the reduction in initial rates of fluorescence generation in roots which were exposed to 1mM OAbz-GSNO as the concentration of GSNO was

increased. The general decrease in fluorescence generation indicates that the fluorescence increase visualized in **Figure 2.3.3-1**, was likely a result of the interaction between OAbz-GSNO and SIGSNOR in roots. The inhibition constant (K_i) can be estimated by the half-maximal rate of fluorescence increase to be at approximately 0.6mM GSNO. However, despite an overall decrease in fluorescent generation, when performing these experiments there was consistently an increase in fluorescence between the first two points at 0mM GSNO and 0.25mM GSNO. Previous studies have suggested that GSNO is capable of modifying GSNOR activity through a PTM at an allosteric site. If the PTM site is specific for GSNO and does not interact with OAbz-GSNO, this may describe the increase upon the addition of GSNO.

Additionally, the inhibitor N6022 has been shown to be highly specific for HmGSNOR. Previous studies have demonstrated that N6022 can also be used in plant studies to selectively inhibit plant GSNOR. The rates of GSNOR activity in roots containing the N6022 inhibitor in comparison to those in control conditions were measured using OAbz-GSNO in **Figure 2.3.3-3**. The roots preincubated with N6022 did not show fluorescence increase in the presence of OAbz-GSNO, indicating that it is inhibiting OAbz-GSNO reduction by GSNOR in the roots. There was however, a more significant fluorescence decrease in blank rates in roots pre-incubated with N6022. This is expected due to the nature of the N6022 inhibitor which promotes the accumulation of the co-factor NADH which acts as a fluorophore with a similar excitation/emission to OAbz-GSNO.

The above experiments suggest that OAbz-GSNO can be used to demonstrate GSNOR activity. Localization experiments were done to ascertain where within the root structures the increase in fluorescence was the highest, to determine where GSNOR activity may be localized (**Figure 2.3.3-4**). The rate of activity varies slightly across tissues; however,

this is contrasted with starkly varying autofluorescence decreases which are proposed to indicate locations with the highest lignin content. Because lignin absorbs in the same region as OAbz-GSNO excitation (300-400nm), it may be possible that there is some fluorescence quenching or shielding attenuating the fluorescent generation in the vascular tissue where GSNOR content is predicted to be highest and where lignin is also known to be highest, however, this interaction must be explored further.

The patterns of increased rate of fluorescence with the addition of the pseudo-substrate, OAbz-GSNO, along with a reduction of fluorescence generation when competitively inhibited by GSNO as well as inhibition by the known GSNOR inhibitor, N6022, was indicative of enzyme catalysis.

The trend of enzymatic activity was further demonstrated through Michaelis Menten kinetics depicted in **Figure 2.3.3-3**. When assessing rates of fluorescence increase over time in increasing concentrations of OAbz-GSNO (0.25mM, 0.375mM, 0.75mM, 1mM, 2mM, 4mM), the increase in the rate of substrate reduction was shown to model classical Michaelis Menten character. The Michaelis constant, K_M , was determined to be 0.46mM in the SIGSNOR *in vivo* model, which is consistent with the known K_M for HmGSNOR *in vitro*, of 0.32mM. In Michaelis Menten experiments the V_{max} of these studies was inconsistent, most likely caused by variations in enzyme content among roots.

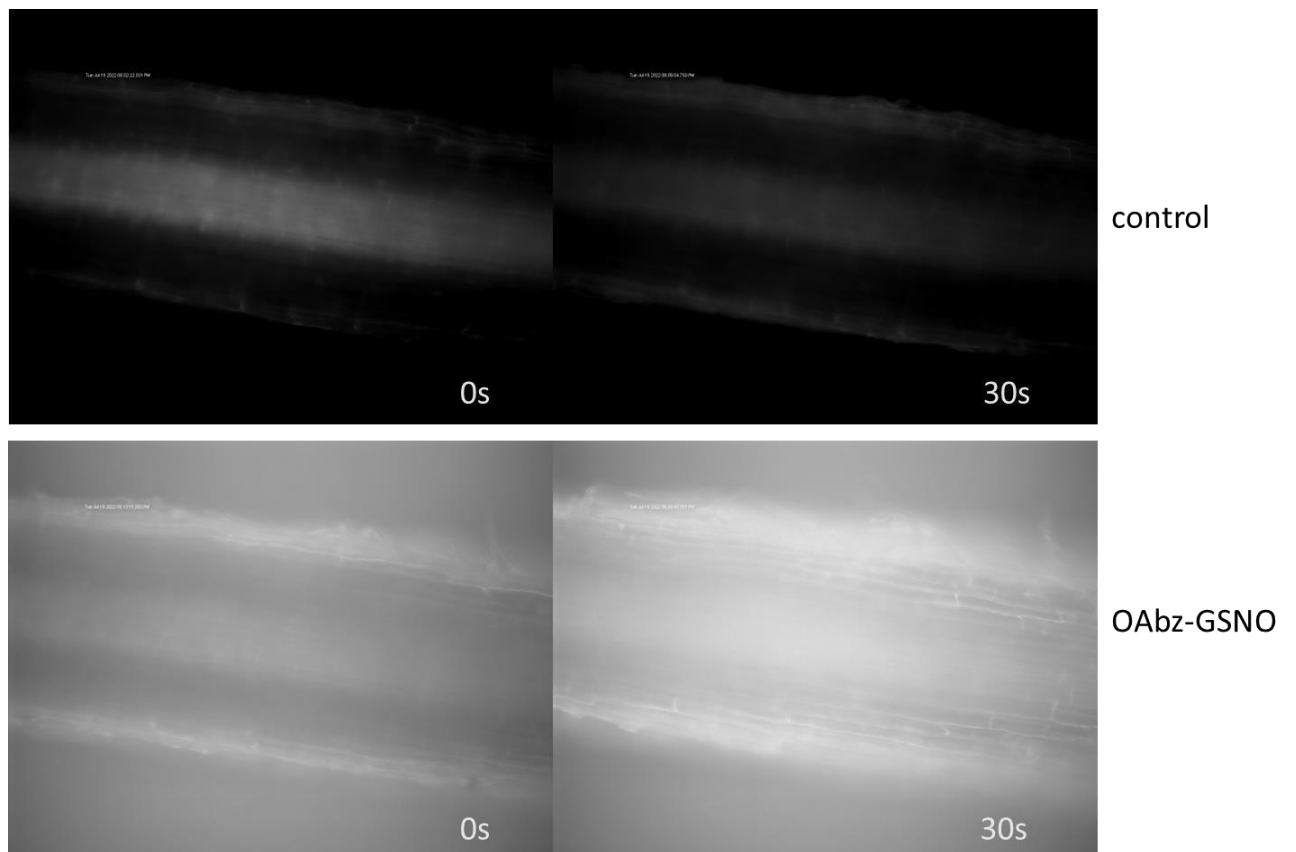


Figure 2.3.3-1 *S. lycopersicum* roots displaying fluorescence increase over time when exposed to OAbz-GSNO. Control roots were mounted in the flow chamber (**Figure 2.3.2-1**) in 10mM MES buffer pH 5.7 and images taken on an epifluorescence microscope at 0s and 30s at 200x magnification and 300ms exposure. OAbz-GSNO images were taken after controls on the same roots, where the MES buffer was removed and replaced with MES buffer containing 1mM OAbz-GSNO, and images taken in the same manner as in controls.

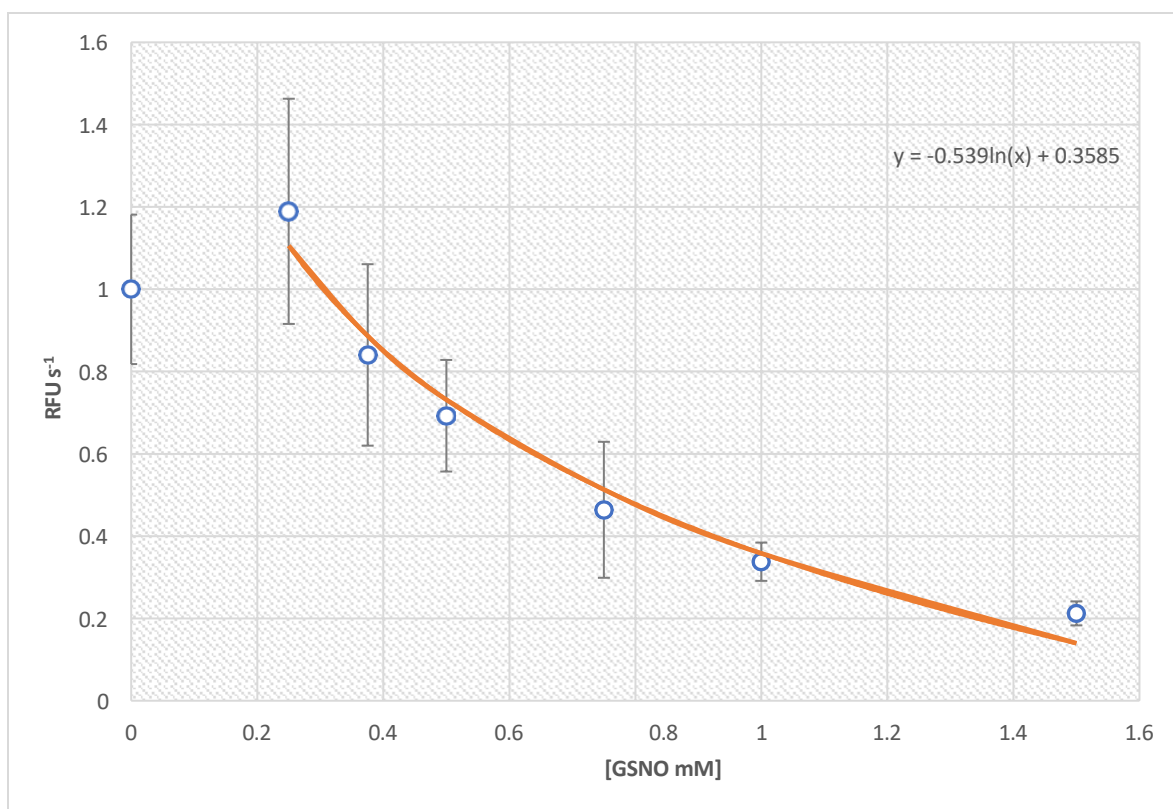


Figure 2.3.3-2 Competitive Inhibition of OAbz-GSNO as a function of [GSNO]. Initial rates were determined by exposing roots to 1mM OAbz-GSNO and increasing concentrations of GSNO, images were taken every 2 seconds and each image analyzed using ImageJ software (NIH and LOCI, University of Wisconsin) for total root grey scale value reported as relative fluorescence units (RFU). The initial rates, in RFU s⁻¹, were plotted against increasing concentrations of GSNO where a general fluorescence decrease was observed and, omitting the first point, fit to a negative logarithmic curve.

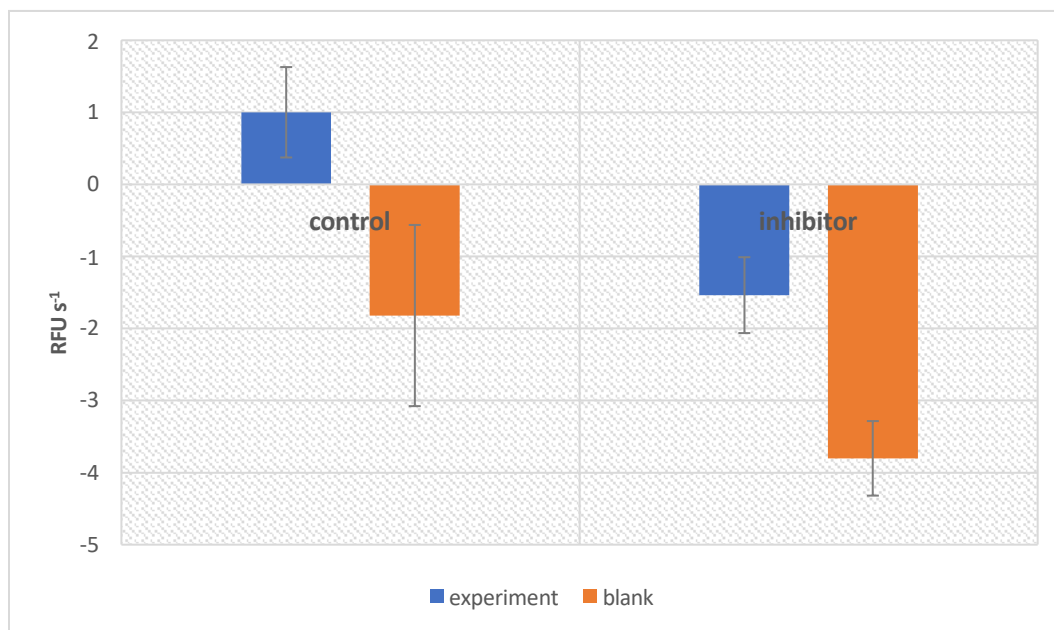


Figure 2.3.3-3 GSNOR activity reduction by N6022 Inhibitor. The initial rates were determined by incubating a root mounted in a flow chamber in a solution containing MES and 50 μ M N6022 (inhibitor) dissolved in DMSO, or MES buffer (control) for 5 minutes. Blank rates (orange) show a decrease in fluorescence. Roots were imaged using an inverted epifluorescence microscope at 300ms every 2 seconds for 30 seconds and each image analyzed for greyscale using ImageJ Software (NIH and LOCI, University of Wisconsin). Initial rates were determined by calculating the slope of the initial linear greyscale increase and reported in RFU s⁻¹ (relative fluorescent units per second). Experimental rates were taken on the same roots where the MES buffer or 50 μ M N6022 in MES were aspirated and replaced with MES containing 0.5mM OAbz-GSNO. The change in fluorescence was reported similarly as in blank rates.

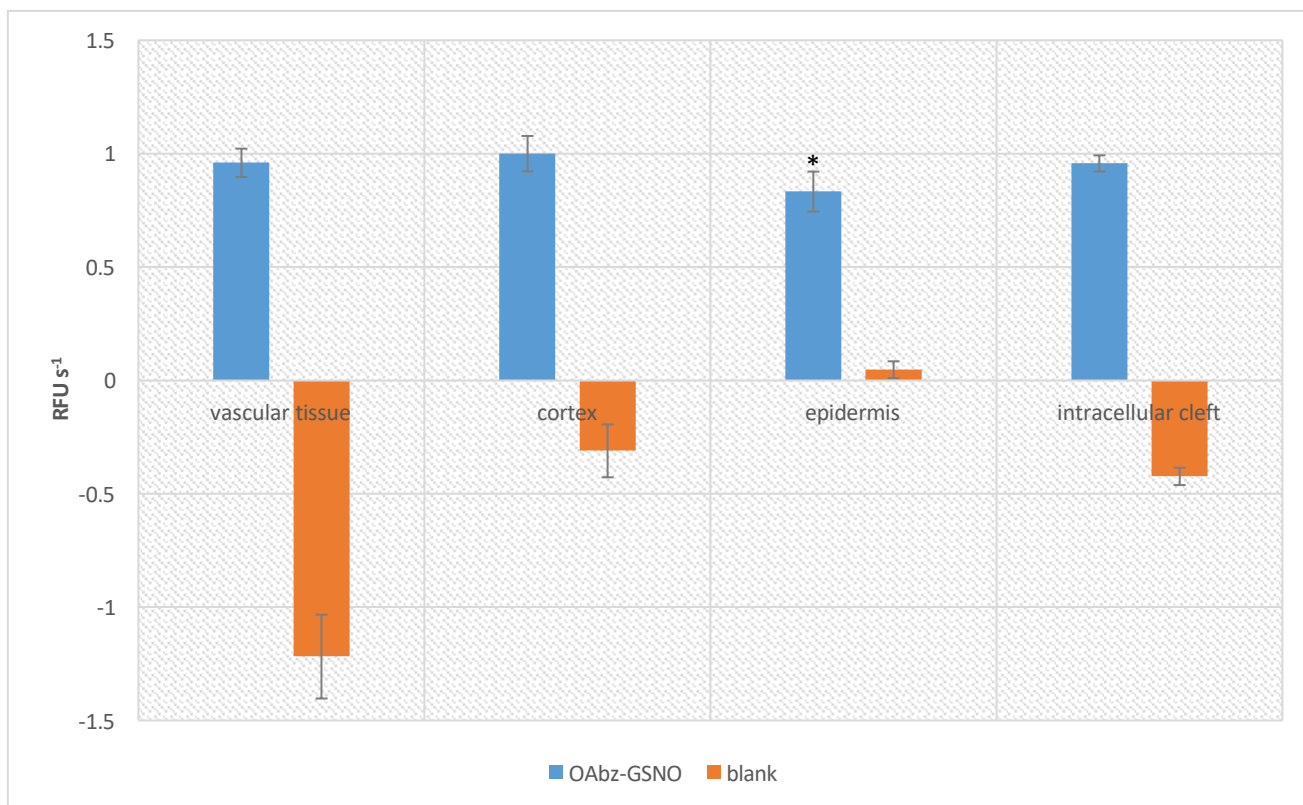


Figure 2.3.3-4 GSNOR activity localization assay. Initial rates of fluorescence increase in RFU s^{-1} were determined by mounting a root in a flow chamber and incubating roots in MES. Blank rates were determined by imaging roots every 2 seconds for 30 seconds on an inverted epifluorescence microscope. Subsequently the MES buffer was aspirated and replaced with MES buffer containing 1mM OAbz-GSNO and images taken in a similar manner. Images were analyzed using ImageJ software (NIH and LOCI, University of Wisconsin). Localization experiments were performed on the same image sets where locations were selected for measurement in correspondence with the vascular tissue, cortex cells, epidermis, and intracellular cleft where $n=3$.

* Statistical significance was determined using a students t-test where p value = 0.028267 and statistical significance is defined as $p < 0.05$

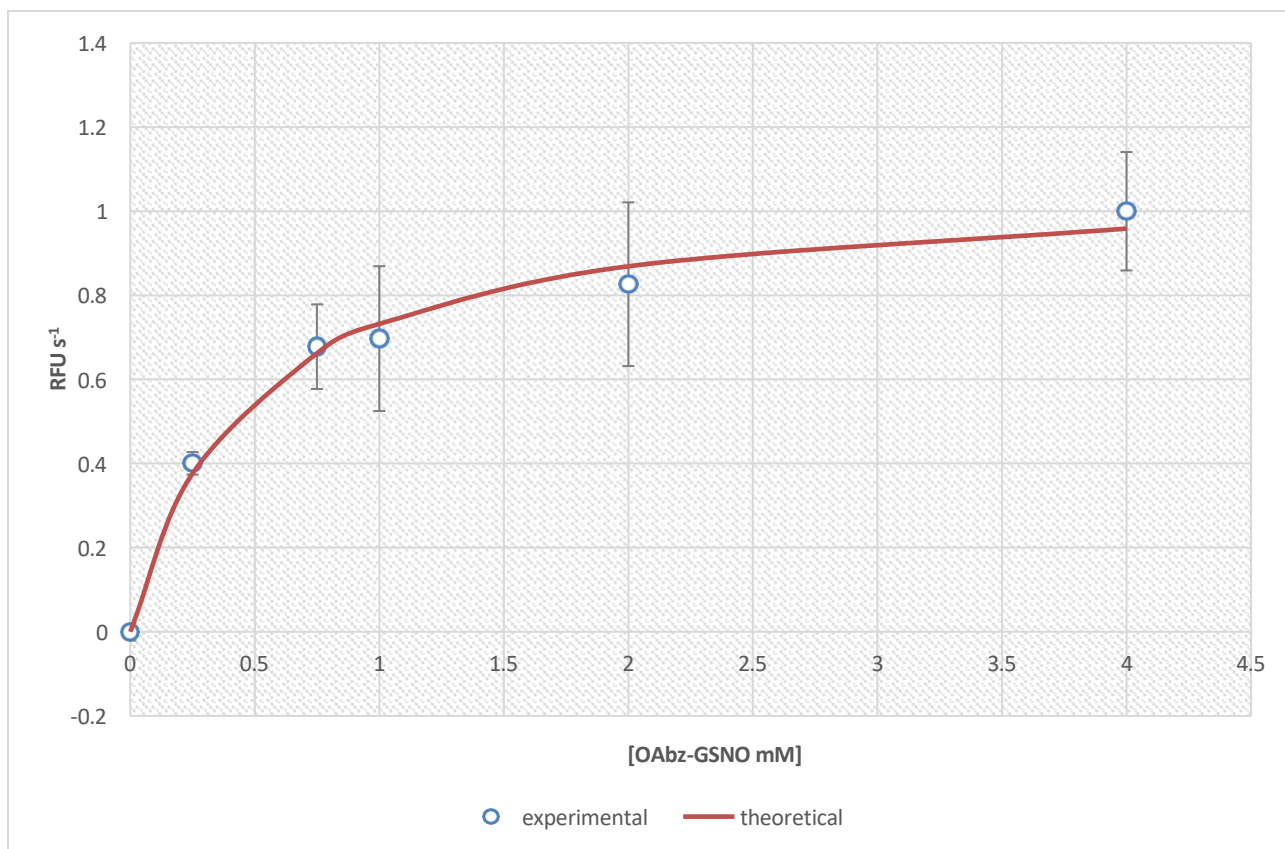


Figure 2.3.3-5 Initial rates of OAbz-GSNO reduction as a function of [OAbz-GSNO]. The tomato root was exposed to increasing concentrations of OAbz-GSNO (0.25mM to 4mM). The root images were collected every 2 seconds for 30 seconds and the initial rates of fluorescence increase, in the area of interest, were calculated from the image stack by using ImageJ software (NIH and LOCI, University of Wisconsin). The data was fitted to the Michaelis-Menten equation. The best fit line is shown by the red line. The error bars represent standard deviation n=3.

2.3.4 CHANGES IN ACTIVITY DUE TO AMMONIUM STRESS

Because GSNOR activity can be demonstrated using the fluorogenic properties of OAbz-GSNO and fluorescence microscopy, it was attempted to use these techniques to elucidate the changes in GSNOR activity under ammonium stress conditions.

Solanum lycopersicum seedlings were grown in MS media containing 10mM ammonium. In **Figure 2.3.4-1** there is observable growth suppression in seedlings grown in NH_4^+ in comparison to control conditions, this is consistent with previously reported effects of ammonium stress which also report growth suppression in apical root and shoot growth ⁹⁹. A western blot was performed to determine whether there was a difference in GSNOR expression between the control and NH_4^+ seedlings. Results in **Figure 2.3.4-2** and **Table 2.3.4-2** show that GSNOR content more than doubled when exposed to ammonium, in comparison to the concentration of the loading control APX3 which remains the same. These results are also consistent with previous reports which suggest that GSNOR activity increases in the presence of ammonium stress conditions ⁹⁹.

A similar increase in GSNOR activity was expected when roots grown in 10mM ammonium were exposed to OAbz-GSNO. The opposite effect was apparent as shown in **Figure 2.3.4-3**, where seedlings grown in ammonium conditions experienced higher GSNOR content but lower activity. These results suggest that GSNOR is inhibited. It is understandable that GSNOR could be inhibited under very high concentrations of NH_4^+ because NH_4^+ is a principal product of GSNOR catalyzed GSNO reduction. Because ammonium stress also causes the disruption in K^+ uptake in roots along with the uptake of cations necessary to growth, so NH_4^+ cannot be utilized in enhanced amino acid synthesis. NH_4^+ is associated with the upregulation of GSNOR transcription. Under normal conditions this could lead to enhanced growth, however under, cation disrupted conditions where

environmental ammonium is too high, GSNOR accumulates and must be inhibited to prevent the further accumulation of ammonium. GSNOR may be controlled by *S*-nitrosylation. Under ammonium stress conditions NO production is upregulated, so both GSNO and NO could be in high concentration. Previous studies have indicated that when GSNOR is exposed to NO donors, GSNOR can be *S*-nitrosylated leading to inhibition. Perhaps GSNOR can be inhibited under conditions where free NO is also high. However more experiments must be done to support this explanation.



Figure 2.3.4-1 The phenotypic changes in seedlings when grown in ammonium vs control conditions **A.** 14-day old *Solanum lycopersicum* seedlings grown in MS media pH 5.7. **B.** 14-day old *Solanum lycopersicum* seedlings grown in MS media containing 10mM ammonium chloride pH 5.7. Both sets of seedlings pictured were selected when cotyledons have just emerged. Ammonium treated seedlings appear slightly smaller than control seedlings with shorter apical root meristems, little lateral root formation, and shorter shoots. Typically, ammonium treated roots lag behind control roots in growth in early growth milestones.

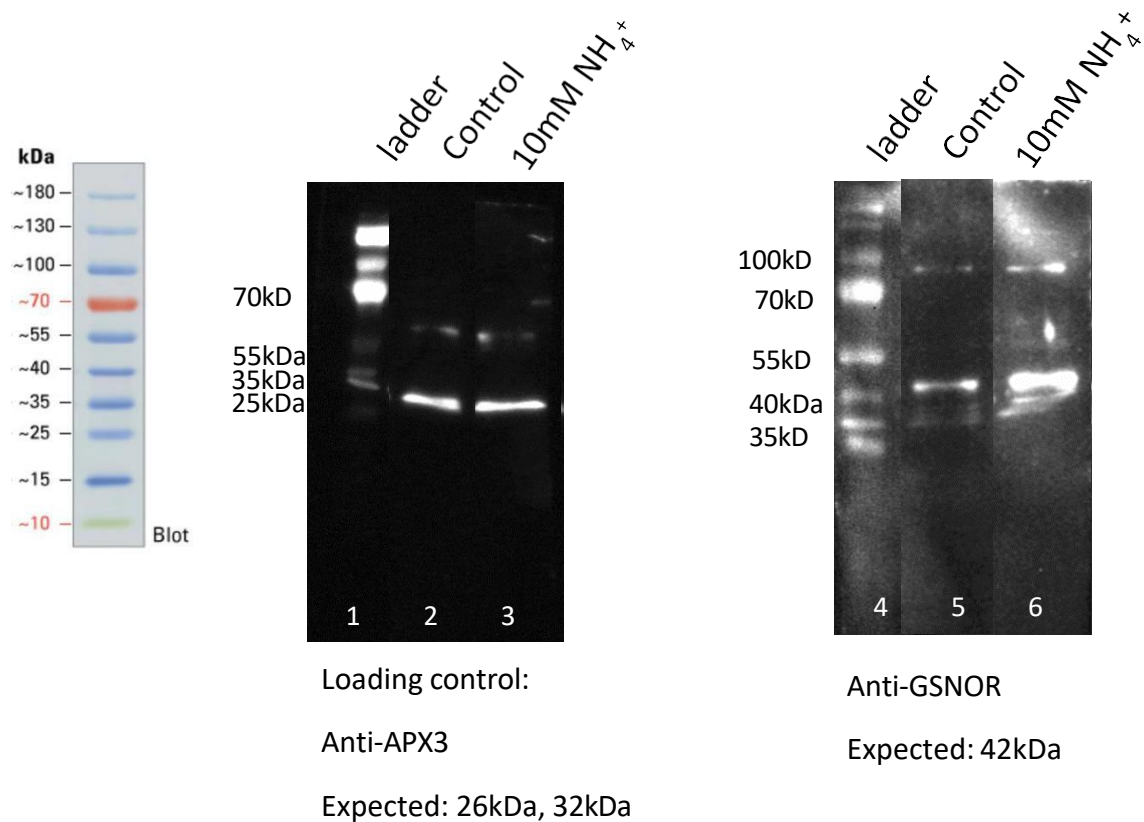


Figure 2.3.4-2 Western Blot to determine GSNOR content in ammonium vs control roots. Root extracts of 30-day old *S. lycopersicum* seedlings were diluted to 100 $\mu\text{g}/\text{ml}$. Wells 1 and 4 contain the protein ladder as depicted in the well to the left. Wells 2 and 5 contain control cell lysates and wells 3 and 6 contain NH_4^+ lysates.

Table 2.3.4-2 Western blot band intensities

	Control	NH_4^+
APX3	1	1.10
GSNOR	1	2.12

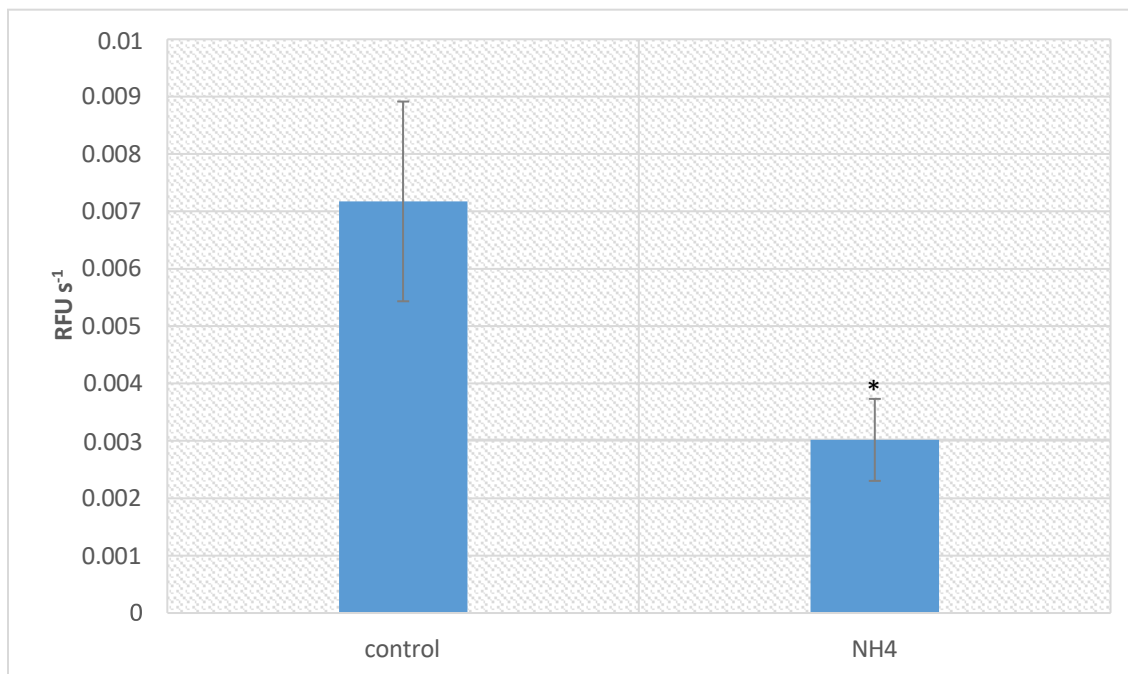


Figure 2.3.4-3 GSNOR activity in ammonium treated roots as determined by Oabz-GSNO reduction *in vivo*. Initial rates of fluorescence increase in RFU s⁻¹ were determined by mounting a root in a flow chamber and incubating roots in MES and taking a blank rate to ensure fluorescent decrease. Subsequently the MES buffer was aspirated and replaced with MES buffer containing 1mM Oabz-GSNO and images taken every 2 seconds for 30 seconds. Images were analyzed using ImageJ software (NIH and LOCI, University of Wisconsin). Error bars represent standard deviation where n=4.

* Statistical significance was determined using a students t-test where p value = 0.02531 and statistical significance is defined as $p < 0.05$

2.4 CONCLUSION

GSNOR is known as the master regulator of oxidative stress in plants, but little is known about its mechanism of control. Studies often employ the NADH assay on plant extracts to assess GSNOR activity under various growth conditions, however this method is limited because it cannot be done in native cellular conditions. In this project, OAbz-GSNO has been identified as a promising pseudo-substrate for the study of endogenous GSNOR activity in the living plant model. Additionally, the flow chamber was developed, which allows intact organs to be visualized using microscopy in a variety of conditions. Localization studies indicate that GSNOR activity may vary across structures. Moreover, NH_4^+ studies suggest that despite higher levels of GSNOR observed when plants are exposed to ammonium stress, GSNOR activity may decrease. This highlights a possibility of GSNOR control by post translational modification.

CHAPTER 3

**DEVELOPING A PHOTOREACTIVE AFFINITY LABEL FOR THE
CHARACTERIZATION OF S-NITROSOGLUTATHIONE
REDUCTASE**

3.1 INTRODUCTION

3.1.1 GSNOR ACTIVITY IS MODIFIED POST-TRANSLATIONALLY BY GSNO

Multiple sources indicate that GSNOR is mediated by the bioavailability of its principal substrate, GSNO^{40,63,70–72,109}. In addition to its active site, GSNOR is proposed to have a secondary allosteric site where GSNO may interact with the enzyme reversibly and elicit a conformational change leading to changes in activity⁷². Studies report that in the presence of highly nitrosative cellular conditions, and thus high concentrations of GSNO, GSNOR activity is downregulated^{40,109}. Because GSNO elicits its control on associated redox-active proteins through *S*-nitrosylation, it was proposed that GSNOR activity is mediated in a similar manner¹¹⁰. When exposed to NO donors *in vitro*, *Arabidopsis* GSNOR activity is inhibited and subsequently restored when exposed to a strong reducing agent, like DTT⁷¹. Additionally, when AtGSNOR was exposed to a NO donor it increased the K_M of GSNO indicating a NO interaction at an available thiol. Because GSNOR is cysteine rich, sequence analysis elucidated conserved cysteines, and molecular modeling indicated that there are conserved cysteine residues which are solvent accessible^{63,111,112}. It is suggested that GSNOR is controlled through a covalent S-NO interaction to an available cysteine residue. The site was further supported by a reduced inhibition of GSNOR activity in enzymes containing cysteine to alanine mutations in residues C10, C271, and C370 indicating that these residues may be targets for *S*-nitrosylation^{40,71}.

3.1.2 AN ALLOSTERIC SITE FOR GSNO MODIFICATION ON GSNOR WAS IDENTIFIED

Though many sources accept *S*-nitrosylation as the manner by which GSNO mediates GSNOR, a previous study in our group has identified an alternative binding site for GSNO (**Figure 3.1.2-1**)⁷². The site was identified initially by enzyme kinetics where a sigmoidal relationship was demonstrated when human GSNOR was subjected to increasing concentrations of GSNO *in vitro*. This relationship indicates the existence of an allosteric site capable of binding to GSNO when it is in abundance and upregulating GSNOR activity. The site was further identified using molecular modeling at Lys323, Gly321, Asn185, and Lys188 and site-directed mutagenesis at each of the lysine residues to alanine, where single and double mutants displayed a significant decrease in GSNO reduction compared to wtGSNOR.

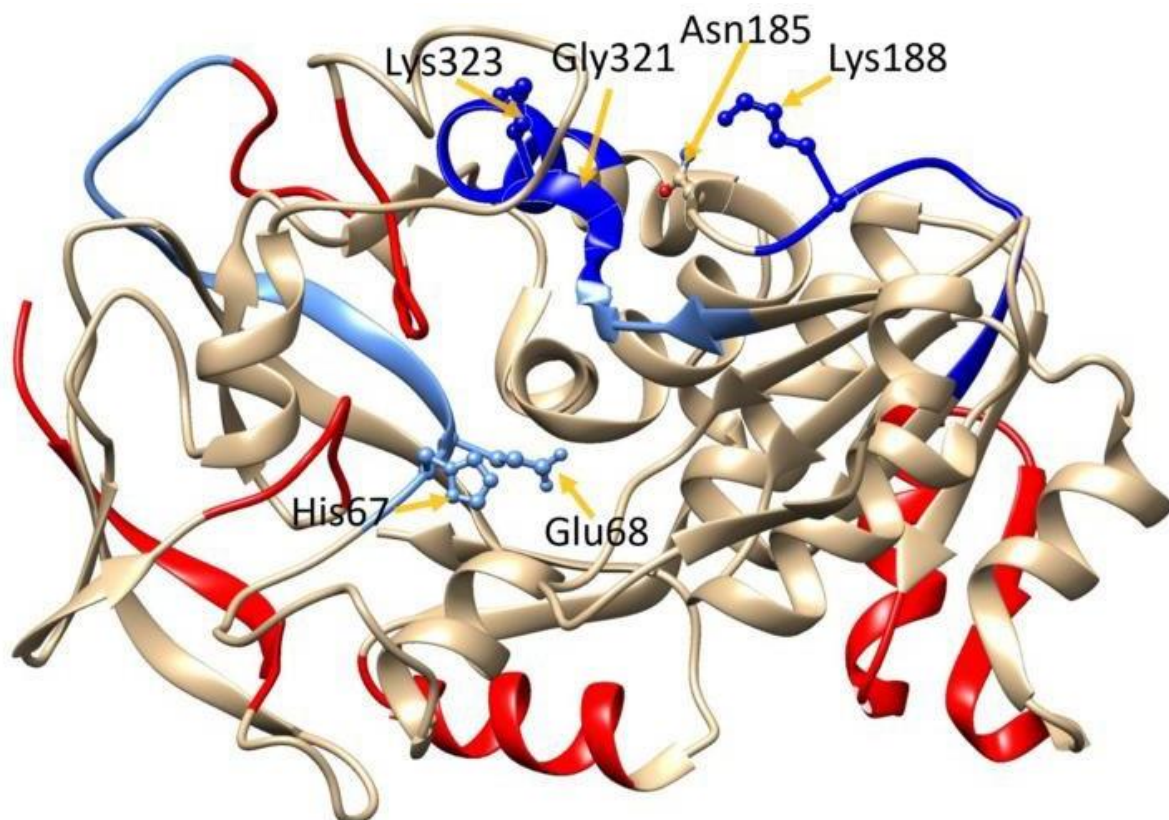


Figure 3.1.2-1 GSNO Binding Site on GSNOR at residues Lys323, Gly321, Asn185, Lys188 indicated by molecular modeling and supported using mass spectrometry ⁷²

Data from Antioxidants (Basel). 2019 Nov 13;8(11):545. doi: 10.3390/antiox8110545.

PMID: 31766125; PMCID: PMC6928738.

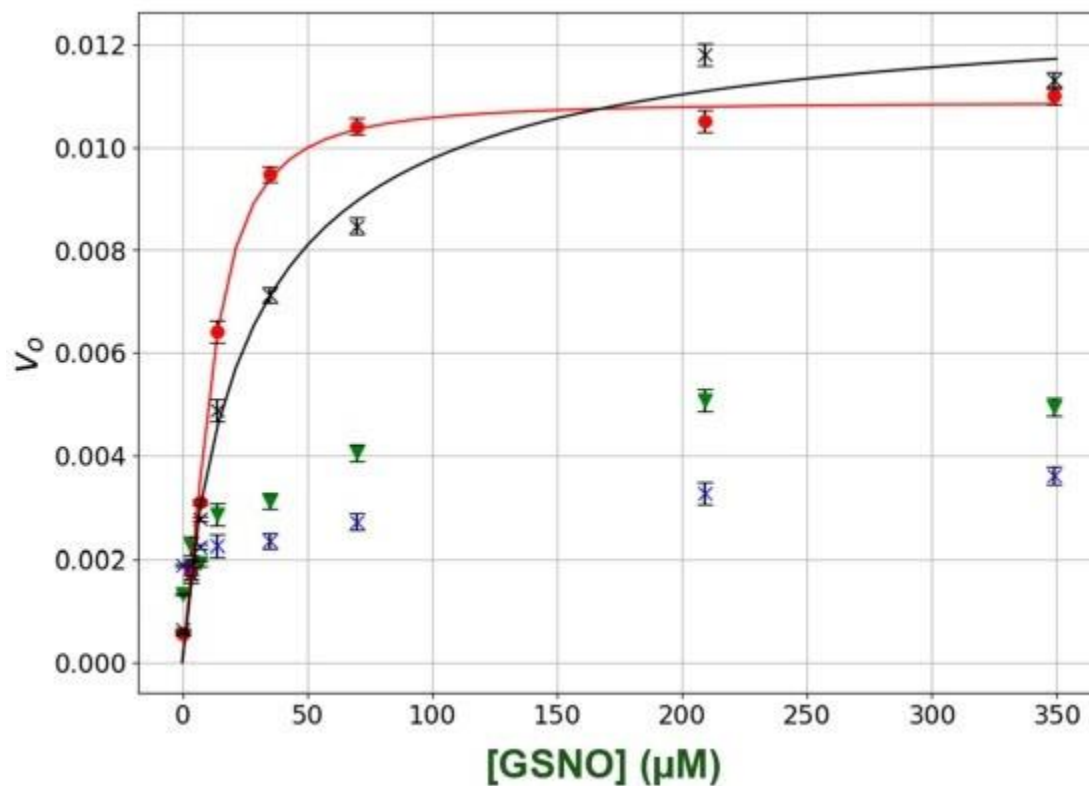


Figure 3.1.2-2 wtGSNOR activity vs mutants. Red indicates wtGSNOR activity, black is K188A mutant, blue is K323A mutant, and green is K188A/K323A double mutant.

Mutations on GSNOR at the proposed allosteric site show significantly decreased GSNOR activity, supporting its identification as an allosteric activation site. Figure reproduced with permission. Fontana K, Onukwue N, Sun BL, Lento C, Ventimiglia L, Nikoo S, Gauld JW, Wilson DJ, Mutus B. Evidence for an Allosteric *S*-Nitrosoglutathione Binding Site in *S*-Nitrosoglutathione Reductase (GSNOR).

Data from Antioxidants (Basel). 2019 Nov 13;8(11):545. doi: 10.3390/antiox8110545.

PMID: 31766125; PMCID: PMC6928738.

3.1.3 P-AZIDIOPHENACYL BROMIDE

p-azidophenacyl bromide (papaBr) is a photo-labile reagent which is capable of covalently binding to reactive thiol groups on macromolecules and enzymes ¹¹³. Because of its nature to interact mainly with thiols, in enzyme studies, papaBr will bind to reactive cysteine residues within active sites ¹¹⁴. papaBr reacts readily because it consists of a highly reactive bromo acetyl group by which it may perform a nucleophilic displacement with cysteine ¹¹⁵. In addition, papaBr is photo-reactive owing to its azide group. When irradiated at around 330nm the azide group on papaBr will form a carbene or nitrene, which is highly reactive and non-specific ¹¹⁶. Within an active site papaBr, which will have little effect on activity when non-irradiated, however, upon irradiation is capable of completely inhibiting enzyme activity through crosslinking ^{115,116}. Additional azide containing probes have been developed and utilized in a similar manner to papaBr, however due to their non-specific binding they label enzymes randomly rather than at the active site. papaBr is ‘bifunctional’ due to its reactive thiol specificity and photo lability ¹¹⁵.

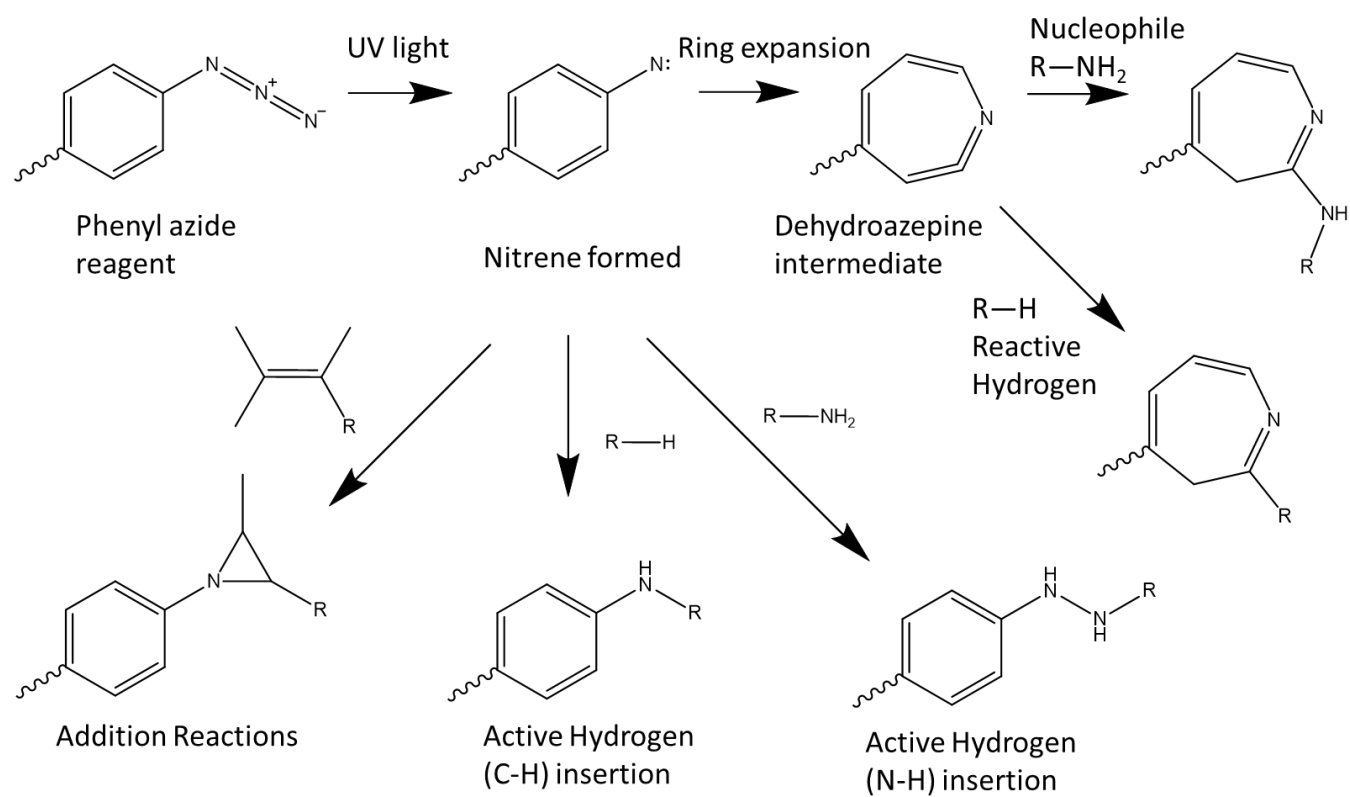


Figure 3.1.3-1 Possible structural changes in azide group in response to irradiation ¹¹⁷.

3.2 MATERIALS AND METHODS

3.2.1 Materials

p-azidophenacyl bromide (Toronto research chemical Inc.), reduced glutathione, Sodium Carbonate, G-25 sephadex, Tris-HCl, kanamycin, IPTG, NaCl, imidazole, DTT, PMSF, Triton X-100, DNase I, lysozyme, HIS-select nickel affinity column, glycerol, sodium phosphate dibasic, sodium phosphate monobasic, NADH, iodoacetamide, trypsin digestion buffer (promega), B+J H₂O (Thermo Fischer), formic acid, acetonitrile

3.2.2 Methods

3.2.3 papaGS synthesis and purification

28.8mg of *p*-azidophenacyl bromide was dissolved into 0.5ml of MeOH. 17.8mg of reduced glutathione was added to this mixture along with 5ml of additional MeOH 5ml of Carbonate buffer, pH 9. The mixture was allowed to mix in the dark at room temperature for 1hr. The insoluble salts were removed by centrifugation at 100 rpm for 5 minutes. 2ml of the clear and colourless supernatant was applied to a 1.5 meter long BioRad econo-column with a 1.5 centimeter diameter packed carefully with G-25 sephadex and equilibrated a pH 7.5 0.1M Tris buffer, and the components were allowed to separate through the column using size exclusion chromatography, in the dark. The outflow was monitored using a BioRad Biologic LP spectrometer, where the first peak, which appeared after about an hour, corresponded to the unreacted glutathione and the second peak, appearing shortly after the first corresponded to the *p*-azidophenacyl glutathione (papaGS) product. The product was then frozen and lyophilized until it was a powder then reconstituted with 1 ml of 20mM Tris buffer pH 8.5. Concentration was measured using UV/vis spectroscopy where extinction

coefficient is $\epsilon \approx 10200 \text{ M}^{-1} \text{ cm}^{-1}$ at an absorbance of 298nm. The product was stored at -20°C for up-to a year under strict dark conditions.

3.2.4 HmGSNOR expression and purification

HmGSNOR plasmids (pET28b_ADH5) were transformed into *E. coli* (BL21(DE3)) and inoculated into 2X YT medium containing 50µg/ml kanamycin by previous lab members and stored in 1ml aliquots at -80°C. An aliquot was transferred into a starter culture containing 100ml of 2x YT medium and 50µg/ml kanamycin which was incubated in 37°C shaker overnight. The starter culture was used to inoculate 1.5L of 2X YT medium containing 50µg/ml kanamycin which was incubated in 37°C shaker for 8 hrs. The expression of the GSNOR plasmid was induced at this point using IPTG at a final concentration of 0.4mM and allowed to express on a shaker at room temperature for 24 hours. The cells were separated by centrifugation at 6000 rpm for 30 minutes at 4°C and the supernatant discarded. The pellet was resuspended with a lysis buffer containing 50mM Tris-HCl pH 8, 150mM NaCl, 15mM imidazole, 1mM DTT, 1mM PMSF, 0.5% Triton X-100, 50µg/ml DNase I, 100µg/ml lysozyme. The lysate was incubated on ice for 30 minutes then sonicated in 20 second on/off cycles 8 times. The lysate was further centrifugated at 12000 rpm for 30 minutes at 4°C and the supernatant further purified using a HIS-select nickel affinity column.

Following manufactures guidelines, the nickel affinity column was equilibrated using a wash buffer containing 50mM Tris-HCl, and 150mM NaCl pH 8, then again with the same wash buffer containing 15mM imidazole. The supernatant was then applied to the column and washed with a wash buffer containing 40mM imidazole. HmGSNOR was eluted from the column using an elution buffer containing 50mM Tris-HCl, 150mM NaCl and 300mM imidazole at pH 8. The eluate was buffer exchanged using Amicon 30kDa centrifugal filters

into a storage buffer containing 58mM Na₂HPO₄, 17mM NaH₂PO₄, 68mM NaCl, and 15% glycerol and stored at -80°C.

3.2.5 Kinetic assays

Stock solutions of 20mM NADH and 20mM GSNO were prepared fresh using a 20mM Tris-HCl pH 8.5 buffer. The components 10µl NADH, and varying final concentrations of GSNO (0mM, 0.005mM, 0.01mM, 0.025mM, 0.05mM, 0.1mM, 0.25mM) were added to an absorbance cuvette containing 20mM Tris-HCl pH 8.5 buffer with 5µg of HmGSNOR added last to a final volume of 1ml. Activity was monitored using an Edinburgh Instruments DH5 UV/Vis spectrophotometer measuring the rate of NADH depletion at 320nm for 60 seconds at room temperature.

The above assay was also performed in papaGS-dark and papaGS-irradiated conditions. In papaGS-dark conditions the enzyme was mixed with papaGS to a final concentration of 25µM in the reaction mixture, and the assay was performed in the same manner as stated above. In the papaGS irradiated conditions the enzyme was mixed with papaGS to a final concentration of 25µM and that irradiated with an LED light source (365nm, Wilson Analytical, Edmonton AB) light for 5 minutes and a colour change from colourless to orange yellow was observed. The kinetic assays were performed in the same manner as previously stated in this section.

3.2.6 Mass Spectrometry

HmGSNOR proteins at a concentration of 0.5µg/µl were reduced with 10mM DTT (dithiothreitol) at room temperature for 45 minutes, then alkylated with IAM (iodoacetamide) to a final concentration of 20mM IAM in the dark for 1hr. The proteins were then digested in siliconized tubes with TGB (trypsin digestion buffer) to a final concentration of 5ng/µl and

left on a shaker at 37°C overnight. Samples were then transferred into new siliconized tubes along with 100µl B+J H₂O and the digestion quenched with 1% FA (formic acid) then boiled for 5 minutes and allowed to cool. Salts were removed from the samples using Waters Oasis columns. Columns were activated using 200µl ACN then equilibrated with 3 washes of 100µl 0.15% FA, and 1 wash of 100µl 0.15% FA, 1% ACN. Sample volumes were reduced to approximately 50µl using a speed vacuum and resuspended in 150µl 0.15% FA then added to the Oasis columns. Once the sample ran through the column it was washed 3 times with 100µl 0.15% FA. Peptides were eluted off the column in a stepwise manner into new siliconized tubes with 100µl of 20% ACN in 0.12% FA, then 100µl of 50% ACN in 0.075% FA, then twice with 80% ACN in 0.03% FA. The resulting peptides were dried with a speed vacuum and reconstituted in 20µl of 0.1% FA and stored at -20°C. Mass spectrometry was performed and analyzed by Dr. Otis Vacratsis, University of Windsor, and by Simon Plaize, Université Laval.

3.3 RESULTS AND DISCUSSION

3.3.1 THE DEVELOPMENT OF PAPAGS

Previous studies in our lab group have identified an allosteric GSNO binding site on human GSNOR ⁷². This site is responsible for enzyme activation, and unlike previous studies have suggested, the interaction is not elicited through *S*-nitrosylation. To further characterize mechanisms of GSNOR control by GSNO, a novel reagent was developed which was capable of interacting with the enzyme in a similar manner to GSNO. Because GSH is a precursor to GSNO, it is thought to interact with the allosteric or catalytic site on its own. Additionally, GSH contains a reactive thiol, which is capable of reacting with a photo-labile label like papaBr. When reacted together to form papaGS (*p*-azidophenacyl glutathione, **Figure 3.3.1-1**) the probe was hypothesized be capable of interacting with either the catalytic site or the allosteric site, due to structural similarities between GSH and GSNO, and once proximity to this site was established, irradiation was expected to cause the enzyme activity to change in response to highly reactive nitrene or carbene formation, and subsequently, non-specific crosslinking at this site.

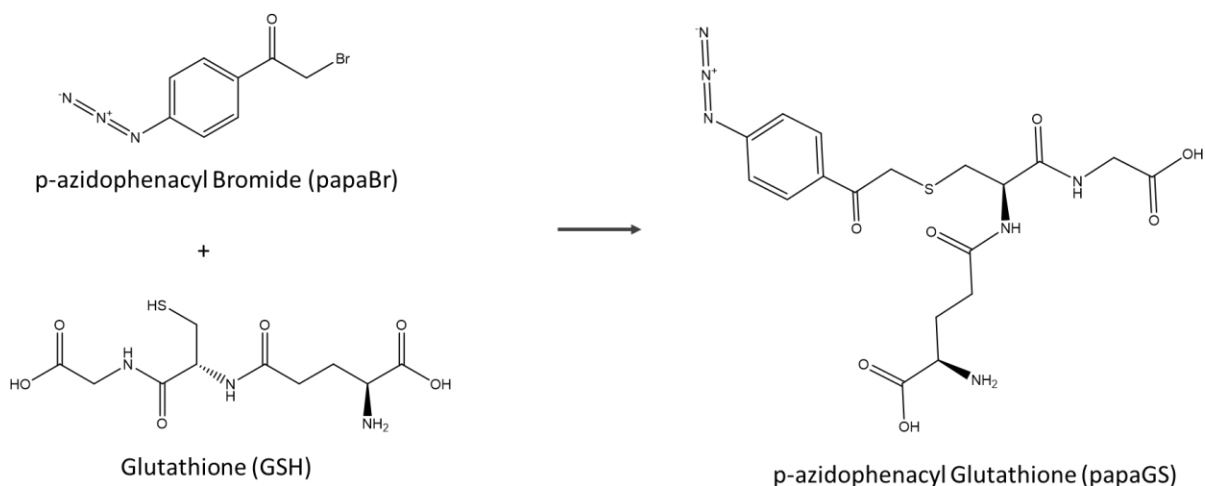


Figure 3.3.1-1 The proposed structure of photo-labile papaGS (*p*-azidophenacyl glutathione) when formed from Glutathione (GSH) and papaBr (*p*-azidophenacyl bromide).

3.3.2 EVIDENCE OF SUCCESSFUL PAPAGS SYNTHESIS AND ACTIVITY

The protocol for papaGS synthesis was developed by Dr. Bulent Mutus and described in section 3.2 of this document. Upon papaGS synthesis and purification, papaGS which was a clear and colourless solution, was subjected to irradiation at 365nm to determine whether the compound was photo sensitive. **Figure 3.3.2-1** shows that there was a very apparent colour change between the non-irradiated and irradiated papaGS, indicative of a structural change. To determine whether the observed structural change would have an effect on GSNOR, papaGS was interacted with GSNOR in dark vs irradiated conditions. The resulting GSNOR activity was determined using an NADH assay shown in **Figure 3.3.2-2**. It did not appear that GSNOR activity was affected by exposure to papaGS under dark conditions however exposure to irradiated papaGS significantly reduced GSNOR activity. This suggests that papaGS may interact with the allosteric site, where irradiation causes an inhibitory effect on GSNOR, similar to the K323A point mutation described in section 3.1.2.

To determine whether papaGS may be capable of causing a change to activity depending on concentration, GSNOR activity was determined while exposing the enzyme to increasing concentrations of papaGS in **Figure 3.3.2-3**, where it was found that there is no significant change in the activity of GSNOR when exposed to high concentrations of non-irradiated papaGS. These are similar findings to the reported activity of azide containing photo-labile reagents which are shown to only cause major changes to enzyme activity when exposed to light.

Finally, the structure of papaGS shown in **Figure 3.3.2-5** was verified by Mass spectrometry performed by Dr. Otis Vacratsis, shown in **Figure 3.3.2-4**. The calculated mass of papaGS is 466 Da, which is observed at 467 Da when ionized by ESI. An additional peak was observed at 441 Da which may result from the structural change of papaGS when irradiated. The proposed structural change upon irradiation is a ring expansion as suggested in **Figure 3.1.3-1** where possible structural changes are indicated. The molecular weights of the other possible structures were calculated and are indicated in **Appendix C**. The proposed structure has a molecular weight of 440 Da, which may be observed at 441 Da when ionized.

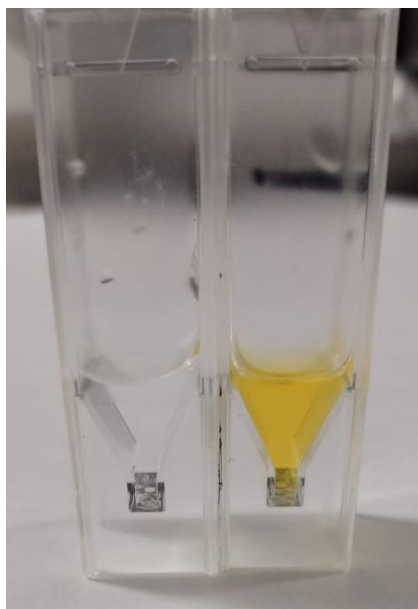


Figure 3.3.2-1 papaGS light-sensitivity indicated by a colour change. Left, clear and colourless papaGS stored in dark conditions. Right, papaGS exhibiting an orange-yellow colour change after direct exposure to 365nm light for 5 minutes.

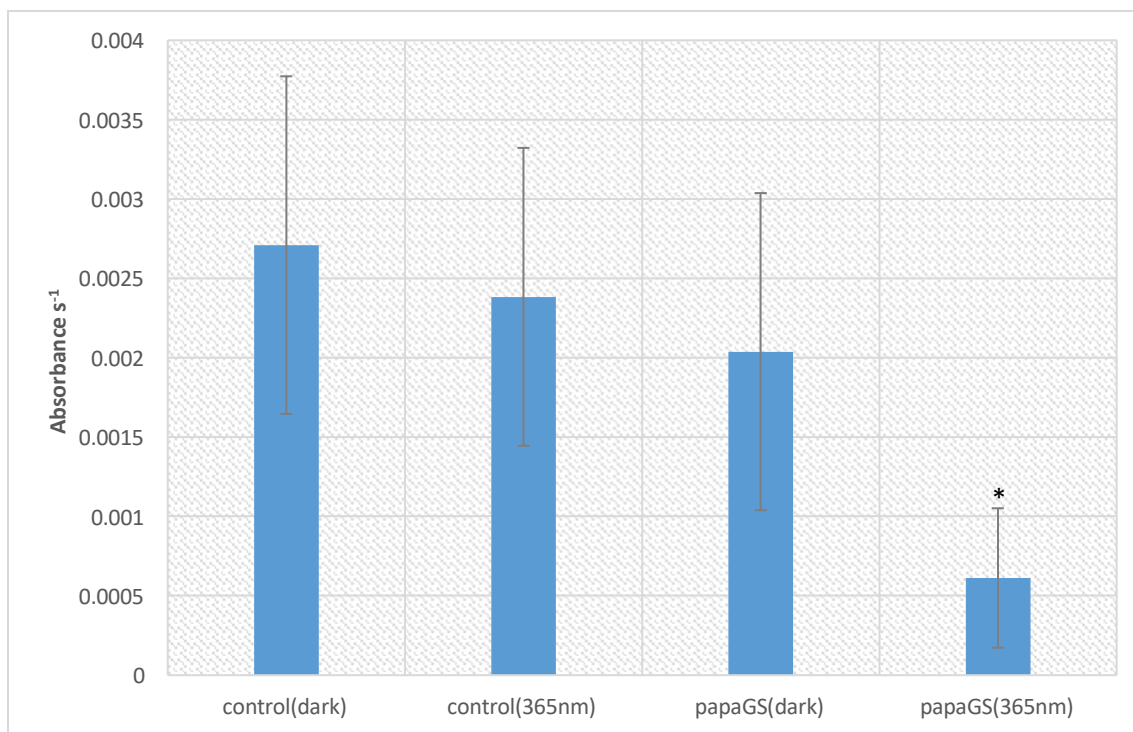


Figure 3.3.2-2 GSNOR kinetic activity when exposed to papaGS in light and dark conditions vs control. Control indicates samples which contain GSNOR in a pH 8 phosphate buffer with no papaGS and those which at label papaGS, contain 100 μ M papaGS. Dark experiments were performed in low light conditions and in the irradiation experiments, the samples were irradiated for 5 minutes with 365nm light. Kinetics of GSNOR was determined using the NADH assay to measure NADH depletion using absorbance at 340nm and the inverse rates ($V_{o, \text{plotted}} = v_o \cdot X_{-1}$) where plotted Error bars represent (n=3).

* Statistical significance was determined using a students t-test where p value = 0.013494 and statistical significance is defined as $p < 0.05$

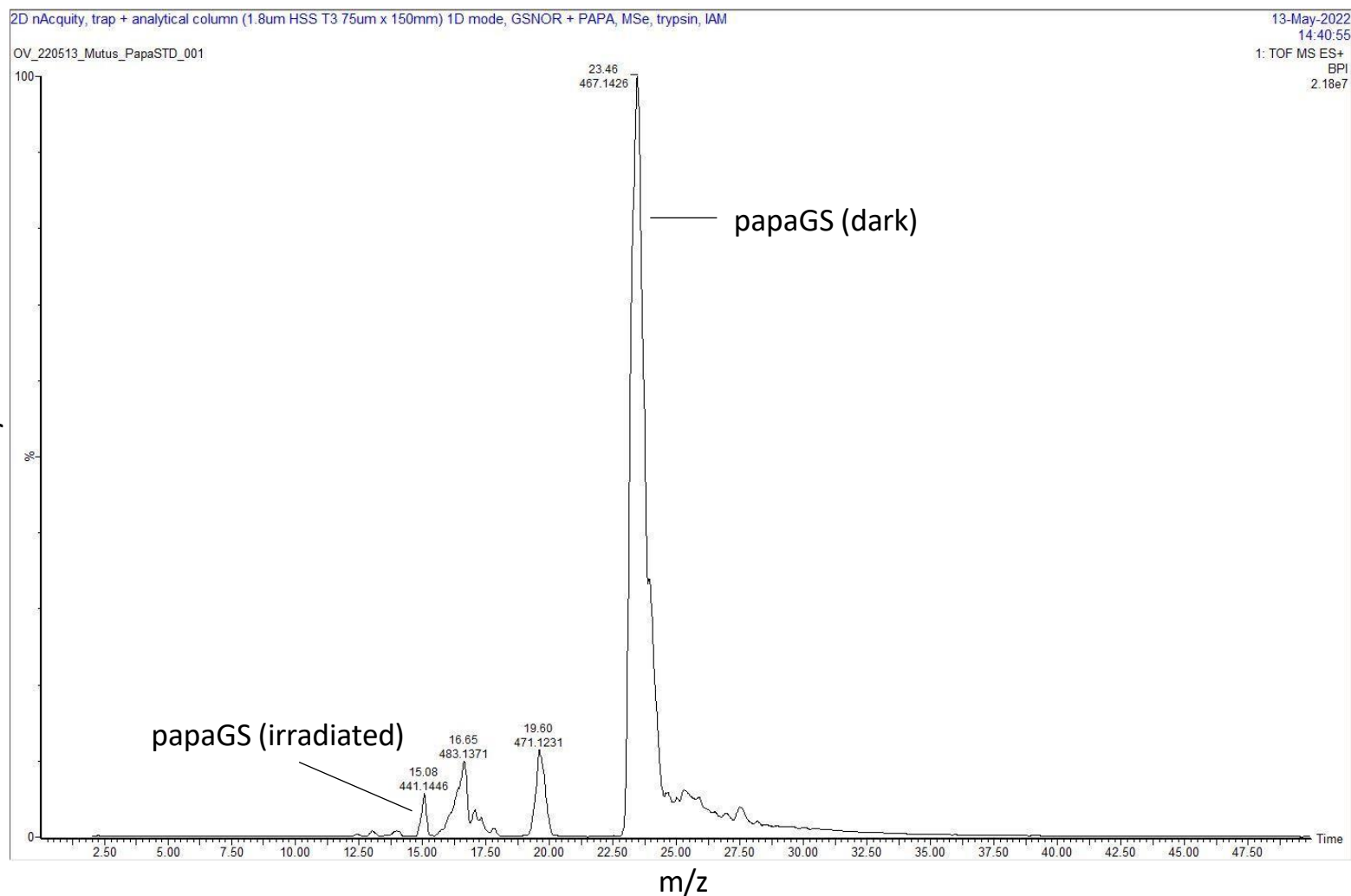


Figure 3.3.2-4 Mass spectral analysis of papaGS. Mass Spectrometry was performed using electrospray ionization (ESI) and Time of Flight (TOF) MS on papaGS exposed to 365nm for 5 minutes verifying both the molecular weight of 466 Da unexposed papaGS and providing insight to the molecular weight of the structural change when exposed to 365nm light.

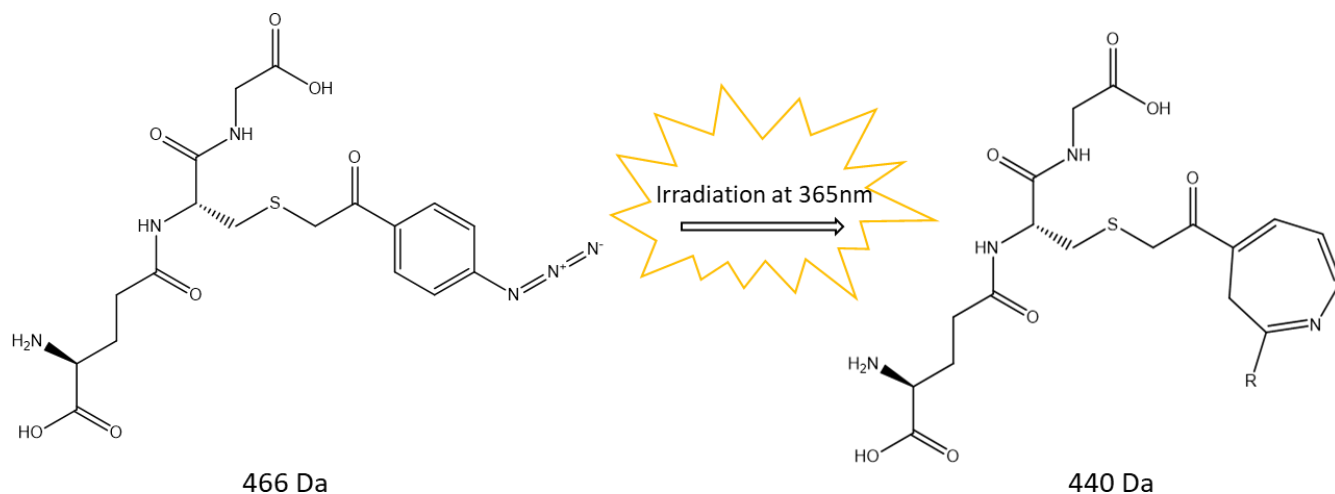


Figure 3.3.2-5 Proposed structural changes based on Mass Spectral analysis of irradiated papaGS.

3.3.3 EVIDENCE OF PAPAGS BINDING TO THE ALLOSTERIC SITE

Because it is proposed that papaGS can bind to the same allosteric activation site as GSNO, which was determined in earlier studies, kinetic assays were done similarly to those done previously with GSNO to determine their fit (**Figure 3.3.3-1**). All three conditions can be modeled using Michaelis-Menten enzyme kinetics with increasing concentrations of GSNO ranging from 0.005mM to 0.25mM. There is no significant difference in Michaelis-Menten kinetic parameters, K_M and V_{max} for GSNOR only and non-irradiated papaGS experiments. However, there is a significant reduction in GSNOR activity when exposed to irradiated papaGS, where there is a significant decrease in both V_{max} and K_M (**Table 3.3.3-1**). A reduction in K_M indicates enhanced enzyme-substrate interaction at the active site. This may be evidence in favour of allosteric binding due to a change in conformation of the active site to increase its affinity for GSNO, however a low V_{max} also indicates a reduction in

catalysis. Because the irradiation of azide containing affinity labels usually leads to non-specific crosslinking, if papaGS was interacting with an allosteric site it would be expected to disable the active site upon irradiation. Therefore, this reduction in catalysis is indicative of papaGS interaction with an allosteric site.

It has been shown previously that normal GSNOR kinetics follows sigmoidal behaviour modeled by cooperativity binding in the Hill–Langmuir relationship (**Equation 3.3.3-1**). As the concentration of GSNO increases, GSNO interacts with an allosteric site leading to an increase in enzyme activity, described as positive cooperativity. The plots in **Figure 3.3.3-1** were analyzed for their cooperativity in **Figure 3.3.3-2**. Cooperativity is represented by the Hill coefficient n , when n is higher than 1 there is positive cooperativity and when it is below 1 there is negative cooperativity. In both conditions, control and papaGS indicate positive cooperativity binding, however, when exposed to papaGS the Hill constant decreases, indicating diminished cooperativity. This loss in cooperativity in the presence of papaGS may indicate that papaGS can disrupt GSNO interaction at the allosteric site of GSNOR.

$$v_o = \frac{v_{max}[S]^n}{k_D^n + [S]^n}$$

Equation 3.3.3-1 The Hill-Langmuir relationship

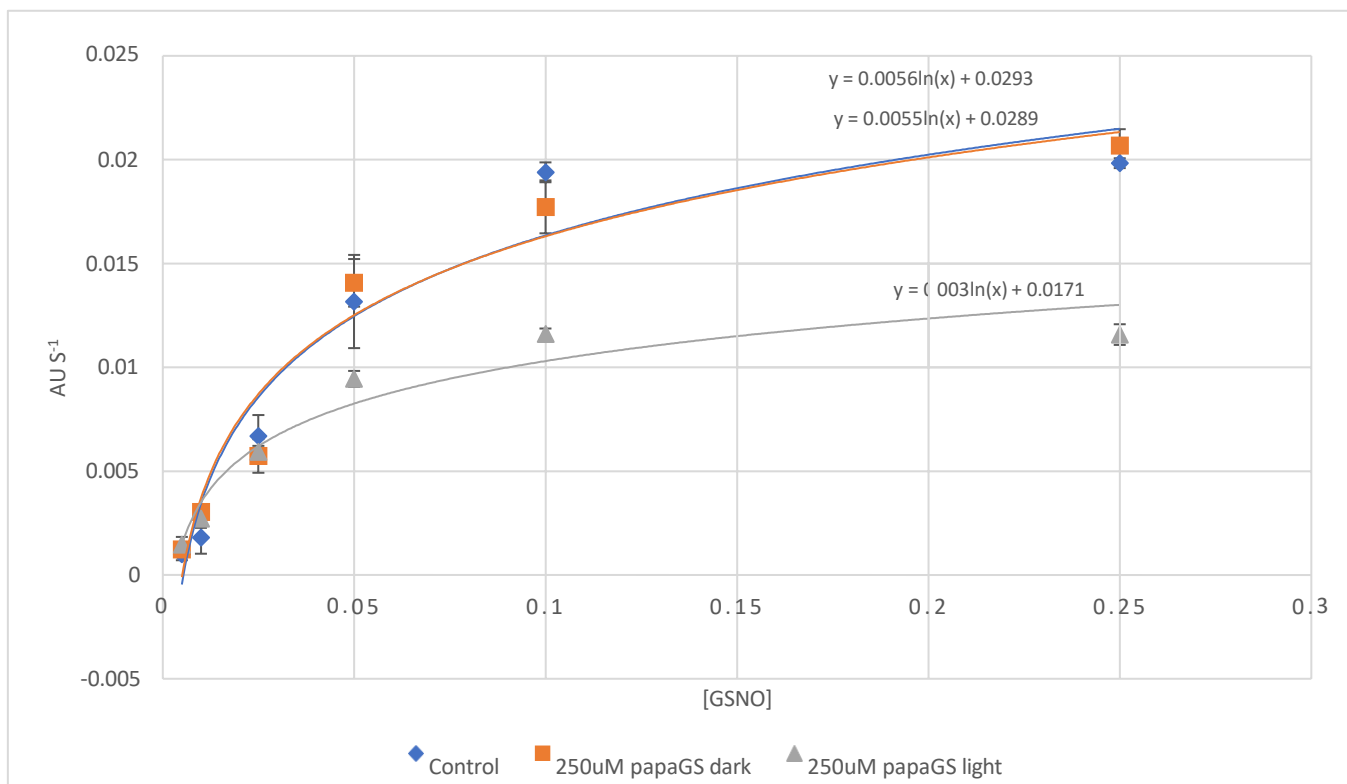


Figure 3.3.3-1 Michaelis-Menten GSNOR kinetics in samples containing papaGS. Initial rates were determined using the NADH assay to measure NADH depletion using absorbance at 340nm and the inverse rates ($v_{o, \text{plotted}} = v_o \cdot x^{-1}$) were plotted for samples of varying GSNO concentrations (0mM to 0.25mM). Control (blue) contain no papaGS, where orange contains 250μM papaGS which was done in dark conditions and grey contains 250μM papaGS which has been irradiated when combined with GSNOR. Where plotted Error bars represent (n=3).

Table 3.3.3-1 Michaelis-Menten parameters from **Figure 3.3.3-1**

experiment	kM μM	vmax AU s ⁻¹
Control	58.58739	0.02653356
250μM papaGS dark	55.89169	0.026236311
250μM papaGS light	24.21357	0.013350088

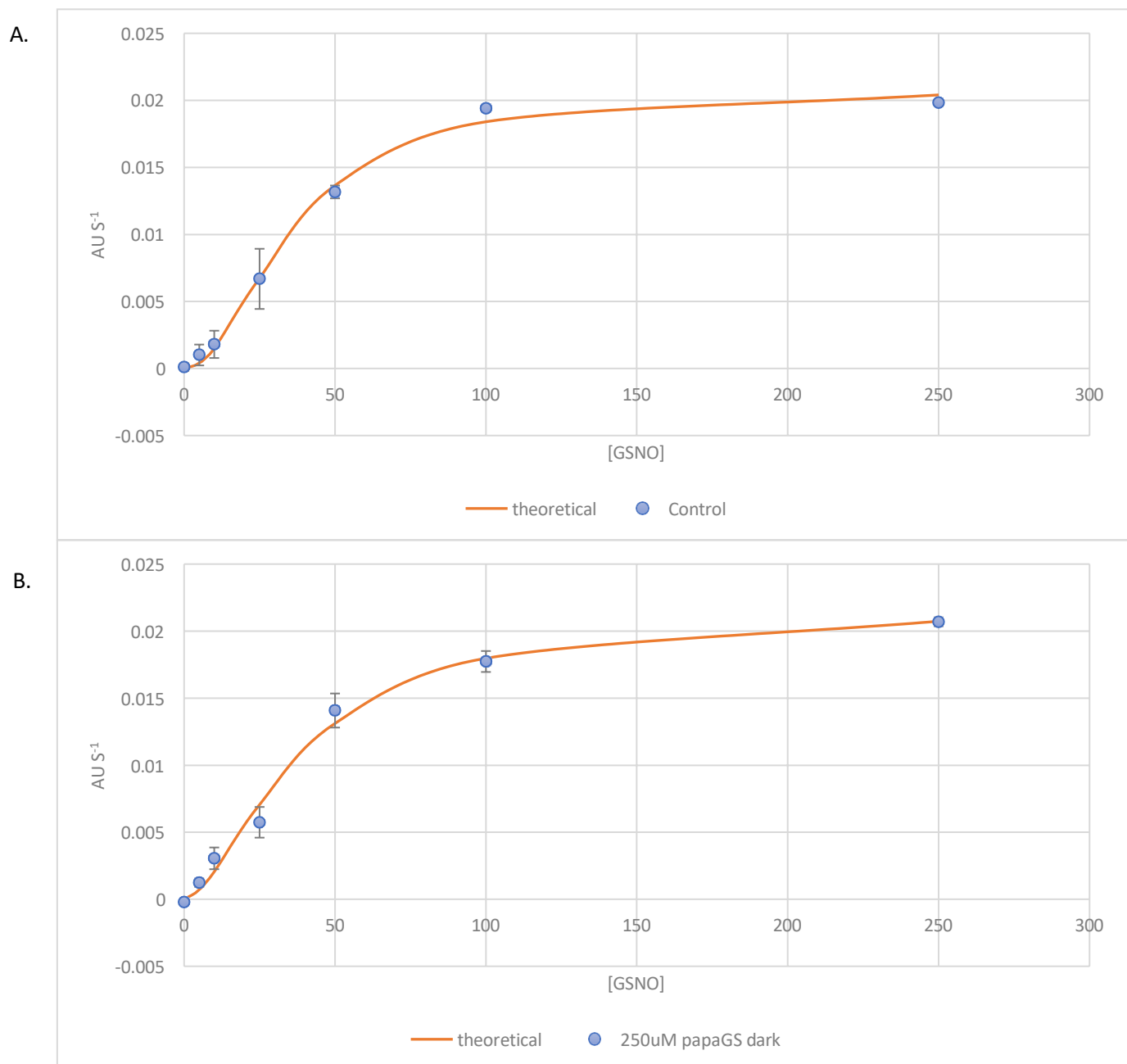


Figure 3.3.3-2 Cooperativity binding indicating possible allosteric binding site. The data collected from **Figure 3.3.3-1** was fit to the Hill-Langmuir relationship (**Equation 3.3.3-1**). A. indicates the fit to control conditions and B. indicates papaGS 250 μ M in dark conditions.

Table 3.3.3-2 Hill-Langmuir parameters from **Figure 3.3.3-2**

experiment	K_D μM	v_{max} AU s^{-1}	Hill coefficient n
Control	37.28995	0.02039	2.272618
250uM papaGS dark	38.66555	0.02166	1.667593

3.3.4 MASS SPECTROMETRY TO DETERMINE PAPAGS BINDING SITE

In order to determine whether papaGS was interacting with the allosteric site at residues Lys323, Gly321, Asn185, and Lys188, mass spectrometry was performed on trypsin digested HmGSNOR which was incubated with papaGS, papaGS combined with GSNO, and under control conditions. The peaks generated under control conditions were compared to those which contained irradiated papaGS. **Appendix B** indicates possible molecular weights of peptide fragments. PapaGS was expected to interact with the peptide fragments at 1897 +441 Da and 823 +441 Da, however there were no observed peaks in these ranges. A peak was present at m/z 1391 in the sample containing papaGS which was not present in the control (**Figure 3.3.4-1**). This is closest in molecular weight to the 956 Da peptide fragment combined with irradiated papaGS (441 Da). When irradiated papaGS exhibits non-specific crosslinking, so it may interact with a nearby peptide. Additionally, a large amount of papaGS was found to fall off the peptides either during purification or during ESI, additional MS studies should be done using a softer ionization method. As a result, the only piece of evidence indicating that papaGS is acting at the allosteric site is the kinetic results showing the decrease in the allosteric behaviour of GSNOR in the presence of papaGS.

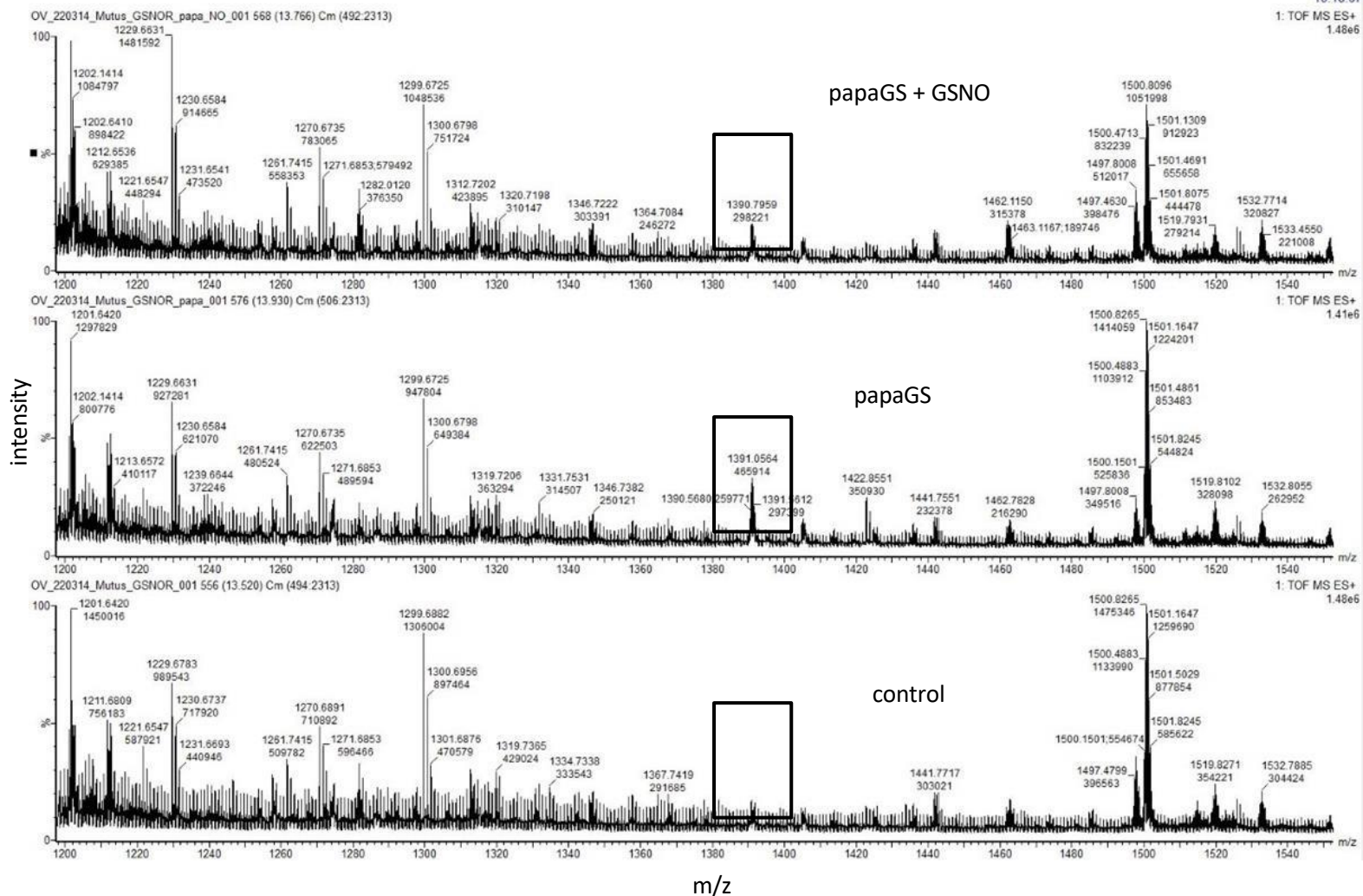


Figure 3.3.4-1 Mass analysis of trypsin digested GSNOR with papaGS. Mass Spectrometry was performed by Dr. Otis Vacratsis on a Waters Synapt G2 Mass spectrometer of GSNOR containing irradiated papaGS, papaGS and GSNO and under control conditions. Peptide fragments were separated using UPLC, then ionized using ESI, the MS/MS was a quadrupole combined with a TOF mass analyzer. Peak at m/z 1391 is absent in controls.

3.4 CONCLUSION

Previous studies have highlighted the importance of elucidating how GSNOR can be controlled by its environment. Though some studies indicate that GSNO may inhibit GSNOR at an *S*-nitrosylation site, in our lab we have shown that GSNOR activity is upregulated as the concentration of GSNO increases. This was demonstrated using enzyme kinetic assays modeled to the Hill-Langmuir cooperativity equation. A photo-reactive affinity label, papaGS, is structurally similar to GSNO and contains a reactive azide group which undergoes non-specific binding when irradiated. In dark conditions the affinity label was shown to augment normal cooperativity binding by GSNO, suggesting that it interacts with the allosteric site. Upon irradiation, papaGS reduces the activity of GSNOR by 50% suggesting that it was interacting with the GSNO binding allosteric site. Additionally, MS analysis highlights a peak at 1391 m/z when exposed to papaGS which must be further analyzed.

CHAPTER 4: GENERAL CONCLUSION

Plants are incredibly adaptable to their changing environments and have developed highly attuned stress response mechanisms to mitigate the, often extreme, changes in their environments. Studying how plants respond to stress conditions is of emerging importance as the environmental conditions of the planet shift. All stress conditions result in some kind of ROS/RNS generation which leads to downstream events, leading to observable changes in plant growth. At the center of stress response is the redox enzyme and master regulator of oxidative stress, GSNOR. GSNOR metabolizes GSNO, a LMM NO transporter which is capable of spontaneously *S*-nitrosylating reactive thiols on proteins, a PTM which is capable of controlling activity. Therefore, GSNOR is a pleiotropic enzyme, and its activity leads to a variety of downstream events. There is particular interest in determining how GSNOR changes in activity in various stress conditions, to further elucidate mechanisms of GSNOR control. In chapter 2 a previously designed pseudo-substrate, OAbz-GSNO, was applied to the study of GSNOR activity in *Solanum lycopersicum* roots. Exogenously applied OAbz-GSNO on roots grown in ammonium stress conditions indicated that GSNOR activity reduces in response to high ammonium exposure. GSNOR content is reported to increase in concentration in ammonium stress conditions, so the loss in activity under these conditions highlights the utility in using OAbz-GSNO as a method of determining GSNOR activity under stress conditions.

In chapter 3 a previously identified site of GSNOR control was further assessed using a novel photo-reactive affinity label.

REFERENCES

- (1) Pérez-Clemente, R. M.; Vives, V.; Zandalinas, S. I.; López-Climent, M. F.; Muñoz, V.; Gómez-Cadenas, A. Biotechnological Approaches to Study Plant Responses to Stress. *BioMed Res. Int.* **2013**, *2013*, 654120. <https://doi.org/10.1155/2013/654120>.
- (2) Hasanuzzaman, M.; Hossain, M. A.; da Silva, J. A. T.; Fujita, M. Plant Response and Tolerance to Abiotic Oxidative Stress: Antioxidant Defense Is a Key Factor. In *Crop Stress and its Management: Perspectives and Strategies*; Venkateswarlu, B., Shanker, A. K., Shanker, C., Maheswari, M., Eds.; Springer Netherlands: Dordrecht, 2012; pp 261–315. https://doi.org/10.1007/978-94-007-2220-0_8.
- (3) *Phytohormones and Abiotic Stress Tolerance in Plants*; Khan, N. A., Nazar, R., Iqbal, N., Anjum, N. A., Eds.; Springer Berlin Heidelberg: Berlin, Heidelberg, 2012. <https://doi.org/10.1007/978-3-642-25829-9>.
- (4) Begara-Morales, J. C.; Chaki, M.; Valderrama, R.; Sánchez-Calvo, B.; Mata-Pérez, C.; Padilla, M. N.; Corpas, F. J.; Barroso, J. B. Nitric Oxide Buffering and Conditional Nitric Oxide Release in Stress Response. *J. Exp. Bot.* **2018**, *69* (14), 3425–3438. <https://doi.org/10.1093/jxb/ery072>.
- (5) Choudhury, S.; Panda, P.; Sahoo, L.; Panda, S. K. Reactive Oxygen Species Signaling in Plants under Abiotic Stress. *Plant Signal. Behav.* **2013**, *8* (4), e23681. <https://doi.org/10.4161/psb.23681>.
- (6) Kapoor, D.; Singh, S.; Kumar, V.; Romero, R.; Prasad, R.; Singh, J. Antioxidant Enzymes Regulation in Plants in Reference to Reactive Oxygen Species (ROS) and Reactive Nitrogen Species (RNS). *Plant Gene* **2019**, *19*, 100182. <https://doi.org/10.1016/j.plgene.2019.100182>.
- (7) Foyer, C. H.; Noctor, G. Ascorbate and Glutathione: The Heart of the Redox Hub1. *Plant Physiol.* **2011**, *155* (1), 2–18. <https://doi.org/10.1104/pp.110.167569>.
- (8) Hasanuzzaman, M.; Nahar, K.; Anee, T. I.; Fujita, M. Glutathione in Plants: Biosynthesis and Physiological Role in Environmental Stress Tolerance. *Physiol. Mol. Biol. Plants* **2017**, *23* (2), 249–268. <https://doi.org/10.1007/s12298-017-0422-2>.
- (9) Noctor, G.; Foyer, C. H. ASCORBATE AND GLUTATHIONE: Keeping Active Oxygen Under Control. *Annu. Rev. Plant Physiol. Plant Mol. Biol.* **1998**, *49*, 249–279. <https://doi.org/10.1146/annurev.arplant.49.1.249>.
- (10) Berthe-Corti, L.; Hulsch, R.; Nevries, U.; Eckardt-Schupp, F. Use of Batch and Fed-Batch Fermentation for Studies on the Variation of Glutathione Content and Its Influence on the Genotoxicity of Methyl-Nitro-Nitrosoguanidine in Yeast. *Mutagenesis* **1992**, *7* (1), 25–30. <https://doi.org/10.1093/mutage/7.1.25>.
- (11) Hasanuzzaman, M.; Bhuyan, M. H. M. B.; Anee, T. I.; Parvin, K.; Nahar, K.; Mahmud, J. A.; Fujita, M. Regulation of Ascorbate-Glutathione Pathway in Mitigating

- Oxidative Damage in Plants under Abiotic Stress. *Antioxidants* **2019**, *8* (9), 384. <https://doi.org/10.3390/antiox8090384>.
- (12) Forman, H. J.; Zhang, H.; Rinna, A. Glutathione: Overview of Its Protective Roles, Measurement, and Biosynthesis. *Mol. Aspects Med.* **2009**, *30* (1–2), 1–12. <https://doi.org/10.1016/j.mam.2008.08.006>.
- (13) Pizzorno, J. Glutathione! *Integr. Med. Clin. J.* **2014**, *13* (1), 8–12.
- (14) Kovacs, I.; Lindermayr, C. Nitric Oxide-Based Protein Modification: Formation and Site-Specificity of Protein S-Nitrosylation. *Front. Plant Sci.* **2013**, *4*, 137. <https://doi.org/10.3389/fpls.2013.00137>.
- (15) Ghanta, S.; Chattopadhyay, S. Glutathione as a Signaling Molecule. *Plant Signal. Behav.* **2011**, *6* (6), 783–788. <https://doi.org/10.4161/psb.6.6.15147>.
- (16) Mhamdi, A.; Han, Y.; Noctor, G. Glutathione-Dependent Phytohormone Responses. *Plant Signal. Behav.* **2013**, *8* (5), e24181. <https://doi.org/10.4161/psb.24181>.
- (17) Baldelli, S.; Ciccarone, F.; Limongi, D.; Checconi, P.; Palamara, A. T.; Ciriolo, M. R. Glutathione and Nitric Oxide: Key Team Players in Use and Disuse of Skeletal Muscle. *Nutrients* **2019**, *11* (10), 2318. <https://doi.org/10.3390/nu11102318>.
- (18) Zhou, X.; Joshi, S.; Khare, T.; Patil, S.; Shang, J.; Kumar, V. Nitric Oxide, Crosstalk with Stress Regulators and Plant Abiotic Stress Tolerance. *Plant Cell Rep.* **2021**. <https://doi.org/10.1007/s00299-021-02705-5>.
- (19) Domingos, P.; Prado, A. M.; Wong, A.; Gehring, C.; Feijo, J. A. Nitric Oxide: A Multitasked Signaling Gas in Plants. *Mol. Plant* **2015**, *8* (4), 506–520. <https://doi.org/10.1016/j.molp.2014.12.010>.
- (20) Begara-Morales, J. C.; Sánchez-Calvo, B.; Chaki, M.; Valderrama, R.; Mata-Pérez, C.; Padilla, M. N.; Corpas, F. J.; Barroso, J. B. Antioxidant Systems Are Regulated by Nitric Oxide-Mediated Post-Translational Modifications (NO-PTMs). *Front. Plant Sci.* **2016**, *7*.
- (21) Fancy, N. N.; Bahlmann, A.-K.; Loake, G. J. Nitric Oxide Function in Plant Abiotic Stress. *Plant Cell Environ.* **2017**, *40* (4), 462–472. <https://doi.org/10.1111/pce.12707>.
- (22) Yin, H.; Xu, L.; Porter, N. A. Free Radical Lipid Peroxidation: Mechanisms and Analysis. *Chem. Rev.* **2011**, *111* (10), 5944–5972. <https://doi.org/10.1021/cr200084z>.
- (23) Lam, M. A.; Pattison, D. I.; Bottle, S. E.; Keddie, D. J.; Davies, M. J. Nitric Oxide and Nitroxides Can Act as Efficient Scavengers of Protein-Derived Free Radicals. *Chem. Res. Toxicol.* **2008**, *21* (11), 2111–2119. <https://doi.org/10.1021/tx800183t>.
- (24) Corpas, F.; Palma, J.; del Río, L.; Barroso, J. Protein Tyrosine Nitration in Higher Plants Grown under Natural and Stress Conditions. *Front. Plant Sci.* **2013**, *4*.
- (25) Fernando, V.; Zheng, X.; Walia, Y.; Sharma, V.; Letson, J.; Furuta, S. S-Nitrosylation: An Emerging Paradigm of Redox Signaling. *Antioxidants* **2019**, *8* (9), 404. <https://doi.org/10.3390/antiox8090404>.

- (26) Martínez-Ruiz, A.; Araújo, I. M.; Izquierdo-Álvarez, A.; Hernansanz-Agustín, P.; Lamas, S.; Serrador, J. M. Specificity in S-Nitrosylation: A Short-Range Mechanism for NO Signaling? *Antioxid. Redox Signal.* **2013**, *19* (11), 1220–1235. <https://doi.org/10.1089/ars.2012.5066>.
- (27) Marino, S. M.; Gladyshev, V. N. Structural Analysis of Cysteine S-Nitrosylation: A Modified Acid-Based Motif and the Emerging Role of Trans-Nitrosylation. *J. Mol. Biol.* **2010**, *395* (4), 844–859. <https://doi.org/10.1016/j.jmb.2009.10.042>.
- (28) Liu, M.; Hou, J.; Huang, L.; Huang, X.; Heibeck, T. H.; Zhao, R.; Pasa-Tolic, L.; Smith, R. D.; Li, Y.; Fu, K.; Zhang, Z.; Hinrichs, S. H.; Ding, S.-J. Site-Specific Proteomics Approach for Study Protein S-Nitrosylation. *Anal. Chem.* **2010**, *82* (17), 7160–7168. <https://doi.org/10.1021/ac100569d>.
- (29) Gong, B.; Yan, Y.; Zhang, L.; Cheng, F.; Liu, Z.; Shi, Q. Unravelling GSNOR-Mediated S-Nitrosylation and Multiple Developmental Programs in Tomato Plants. *Plant Cell Physiol.* **2019**, *60* (11), 2523–2537. <https://doi.org/10.1093/pcp/pcz143>.
- (30) Kiley, P. J.; Storz, G. Exploiting Thiol Modifications. *PLOS Biol.* **2004**, *2* (11), e400. <https://doi.org/10.1371/journal.pbio.0020400>.
- (31) Leichert, L. I.; Jakob, U. Protein Thiol Modifications Visualized In Vivo. *PLoS Biol.* **2004**, *2* (11), e333. <https://doi.org/10.1371/journal.pbio.0020333>.
- (32) Xiong, Y.; Uys, J. D.; Tew, K. D.; Townsend, D. M. S-Glutathionylation: From Molecular Mechanisms to Health Outcomes. *Antioxid. Redox Signal.* **2011**, *15* (1), 233–270. <https://doi.org/10.1089/ars.2010.3540>.
- (33) Alderton, W. K.; Cooper, C. E.; Knowles, R. G. Nitric Oxide Synthases: Structure, Function and Inhibition. *Biochem. J.* **2001**, *357* (Pt 3), 593–615.
- (34) Foresi, N.; Correa-Aragunde, N.; Parisi, G.; Caló, G.; Salerno, G.; Lamattina, L. Characterization of a Nitric Oxide Synthase from the Plant Kingdom: NO Generation from the Green Alga *Ostreococcus Tauri* Is Light Irradiance and Growth Phase Dependent. *Plant Cell* **2010**, *22* (11), 3816–3830. <https://doi.org/10.1105/tpc.109.073510>.
- (35) Jeandroz, S.; Wipf, D.; Stuehr, D. J.; Lamattina, L.; Melkonian, M.; Tian, Z.; Zhu, Y.; Carpenter, E. J.; Wong, G. K.-S.; Wendehenne, D. Occurrence, Structure, and Evolution of Nitric Oxide Synthase-like Proteins in the Plant Kingdom. *Sci. Signal.* **2016**, *9* (417), re2–re2. <https://doi.org/10.1126/scisignal.aad4403>.
- (36) Astier, J.; Gross, I.; Durner, J. Nitric Oxide Production in Plants: An Update. *J. Exp. Bot.* **2018**, *69* (14), 3401–3411. <https://doi.org/10.1093/jxb/erx420>.
- (37) Rockel, P.; Strube, F.; Rockel, A.; Wildt, J.; Kaiser, W. M. Regulation of Nitric Oxide (NO) Production by Plant Nitrate Reductase in Vivo and in Vitro. *J. Exp. Bot.* **2002**, *53* (366), 103–110.

- (38) Chamizo-Ampudia, A.; Sanz-Luque, E.; Llamas, A.; Galvan, A.; Fernandez, E. Nitrate Reductase Regulates Plant Nitric Oxide Homeostasis. *Trends Plant Sci.* **2017**, *22* (2), 163–174. <https://doi.org/10.1016/j.tplants.2016.12.001>.
- (39) Cookson, S. J.; Williams, L. E.; Miller, A. J. Light-Dark Changes in Cytosolic Nitrate Pools Depend on Nitrate Reductase Activity in Arabidopsis Leaf Cells. *Plant Physiol.* **2005**, *138* (2), 1097–1105. <https://doi.org/10.1104/pp.105.062349>.
- (40) Frungillo, L.; Skelly, M. J.; Loake, G. J.; Spoel, S. H.; Salgado, I. S-Nitrosothiols Regulate Nitric Oxide Production and Storage in Plants through the Nitrogen Assimilation Pathway. *Nat. Commun.* **2014**, *5*, 5401. <https://doi.org/10.1038/ncomms6401>.
- (41) Little, D. Y.; Rao, H.; Oliva, S.; Daniel-Vedele, F.; Krapp, A.; Malamy, J. E. The Putative High-Affinity Nitrate Transporter NRT2.1 Represses Lateral Root Initiation in Response to Nutritional Cues. *Proc. Natl. Acad. Sci.* **2005**, *102* (38), 13693–13698. <https://doi.org/10.1073/pnas.0504219102>.
- (42) Campbell, W. H. Structure and Function of Eukaryotic NAD(P)H:Nitrate Reductase. *Cell. Mol. Life Sci. CMLS* **2001**, *58* (2), 194–204. <https://doi.org/10.1007/PL00000847>.
- (43) Gupta, K. J.; Igamberdiev, A. U. The Anoxic Plant Mitochondrion as a Nitrite: NO Reductase. *Mitochondrion* **2011**, *11* (4), 537–543. <https://doi.org/10.1016/j.mito.2011.03.005>.
- (44) Tejada-Jimenez, M.; Llamas, A.; Galván, A.; Fernández, E. Role of Nitrate Reductase in NO Production in Photosynthetic Eukaryotes. *Plants* **2019**, *8* (3), 56. <https://doi.org/10.3390/plants8030056>.
- (45) Chamizo-Ampudia, A.; Sanz-Luque, E.; Llamas, Á.; Ocaña-Calahorra, F.; Mariscal, V.; Carreras, A.; Barroso, J. B.; Galván, A.; Fernández, E. A Dual System Formed by the ARC and NR Molybdoenzymes Mediates Nitrite-Dependent NO Production in Chlamydomonas. *Plant Cell Environ.* **2016**, *39* (10), 2097–2107. <https://doi.org/10.1111/pce.12739>.
- (46) Sanz-Luque, E.; Ocaña-Calahorra, F.; de Montaigu, A.; Chamizo-Ampudia, A.; Llamas, Á.; Galván, A.; Fernández, E. THB1, a Truncated Hemoglobin, Modulates Nitric Oxide Levels and Nitrate Reductase Activity. *Plant J.* **2015**, *81* (3), 467–479. <https://doi.org/10.1111/tpj.12744>.
- (47) Jourdain, D.; Jourdain, F. L.; Feelisch, M. Oxidation and Nitrosation of Thiols at Low Micromolar Exposure to Nitric Oxide. Evidence for a Free Radical Mechanism. *J. Biol. Chem.* **2003**, *278* (18), 15720–15726. <https://doi.org/10.1074/jbc.M300203200>.
- (48) Gow, A. J.; Buerk, D. G.; Ischiropoulos, H. A Novel Reaction Mechanism for the Formation of S-Nitrosothiol in Vivo*. *J. Biol. Chem.* **1997**, *272* (5), 2841–2845. <https://doi.org/10.1074/jbc.272.5.2841>.
- (49) Basu, S.; Keszler, A.; Azarova, N. A.; Nwanze, N.; Perlegas, A.; Shiva, S.; Broniowska, K. A.; Hogg, N.; Kim-Shapiro, D. B. A Novel Role for Cytochrome c: Efficient

Catalysis of S-Nitrosothiol Formation. *Free Radic. Biol. Med.* **2010**, 48 (2), 255.
<https://doi.org/10.1016/j.freeradbiomed.2009.10.049>.

(50) Leterrier, M.; Chaki, M.; Airaki, M.; Valderrama, R.; Palma, J. M.; Barroso, J. B.; Corpas, F. J. Function of S-Nitrosogluthione Reductase (GSNOR) in Plant Development and under Biotic/Abiotic Stress. *Plant Signal. Behav.* **2011**, 6 (6), 789–793.
<https://doi.org/10.4161/psb.6.6.15161>.

(51) Espunya, M. C.; De Michele, R.; Gómez-Cadenas, A.; Martínez, M. C. S-Nitrosogluthione Is a Component of Wound- and Salicylic Acid-Induced Systemic Responses in *Arabidopsis thaliana*. *J. Exp. Bot.* **2012**, 63 (8), 3219–3227.
<https://doi.org/10.1093/jxb/ers043>.

(52) Corpas, F.; Alché, J.; Barroso, J. Current Overview of S-Nitrosogluthione (GSNO) in Higher Plants. *Front. Plant Sci.* **2013**, 4.

(53) Airaki, M.; Sánchez-Moreno, L.; Leterrier, M.; Barroso, J. B.; Palma, J. M.; Corpas, F. J. Detection and Quantification of S-Nitrosogluthione (GSNO) in Pepper (*Capsicum Annuum* L.) Plant Organs by LC-ES/MS. *Plant Cell Physiol.* **2011**, 52 (11), 2006–2015.
<https://doi.org/10.1093/pcp/pcr133>.

(54) Liu, L.; Hausladen, A.; Zeng, M.; Que, L.; Heitman, J.; Stamler, J. S. A Metabolic Enzyme for S-Nitrosothiol Conserved from Bacteria to Humans. *Nature* **2001**, 410 (6827), 490–494. <https://doi.org/10.1038/35068596>.

(55) Sakamoto, A.; Ueda, M.; Morikawa, H. Arabidopsis Glutathione-Dependent Formaldehyde Dehydrogenase Is an S-Nitrosogluthione Reductase. *FEBS Lett.* **2002**, 515 (1–3), 20–24. [https://doi.org/10.1016/S0014-5793\(02\)02414-6](https://doi.org/10.1016/S0014-5793(02)02414-6).

(56) Edenberg, H. J.; Bosron, W. F. 4.06 - Alcohol Dehydrogenases. In *Comprehensive Toxicology (Second Edition)*; McQueen, C. A., Ed.; Elsevier: Oxford, 2010; pp 111–130.
<https://doi.org/10.1016/B978-0-08-046884-6.00406-1>.

(57) Harry, D. E.; Kimmerer, T. W. Molecular Genetics and Physiology of Alcohol Dehydrogenase in Woody Plants. *For. Ecol. Manag.* **1991**, 43 (3–4), 251–272.
[https://doi.org/10.1016/0378-1127\(91\)90130-N](https://doi.org/10.1016/0378-1127(91)90130-N).

(58) Thompson, C. E.; Freitas, L. B.; Salzano, F. M. Molecular Evolution and Functional Divergence of Alcohol Dehydrogenases in Animals, Fungi and Plants. *Genet. Mol. Biol.* **2018**, 41 (1 suppl 1), 341–354. <https://doi.org/10.1590/1678-4685-gmb-2017-0047>.

(59) Staab, C. A.; Alander, J.; Brandt, M.; Lengqvist, J.; Morgenstern, R.; Grafström, R. C.; Höög, J.-O. Reduction of S-Nitrosogluthione by Alcohol Dehydrogenase 3 Is Facilitated by Substrate Alcohols via Direct Cofactor Recycling and Leads to GSH-Controlled Formation of Glutathione Transferase Inhibitors. *Biochem. J.* **2008**, 413 (3), 493–504. <https://doi.org/10.1042/BJ20071666>.

(60) Strittmatter, P.; Ball, E. G. FORMALDEHYDE DEHYDROGENASE, A GLUTATHIONE-DEPENDENT ENZYME SYSTEM. *J. Biol. Chem.* **1955**, 213 (1), 445–461. [https://doi.org/10.1016/S0021-9258\(18\)71084-3](https://doi.org/10.1016/S0021-9258(18)71084-3).

- (61) Staab, C. A.; Hellgren, M.; Höög, J.-O. Medium- and Short-Chain Dehydrogenase/Reductase Gene and Protein Families : Dual Functions of Alcohol Dehydrogenase 3: Implications with Focus on Formaldehyde Dehydrogenase and S-Nitrosogluthathione Reductase Activities. *Cell. Mol. Life Sci. CMLS* **2008**, *65* (24), 3950–3960. <https://doi.org/10.1007/s00018-008-8592-2>.
- (62) Sanghani, P. C.; Robinson, H.; Bosron, W. F.; Hurley, T. D. Human Glutathione-Dependent Formaldehyde Dehydrogenase. Structures of Apo, Binary, and Inhibitory Ternary Complexes. *Biochemistry* **2002**, *41* (35), 10778–10786. <https://doi.org/10.1021/bi0257639>.
- (63) Kubienová, L.; Kopečný, D.; Tylichová, M.; Briozzo, P.; Skopalová, J.; Šebela, M.; Navrátil, M.; Tâche, R.; Luhová, L.; Barroso, J. B.; Petřivalský, M. Structural and Functional Characterization of a Plant S-Nitrosogluthathione Reductase from *Solanum Lycopersicum*. *Biochimie* **2013**, *95* (4), 889–902. <https://doi.org/10.1016/j.biochi.2012.12.009>.
- (64) Castillo, O. A.; Herrera, G.; Manriquez, C.; Rojas, A. F.; González, D. R. Pharmacological Inhibition of S-Nitrosogluthathione Reductase Reduces Cardiac Damage Induced by Ischemia–Reperfusion. *Antioxidants* **2021**, *10* (4), 555. <https://doi.org/10.3390/antiox10040555>.
- (65) Green, L. S.; Chun, L. E.; Patton, A. K.; Sun, X.; Rosenthal, G. J.; Richards, J. P. Mechanism of Inhibition for N6022, a First-in-Class Drug Targeting S-Nitrosogluthathione Reductase. *Biochemistry* **2012**, *51* (10), 2157–2168. <https://doi.org/10.1021/bi201785u>.
- (66) Donaldson, S. H.; Solomon, G. M.; Zeitlin, P. L.; Flume, P. A.; Casey, A.; McCoy, K.; Zemanick, E. T.; Mandagere, A.; Troha, J. M.; Shoemaker, S. A.; Chmiel, J. F.; Taylor-Cousar, J. L. Pharmacokinetics and Safety of Cavosonstat (N91115) in Healthy and Cystic Fibrosis Adults Homozygous for F508DEL-CFTR. *J. Cyst. Fibros.* **2017**, *16* (3), 371–379. <https://doi.org/10.1016/j.jcf.2017.01.009>.
- (67) Yu, Z.; Cao, J.; Zhu, S.; Zhang, L.; Peng, Y.; Shi, J. Exogenous Nitric Oxide Enhances Disease Resistance by Nitrosylation and Inhibition of S-Nitrosogluthathione Reductase in Peach Fruit. *Front. Plant Sci.* **2020**, *11*.
- (68) Jedelská; Kraiczová; Berčíková; Činčalová; Luhová; Petřivalský. Tomato Root Growth Inhibition by Salinity and Cadmium Is Mediated By S-Nitrosative Modifications of ROS Metabolic Enzymes Controlled by S-Nitrosogluthathione Reductase. *Biomolecules* **2019**, *9* (9), 393. <https://doi.org/10.3390/biom9090393>.
- (69) Jahnová, J.; Luhová, L.; Petřivalský, M. S-Nitrosogluthathione Reductase—The Master Regulator of Protein S-Nitrosation in Plant NO Signaling. *Plants* **2019**, *8* (2). <https://doi.org/10.3390/plants8020048>.
- (70) Tichá, T.; Lochman, J.; Činčalová, L.; Luhová, L.; Petřivalský, M. Redox Regulation of Plant S-Nitrosogluthathione Reductase Activity through Post-Translational Modifications of Cysteine Residues. *Biochem. Biophys. Res. Commun.* **2017**, *494* (1–2), 27–33. <https://doi.org/10.1016/j.bbrc.2017.10.090>.

- (71) Guerra, D.; Ballard, K.; Truebridge, I.; Vierling, E. S-Nitrosation of Conserved Cysteines Modulates Activity and Stability of S-Nitrosogluthione Reductase (GSNOR). *Biochemistry* **2016**, 55 (17), 2452–2464. <https://doi.org/10.1021/acs.biochem.5b01373>.
- (72) Fontana, K.; Onukwue, N.; Sun, B.-L.; Lento, C.; Ventimiglia, L.; Nikoo, S.; Gauld, J. W.; Wilson, D. J.; Mutus, B. Evidence for an Allosteric S-Nitrosogluthione Binding Site in S-Nitrosogluthione Reductase (GSNOR). *Antioxidants* **2019**, 8 (11), 545. <https://doi.org/10.3390/antiox8110545>.
- (73) Hu, J.; Huang, X.; Chen, L.; Sun, X.; Lu, C.; Zhang, L.; Wang, Y.; Zuo, J. Site-Specific Nitrosoproteomic Identification of Endogenously S-Nitrosylated Proteins in Arabidopsis. *Plant Physiol.* **2015**, 167 (4), 1731–1746. <https://doi.org/10.1104/pp.15.00026>.
- (74) Kovacs, I.; Holzmeister, C.; Wirtz, M.; Geerlof, A.; Fröhlich, T.; Römeling, G.; Kuruthukulangarakoola, G. T.; Linster, E.; Hell, R.; Arnold, G. J.; Durner, J.; Lindermayr, C. ROS-Mediated Inhibition of S-Nitrosogluthione Reductase Contributes to the Activation of Anti-Oxidative Mechanisms. *Front. Plant Sci.* **2016**, 7. <https://doi.org/10.3389/fpls.2016.01669>.
- (75) Li, B.; Sun, C.; Lin, X.; Busch, W. The Emerging Role of GSNOR in Oxidative Stress Regulation. *Trends Plant Sci.* **2021**, 26 (2), 156–168. <https://doi.org/10.1016/j.tplants.2020.09.004>.
- (76) Kubienová, L.; Tichá, T.; Jahnová, J.; Luhová, L.; Mieslerová, B.; Petřivalský, M. Effect of Abiotic Stress Stimuli on S-Nitrosogluthione Reductase in Plants. *Planta* **2014**, 239 (1), 139–146. <https://doi.org/10.1007/s00425-013-1970-5>.
- (77) Zhang, L.; Li, G.; Wang, M.; Di, D.; Sun, L.; Kronzucker, H. J.; Shi, W. Excess Iron Stress Reduces Root Tip Zone Growth through Nitric Oxide-Mediated Repression of Potassium Homeostasis in Arabidopsis. *New Phytol.* **2018**, 219 (1), 259–274. <https://doi.org/10.1111/nph.15157>.
- (78) Romero-Puertas, M. C.; Laxa, M.; Mattè, A.; Zaninotto, F.; Finkemeier, I.; Jones, A. M. E.; Perazzolli, M.; Vandelle, E.; Dietz, K.-J.; Delledonne, M. S-Nitrosylation of Peroxiredoxin II E Promotes Peroxynitrite-Mediated Tyrosine Nitration. *Plant Cell* **2007**, 19 (12), 4120–4130. <https://doi.org/10.1105/tpc.107.055061>.
- (79) Yun, B.-W.; Feechan, A.; Yin, M.; Saidi, N. B. B.; Le Bihan, T.; Yu, M.; Moore, J. W.; Kang, J.-G.; Kwon, E.; Spoel, S. H.; Pallas, J. A.; Loake, G. J. S-Nitrosylation of NADPH Oxidase Regulates Cell Death in Plant Immunity. *Nature* **2011**, 478 (7368), 264–268. <https://doi.org/10.1038/nature10427>.
- (80) Lymperopoulos, P.; Msanne, J.; Rabara, R. Phytochrome and Phytohormones: Working in Tandem for Plant Growth and Development. *Front. Plant Sci.* **2018**, 9. <https://doi.org/10.3389/fpls.2018.01037>.
- (81) París, R.; Iglesias, M. J.; Terrile, M. C.; Casalongué, C. A. Functions of S-Nitrosylation in Plant Hormone Networks. *Front. Plant Sci.* **2013**, 4. <https://doi.org/10.3389/fpls.2013.00294>.

- (82) Terrile, M. C.; París, R.; Calderón-Villalobos, L. I. A.; Iglesias, M. J.; Lamattina, L.; Estelle, M.; Casalongué, C. A. Nitric Oxide Influences Auxin Signaling through S-Nitrosylation of the Arabidopsis TRANSPORT INHIBITOR RESPONSE 1 Auxin Receptor. *Plant J.* **2012**, *70* (3), 492–500. <https://doi.org/10.1111/j.1365-313X.2011.04885.x>.
- (83) Feng, J.; Wang, C.; Chen, Q.; Chen, H.; Ren, B.; Li, X.; Zuo, J. S-Nitrosylation of Phosphotransfer Proteins Represses Cytokinin Signaling. *Nat. Commun.* **2013**, *4* (1), 1529. <https://doi.org/10.1038/ncomms2541>.
- (84) Scott, J. W.; Harbaugh, B. K. *Micro-Tom: A Miniature Dwarf Tomato*; Circular (University of Florida. Agricultural Experiment Station); Agricultural Experiment Station, Institute of Food and Agricultural Sciences, University of Florida: Gainesville, FL, 1989.
- (85) Gonzalez, C.; Ré, M. D.; Sossi, M. L.; Valle, E. M.; Boggio, S. B. Tomato Cv. ‘Micro-Tom’ as a Model System to Study Postharvest Chilling Tolerance. *Sci. Hortic.* **2015**, *184*, 63–69. <https://doi.org/10.1016/j.scienta.2014.12.020>.
- (86) Malacrida, C.; Valle, E. M.; Boggio, S. B. Postharvest Chilling Induces Oxidative Stress Response in the Dwarf Tomato Cultivar Micro-Tom. *Physiol. Plant.* **2006**, *127* (1), 10–18. <https://doi.org/10.1111/j.1399-3054.2005.00636.x>.
- (87) Wen, D.; Gong, B.; Sun, S.; Liu, S.; Wang, X.; Wei, M.; Yang, F.; Li, Y.; Shi, Q. Promoting Roles of Melatonin in Adventitious Root Development of Solanum Lycopersicum L. by Regulating Auxin and Nitric Oxide Signaling. *Front. Plant Sci.* **2016**, *7*. <https://doi.org/10.3389/fpls.2016.00718>.
- (88) Jensen, D. E.; Belka, G. K.; Du Bois, G. C. S-Nitrosoglutathione Is a Substrate for Rat Alcohol Dehydrogenase Class III Isoenzyme. *Biochem. J.* **1998**, *331* (Pt 2), 659–668.
- (89) Pegg, T. J.; Gladish, D. K.; Baker, R. L. Algae to Angiosperms: Autofluorescence for Rapid Visualization of Plant Anatomy among Diverse Taxa. *Appl. Plant Sci.* **2021**, *9* (6), e11437. <https://doi.org/10.1002/aps3.11437>.
- (90) DeVree, B. T.; Steiner, L. M.; Głazowska, S.; Ruhnnow, F.; Herburger, K.; Persson, S.; Mravec, J. Current and Future Advances in Fluorescence-Based Visualization of Plant Cell Wall Components and Cell Wall Biosynthetic Machineries. *Biotechnol. Biofuels* **2021**, *14* (1), 78. <https://doi.org/10.1186/s13068-021-01922-0>.
- (91) Meier, M.; Lucchetta, E. M.; Ismagilov, R. F. Chemical Stimulation of the Arabidopsis Thaliana Root Using Multi-Laminar Flow on a Microfluidic Chip. *Lab. Chip* **2010**, *10* (16), 2147–2153. <https://doi.org/10.1039/C004629A>.
- (92) Grossmann, G.; Guo, W.-J.; Ehrhardt, D. W.; Frommer, W. B.; Sit, R. V.; Quake, S. R.; Meier, M. The RootChip: An Integrated Microfluidic Chip for Plant Science. *Plant Cell* **2011**, *23* (12), 4234–4240. <https://doi.org/10.1105/tpc.111.092577>.
- (93) Donaldson, L. Autofluorescence in Plants. *Molecules* **2020**, *25* (10), 2393. <https://doi.org/10.3390/molecules25102393>.

- (94) García-Plazaola, J. I.; Fernández-Marín, B.; Duke, S. O.; Hernández, A.; López-Arbeloa, F.; Becerril, J. M. Autofluorescence: Biological Functions and Technical Applications. *Plant Sci.* **2015**, *236*, 136–145. <https://doi.org/10.1016/j.plantsci.2015.03.010>.
- (95) Berg, R. H.; Beachy, R. N. Fluorescent Protein Applications in Plants. *Methods Cell Biol.* **2008**, *85*, 153–177. [https://doi.org/10.1016/S0091-679X\(08\)85008-X](https://doi.org/10.1016/S0091-679X(08)85008-X).
- (96) Wikimedia Commons. *English: General Structure of Lignin. Inset of Lignol Monomers*; 2011. <https://commons.wikimedia.org/wiki/File:Lignin.png> (accessed 2022-11-21).
- (97) del Río, J. C.; Rencoret, J.; Gutiérrez, A.; Elder, T.; Kim, H.; Ralph, J. Lignin Monomers from beyond the Canonical Monolignol Biosynthetic Pathway: Another Brick in the Wall. *ACS Sustain. Chem. Eng.* **2020**, *8* (13), 4997–5012. <https://doi.org/10.1021/acssuschemeng.0c01109>.
- (98) Sun, B. L.; Palmer, L.; Alam, S. R.; Adekoya, I.; Brown-Steinke, K.; Periasamy, A.; Mutus, B. O-Aminobenzoyl-S-Nitrosoglutathione: A Fluorogenic, Cell Permeable, Pseudo-Substrate for S-Nitrosoglutathione Reductase. *Free Radic. Biol. Med.* **2017**, *108*, 445–451. <https://doi.org/10.1016/j.freeradbiomed.2017.04.008>.
- (99) Zhang, L.; Song, H.; Li, B.; Wang, M.; Di, D.; Lin, X.; Kronzucker, H. J.; Shi, W.; Li, G. Induction of S-Nitrosoglutathione Reductase Protects Root Growth from Ammonium Toxicity by Regulating Potassium Homeostasis in Arabidopsis and Rice. *J. Exp. Bot.* **2021**, *72* (12), 4548–4564. <https://doi.org/10.1093/jxb/erab140>.
- (100) Hachiya, T.; Sakakibara, H. Interactions between Nitrate and Ammonium in Their Uptake, Allocation, Assimilation, and Signaling in Plants. *J. Exp. Bot.* **2017**, *68* (10), 2501–2512. <https://doi.org/10.1093/jxb/erw449>.
- (101) López-Bucio, J.; Cruz-Ramírez, A.; Herrera-Estrella, L. The Role of Nutrient Availability in Regulating Root Architecture. *Curr. Opin. Plant Biol.* **2003**, *6* (3), 280–287. [https://doi.org/10.1016/S1369-5266\(03\)00035-9](https://doi.org/10.1016/S1369-5266(03)00035-9).
- (102) Meier, M.; Liu, Y.; Lay-Pruitt, K. S.; Takahashi, H.; von Wirén, N. Auxin-Mediated Root Branching Is Determined by the Form of Available Nitrogen. *Nat. Plants* **2020**, *6* (9), 1136–1145. <https://doi.org/10.1038/s41477-020-00756-2>.
- (103) Straub, T.; Ludewig, U.; Neuhäuser, B. The Kinase CIPK23 Inhibits Ammonium Transport in Arabidopsis Thaliana. *Plant Cell* **2017**, *29* (2), 409–422. <https://doi.org/10.1105/tpc.16.00806>.
- (104) Saha, B.; Borovskii, G.; Panda, S. K. Alternative Oxidase and Plant Stress Tolerance. *Plant Signal. Behav.* **2016**, *11* (12), e1256530. <https://doi.org/10.1080/15592324.2016.1256530>.
- (105) Hachiya, T.; Noguchi, K. Integrative Response of Plant Mitochondrial Electron Transport Chain to Nitrogen Source. *Plant Cell Rep.* **2011**, *30* (2), 195–204. <https://doi.org/10.1007/s00299-010-0955-0>.

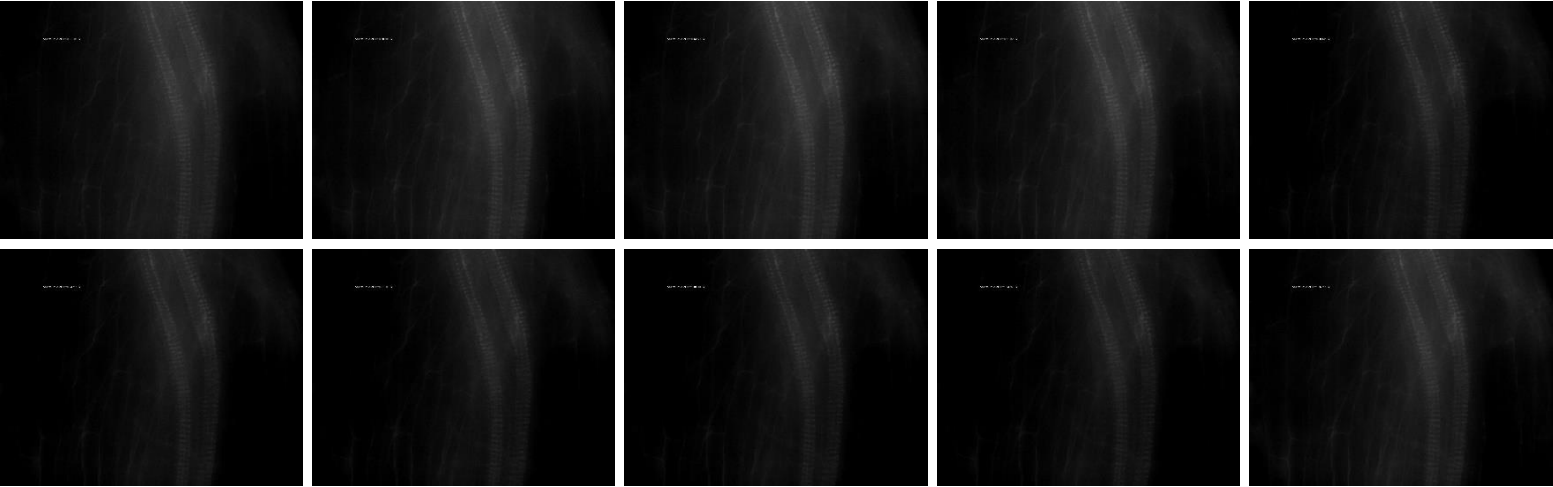
- (106) Kempinski, C. F.; Haffar, R.; Barth, C. Toward the Mechanism of NH_4^+ Sensitivity Mediated by Arabidopsis GDP-Mannose Pyrophosphorylase. *Plant Cell Environ.* **2011**, *34* (5), 847–858. <https://doi.org/10.1111/j.1365-3040.2011.02290.x>.
- (107) Rustérucci, C.; Espunya, M. C.; Díaz, M.; Chabannes, M.; Martínez, M. C. S-Nitrosogluthione Reductase Affords Protection against Pathogens in Arabidopsis, Both Locally and Systemically. *Plant Physiol.* **2007**, *143* (3), 1282–1292. <https://doi.org/10.1104/pp.106.091686>.
- (108) García, M. J.; Corpas, F. J.; Lucena, C.; Alcántara, E.; Pérez-Vicente, R.; Zamarreño, Á. M.; Bacaicoa, E.; García-Mina, J. M.; Bauer, P.; Romera, F. J. A Shoot Fe Signaling Pathway Requiring the OPT3 Transporter Controls GSNO Reductase and Ethylene in Arabidopsis Thaliana Roots. *Front. Plant Sci.* **2018**, *9*. <https://doi.org/10.3389/fpls.2018.01325>.
- (109) Skelly, M. J.; Loake, G. J. Synthesis of Redox-Active Molecules and Their Signaling Functions During the Expression of Plant Disease Resistance. *Antioxid. Redox Signal.* **2013**, *19* (9), 990–997. <https://doi.org/10.1089/ars.2013.5429>.
- (110) Yu, M.; Yun, B.-W.; Spoel, S. H.; Loake, G. J. A Sleigh Ride through the SNO: Regulation of Plant Immune Function by Protein S-Nitrosylation. *Curr. Opin. Plant Biol.* **2012**, *15* (4), 424–430. <https://doi.org/10.1016/j.pbi.2012.03.005>.
- (111) Guerra, D.; Ballard, K.; Truebridge, I.; Vierling, E. S-Nitrosation of Conserved Cysteines Modulates Activity and Stability of S-Nitrosogluthione Reductase (GSNOR). *Biochemistry* **2016**, *55* (17), 2452–2464. <https://doi.org/10.1021/acs.biochem.5b01373>.
- (112) Xu, S.; Guerra, D.; Lee, U.; Vierling, E. S-Nitrosogluthione Reductases Are Low-Copy Number, Cysteine-Rich Proteins in Plants That Control Multiple Developmental and Defense Responses in Arabidopsis. *Front. Plant Sci.* **2013**, *4*, 430. <https://doi.org/10.3389/fpls.2013.00430>.
- (113) Smith, B. D.; Nakanishi, K.; Watanabe, K.; Ito, S. 4-Azido[3,5-[3H]]Phenacylbromide, a Versatile Bifunctional Reagent for Photoaffinity Radiolabeling. Synthesis of Prostaglandin 4-Azido[3,5-[3H]]Phenacyl Esters. *Bioconjug. Chem.* **1990**, *1* (5), 363–364. <https://doi.org/10.1021/bc00005a011>.
- (114) Schwartz, I.; Ofengand, J. Photo-Affinity Labeling of tRNA Binding Sites in Macromolecules. I. Linking of the Phenacyl- *p* -Azide of 4-Thiouridine in (*Escherichia Coli*) Valyl-tRNA to 16S RNA at the Ribosomal P Site. *Proc. Natl. Acad. Sci.* **1974**, *71* (10), 3951–3955. <https://doi.org/10.1073/pnas.71.10.3951>.
- (115) Hixson, S. H.; Hixson, S. S. P-Azidophenacyl Bromide, a Versatile Photolabile Bifunctional Reagent. Reaction with Glyceraldehyde-3-Phosphate Dehydrogenase. *Biochemistry* **1975**, *14* (19), 4251–4254. <https://doi.org/10.1021/bi00690a016>.
- (116) Richter, D.; West, L.-S. (1974 : B. Lipmann Symposium. *Energy Transformation in Biological Systems: [Symposium on Energy Transformation in Biological Systems, London, 2.–4. July, 1974]*; Walter de Gruyter GmbH & Co KG, 2019.

(117) *Photoreactive Crosslinker Chemistry - CA.*

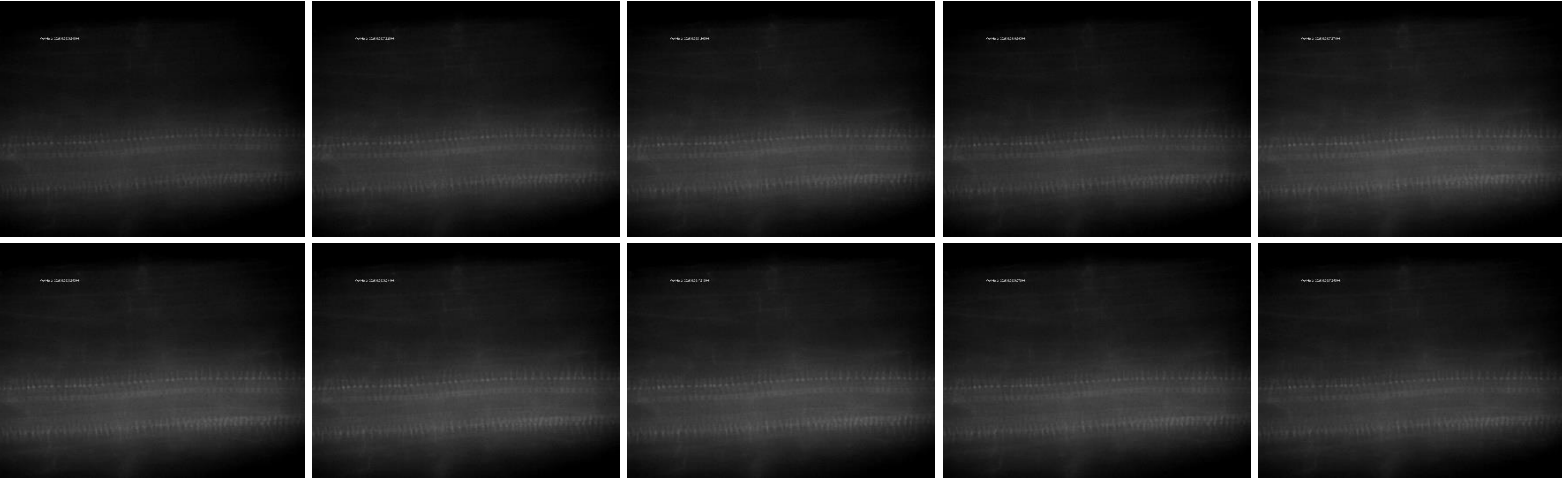
<https://www.thermofisher.com/ca/en/home/life-science/protein-biology/protein-biology-learning-center/protein-biology-resource-library/pierce-protein-methods/photoreactive-crosslinker-chemistry.html> (accessed 2022-11-27).

APPENDICES

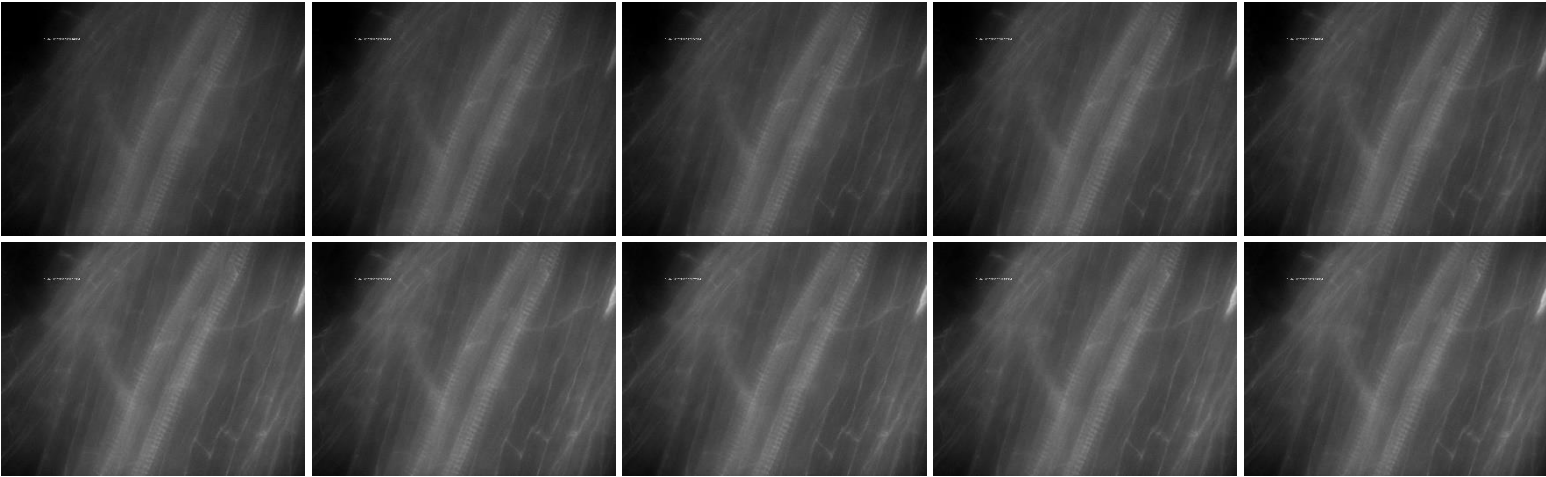
Appendix A—Michaelis Menten Kinetics



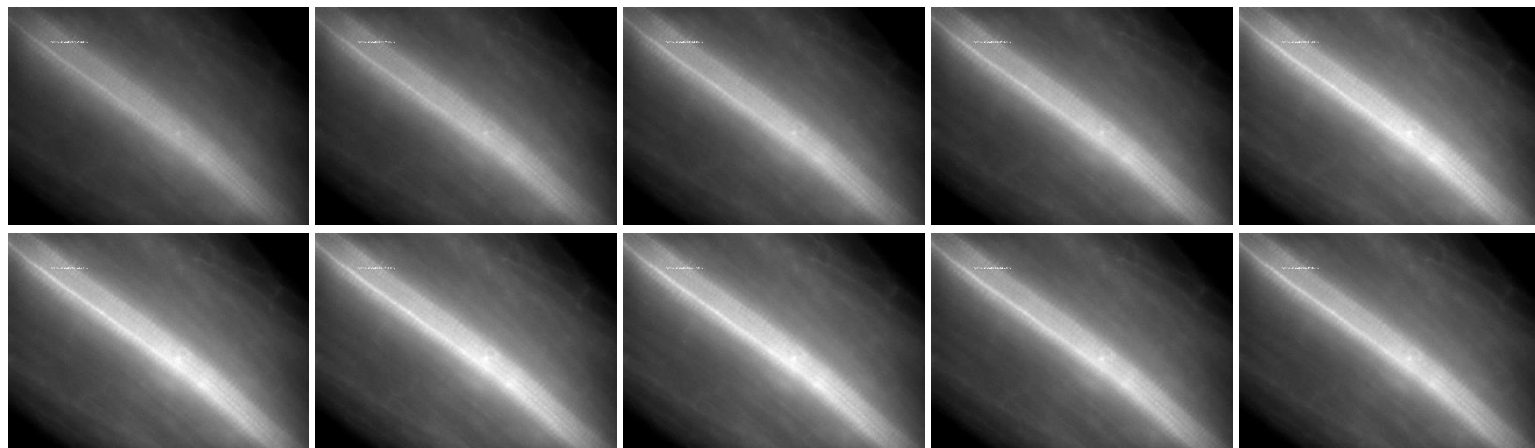
control



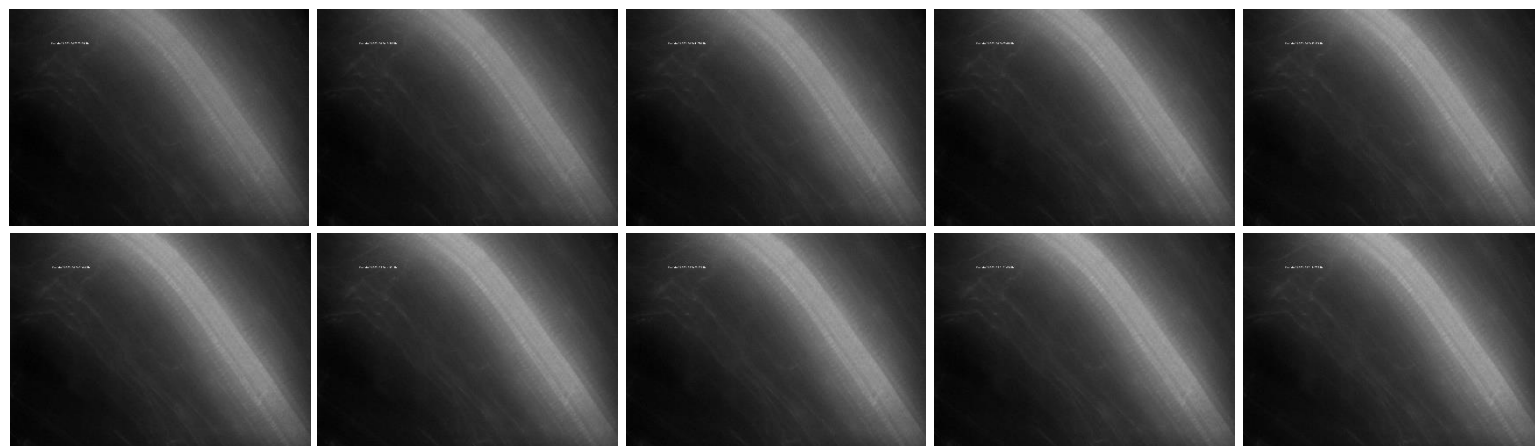
0.25mM



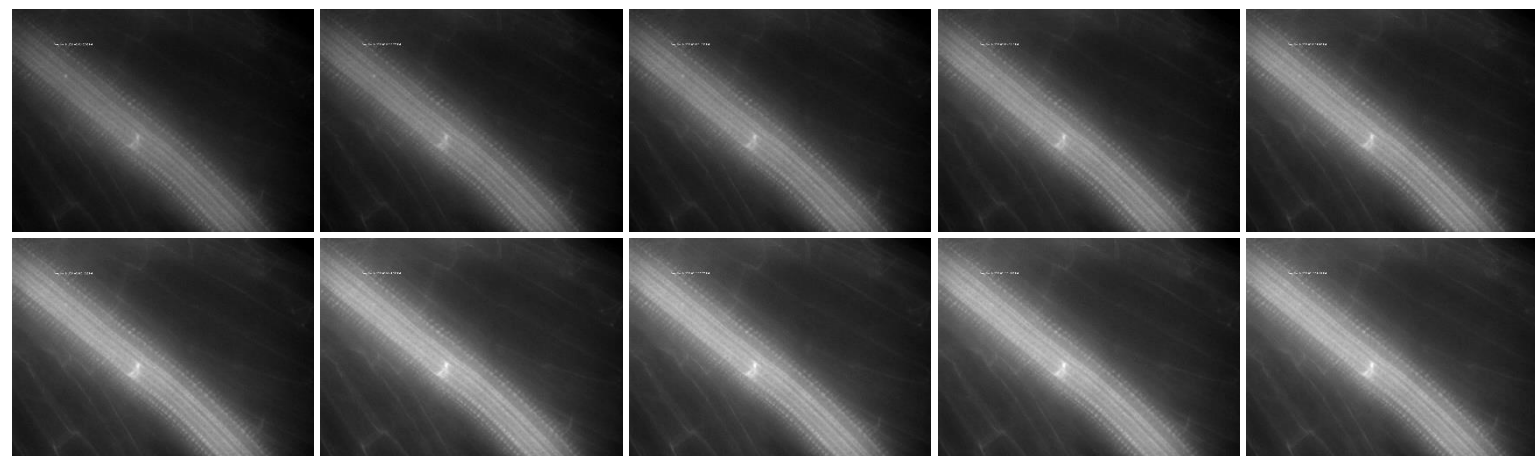
0.75mM



1mM



2mM



4mM

Figure A.1 Image series for Michaelis-Menten experiments

An image series was taken for roots exposed to concentrations of OAbz-GSNO ranging from 0 to 4mM, to determine the change in fluorescent intensity over time at each concentration.

Images were captured using an inverted epifluorescence microscope every 2 seconds for 30 seconds. Each image taken at 400x magnification was exposed for 500ms and analyzed using ImageJ software (NIH and LOCI, University of Wisconsin) for its greyscale value of the total area occupied by the root. The greyscale value corresponds to relative fluorescent units (RFU) which can be plotted and analyzed for slope of RFU per second. When the corrected rates from image series 0.25mM to 4mM (subtracted by control rate) are plotted on a graph where RFU per second is placed on the y-axis and concentration in mM on the x-axis the corresponding relationship resembles Michaelis- Menten kinetics

Appendix B—Human GSNOR sequence used containing tags and start methionine

MGSSHHHHHH₁₀ SSGLVPRGSH₂₀ MANEVIKCKA₃₀ AVAWEAGKPL₄₀ SIEEIEVAPP₅₀
KAHEVRIKII₆₀ ATAVCHTDAY₇₀ TLSGADPEGC₈₀ FPVILGHEGA₉₀ GIVESVGEGV₁₀₀
TKLKAGDTVI₁₁₀ PLYIPQCGEC₁₂₀ KFCLNPKTNL₁₃₀ CQKIRVTQGK₁₄₀
GLMPDGTSRF₁₅₀ TCKGKTILHY₁₆₀ MGTSTFSEYT₁₇₀ VVADISVAKI₁₈₀
DPLAPLDKVC₁₉₀ LLGCGISTGY₂₀₀ GAAVNTAKLE₂₁₀ PGSVCAVFGL₂₂₀
GGVGLAVIMG₂₃₀ CKVAGASRII₂₄₀ GVDINKDKFA₂₅₀ RAKEFGATEC₂₆₀
INPQDFSKPI₂₇₀ QEVLIEMTDG₂₈₀ GVDYSFECIG₂₉₀ NVKVMRAALE₃₀₀
ACHKGWGVSV₃₁₀ VVGVAASGEE₃₂₀ IATRPFQLVT₃₃₀ GRTWKGTAFG₃₄₀
GWKSVESVPK₃₅₀ LVSEYMSKKI₃₆₀ KVDEFVTHNL₃₇₀ SFDEINKAFE₃₈₀
LMHSGKSIRT₄₀₀ VVKILEHHHH₄₁₀ HH

Figure B.1 Sequence of hmGSNOR used containing tags and start methionine with allosteric site residues Asn205, Lys208, Gly341, and Lys343

Table B.1 peptide masses from HmGSNOR trypsin digestion

Fragment mass	Position	Peptide sequence
1899.8892	1-17	MGSSHHHHHHSSGLVPR
1085.5408	18-27	GSHMANEVIK
2305.2437	30-51	AAVAWEAGKPLSIEEIEVAP PK
611.3260	52-56	AHEVR

4384.1474	59-102	IIATAVCHTDAYTLSGADPEGCFPVILGHEGAGIVESVGE GVTK
1806.8764	105-121	AGDTVIPLEYIPQCGECK
721.3701	122-127	FCLNPK
706.3552	128-133	TNLCQK
532.3089	136-140	VTQ GK
933.4458	141-149	GLMPDGTSR
2633.3167	156-179	TILHYMG TSTFSEYTVVADI SVAK
981.5615	180-188	IDPLAPLDK
1897.9510	189-208	VCLLGCGISTGYGAAVNTAK
2277.1803	209-232	LEPGSVCAVFGLGGVGLAVI MGCK
560.3151	233-238	VAGASR
871.5247	239-246	IIGVDINK
4423.0454	254-293	EFGATECINPQDFSKPIQEV LIEMTDGGVDYSFECIGNVK
842.4189	297-304	AALEACHK
2842.5209	305-332	GWGVSVVVGVAAGEEIATR PFQLVTGR
823.4097	336-343	GTAFGGWK
745.4090	344-350	SVESVPK
956.4757	351-358	LVSEYMSK
1906.9181	362-377	VDEFVTHNLSFDEINK
1019.4978	378-386	AFELMHSGK
1196.5820	394-402	ILEHHHHHHH

Appendix C—papaGS adducts

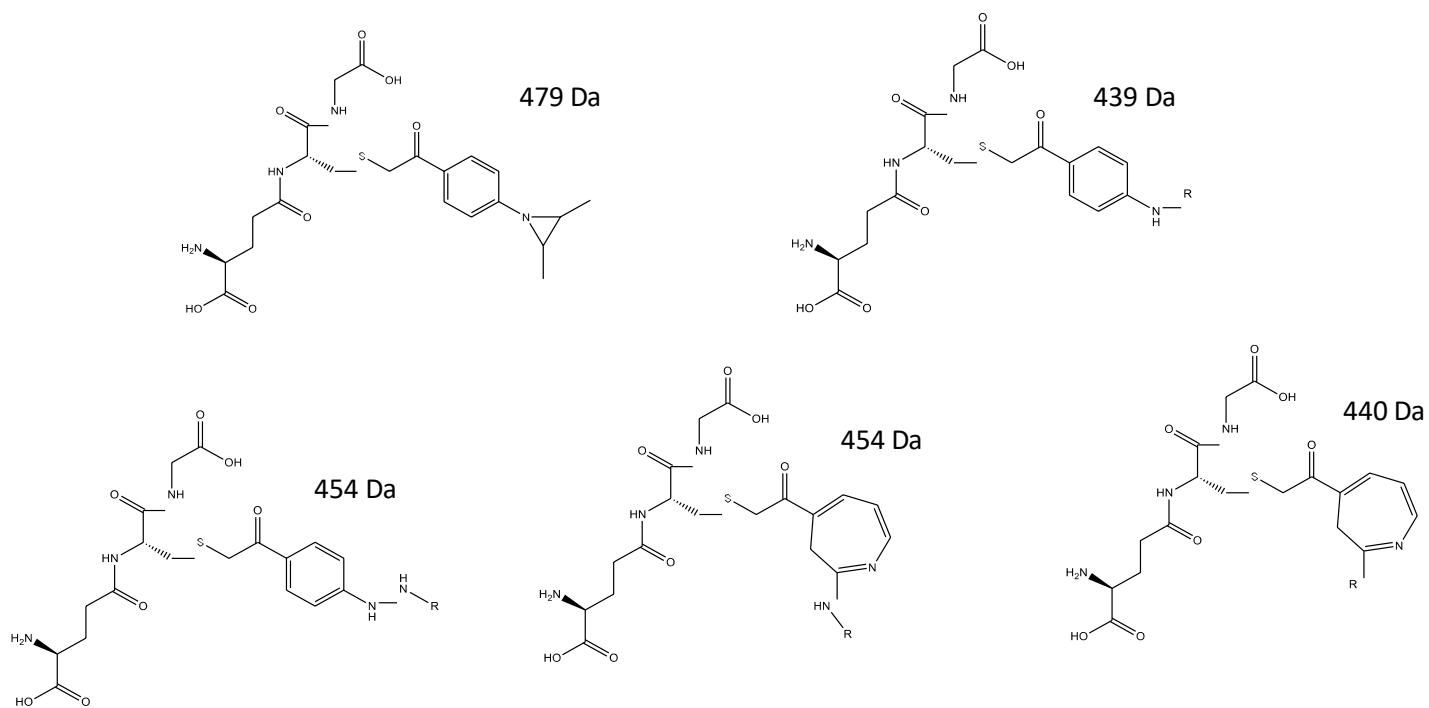


Figure C.1 Possible Molecular Weights of irradiated papaGS adducts.

Appendix D —Protoplast Isolation

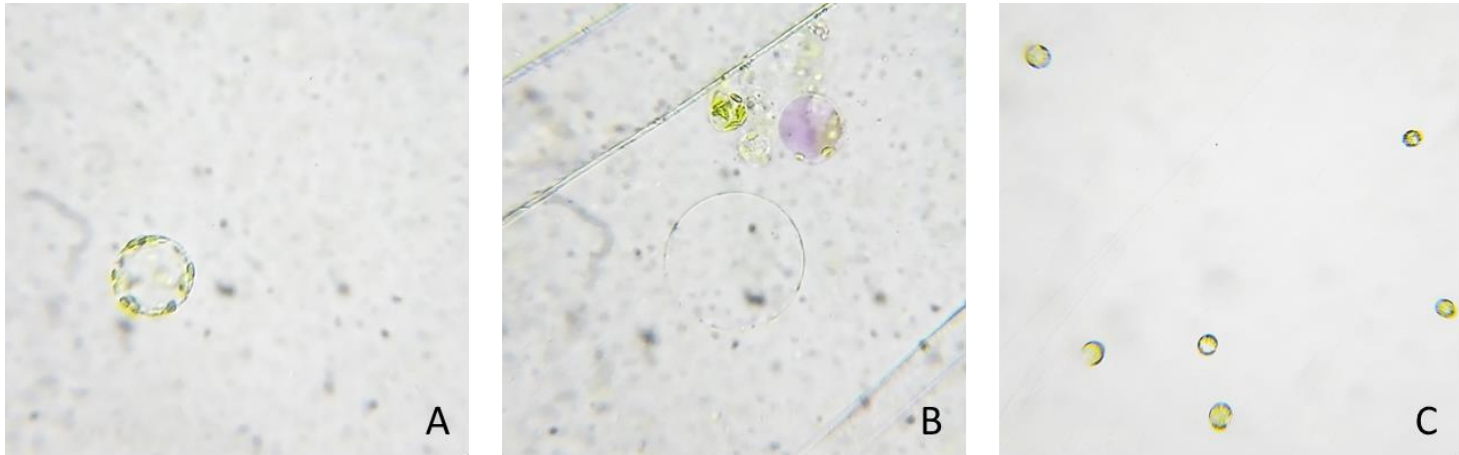


Figure B.1 Extracted protoplasts

Images taken with benchtop light microscope. **A.** 400x magnification. Single protoplast containing green chloroplasts. **B.** 400x magnification. Three different cell types visible as protoplasts, small protoplast containing chlorophyll, medium protoplast with a large vacuole containing violet pigment, and a large clear protoplast. **C.** 100x magnification.

VITA AUCTORIS

NAME: Leslie Ventimiglia

PLACE OF BIRTH: Windsor, Ontario, Canada

EDUCATION: University of Windsor, B.Sc.

Windsor, Ontario, Canada, 2019

PUBLICATIONS:

1. Fontana, K., Ventimiglia, L. and Mutus, B. (2018), Nitric oxide generating copper–chitosan particles for wound healing applications. *J. Chem. Technol. Biotechnol.* 93: 2093-2101. <https://doi.org/10.1002/jctb.5630>
2. Onukwue N, Ventimiglia L, Potter M, Aljoudi S, Mutus B. Simple fluorescent reagents for monitoring disulfide reductase and S-nitroso reductase activities in vitro and in live cells in culture. *Methods*. 2019 Sep 15;168:29-34. doi: 10.1016/j.ymeth.2019.06.028. Epub 2019 Jul 3. PMID: 31278980.
3. Fontana K, Onukwue N, Sun BL, Lento C, Ventimiglia L, Nikoo S, Gauld JW, Wilson DJ, Mutus B. Evidence for an Allosteric S-Nitrosoglutathione Binding Site in S-Nitrosoglutathione Reductase (GSNOR). *Antioxidants (Basel)*. 2019 Nov 13;8(11):545. doi: 10.3390/antiox8110545. PMID: 31766125; PMCID: PMC6928738.
4. Ventimiglia L, Mutus B. The Physiological Implications of S-Nitrosoglutathione Reductase (GSNOR) Activity Mediating NO Signalling in Plant Root Structures. *Antioxidants (Basel)*. 2020 Nov 30;9(12):1206. doi: 10.3390/antiox9121206. PMID: 33266126; PMCID: PMC7760381.